EFFECT OF JOINT FLEXIBILITY ON THE NONLINEAR STATIC AND DYNAMIC BEHAVIOUR OF OFFSHORE JACKET PLATFORMS

HAMIDREZA GOLABI

DISSERTATION SUBMITTED IN FULFILMENT OF THE REQUIREMENTS FOR THE DEGREE OF MASTER OF SCIENCE

INSTITUTE OF GRADUATE STUDIES
UNIVERSITY OF MALAYA
KUALA LUMPUR

2015

UNIVERSITI MALAYA

PERAKUAN KEASLIAN PENULISAN

Nama: HAMIDREZA GOLABI

No. Pendaftaran/Matrik: KGA080063

Nama Ijazah: MASTER OF ENGINEERING SCIENCE

Tajuk Kertas Projek/Laporan Penyelidikan/Disertasi/Tesis ("Hasil Kerja ini"):

EFFECT OF JOINT FLEXIBILITY ON THE NONLINEAR STATIC AND DYNAMIC BEHAVIOUR OF OFFSHORE JACKET PLATFORMS

Bidang Penyelidikan: STRUCTURAL ENGINEERING AND MATERIALS

Saya dengan sesungguhnya dan sebenarnya mengaku bahawa:

(1) Saya adalah satu-satunya pengarang/penulis Hasil Kerja ini;
(2) Hasil Kerja ini adalah asli;
(3) Apa-apa penggunaan mana-mana hasil kerja yang mengandungi hakcipta telah dilakukan secara urusan yang wajar dan bagi maksud yang dibenarkan dan apa-apa petikan, ekstrak, rujukan atau pengeluaran semula daripada atau kepada mana-mana hasil kerja yang mengandungi hakcipta telah dinyatakan dengan sejelasnya dan secukupnya dan satu pengiktirafan tajuk hasil kerja tersebut dan pengarang/penulisnya telah dilakukan di dalam Hasil Kerja ini;
(4) Saya tidak mempunyai apa-apa pengetahuan sebenar atau patut semunasabahnya tahu bahawa penghasilan Hasil Kerja ini melanggar suatu hakcipta hasil kerja yang lain;
(5) Saya dengan ini menyerahkan kesemua dan tiap-tiap hak yang terkandung di dalam hakcipta Hasil Kerja ini kepada Universiti Malaya ("UM") yang seterusnya mula dari sekarang adalah tuan punya kepada hakcipta di dalam Hasil Kerja ini dan apa-apa pengeluaran semula atau penggunaan dalam apa jua bentuk atau dengan apa juga cara sekalipun adalah dilarang tanpa terlebih dahulu mendapat kebenaran bertulis dari UM;
(6) Saya sedar sepenuhnya sekiranya dalam masa penghasilan Hasil Kerja ini saya telah melanggar suatu hakcipta hasil kerja yang lain sama ada dengan niat atau sebaliknya, saya boleh dikenakan tindakan undang-undang atau apa-apa tindakan lain sebagaimana yang diputuskan oleh UM.

Tandatangan Calon Tarikh

Diperbuat dan sesungguhnya diakui di hadapan,

Tandatangan Saksi Tarikh

Nama:

Jawatan:

UNIVERSITI MALAYA

ORIGINAL LITERARY WORK DECLARATION

Name of Candidate: HAMIDREZA GOLABI

Registration/Matric No: KGA080063

Name of Degree: MASTER OF ENGINEERING SCIENCE

Title of Project Paper/Research Report/Dissertation/Thesis ("this Work"):

EFFECT OF JOINT FLEXIBILITY ON THE NONLINEAR STATIC AND DYNAMIC BEHAVIOUR OF OFFSHORE JACKET PLATFORMS

Field of Study: STRUCTURAL ENGINEERING AND MATERIALS

I do solemnly and sincerely declare that:

(1) I am the sole author/writer of this Work;
(2) This Work is original;
(3) Any use of any work in which copyright exists was done by way of fair dealing and for permitted purposes and any excerpt or extract from, or reference to or reproduction of any copyright work has been disclosed expressly and sufficiently and the title of the Work and its authorship have been acknowledged in this Work;
(4) I do not have any actual knowledge nor do I ought reasonably to know that the making of this work constitutes an infringement of any copyright work;
(5) I hereby assign all and every rights in the copyright to this Work to the University of Malaya ("UM"), who henceforth shall be owner of the copyright in this Work and that any reproduction or use in any form or by any means whatsoever is prohibited without the written consent of UM having been first had and obtained;
(6) I am fully aware that if in the course of making this Work I have infringed any copyright whether intentionally or otherwise, I may be subject to legal action or any other action as may be determined by UM.

Candidate's Signature Date

Subscribed and solemnly declared before,

Witness's Signature Date

Name:

Designation:

ABSTRACT

Offshore steel jacket structures consist primarily of tubular members and associated joints. Tubular members have been widely used due to their excellent properties in respect of resistance in compression, tension, bending and torsion forces. In computer analysis, connections between the elements are assumed to be rigid, which means that there would be no axial rotational or deflection at the end of the secondary member against the main member's axis. Nevertheless, the tubular joints have a remarkable amount of flexibility in the elasto-plastic range. Designing these structures based on realistic conditions is important due to the high costs of design and construction. Several studies based on numerical and experimental work have been done on tubular joints in 2-Dimensional states. In this study, finite element (FE) modelling of tubular connections is carried out in 3-Dimensions, to account for the actual platform performance.

In this study a 3-D model of a fixed steel platform existing in the Persian Gulf has been modelled using a nonlinear finite element program. The joints and platform members are modelled using a SHELL element and PIPE element, respectively, through ANSYS software. Moreover, to investigate the effect of joint flexibility on these models, the analysis of rigid and flexible models of the platform and comparison of their static and dynamic behaviours are presented. In addition, push-over analyses were carried out for several joints with and without Joint-cans and also a comparison of $M-\theta$ curves in these two conditions is reported.

The result of the non-linear static analysis shows that the static response of the structure changed considerably with respect to the joints' flexibility in the nonlinear range. The modal features of the structure with flexible joints have significant differences

compared to the rigid joints structure. In addition, performing the dynamic time-history analysis and investigating the exact effect of flexibility based on the flexible model shows that base shear values are reduced by about 30% compared to the rigid model. It is proven that local joint restraint has a considerable effect on the nonlinear static and dynamic behaviour of offshore structures.

ABSTRAK

Struktur keluli untuk pelantar luar pesisir terdiri daripada anggota keratan tiub dan sambungan. Anggota keratan tiub telah digunakan secara meluas kerana ciri-ciri yang cemerlang seperti rintangan dalam mampatan, ketegangan, daya lenturan dan kilasan. Dalam analisis komputer, kebiasaannya sambungan di antara elemen diandaikan sebagai tegar, iaitu tidak akan ada putaran paksi atau pesongan pada hujung anggota sekunder terhadap paksi anggota utama. Walau bagaimanapun, sambungan tiub mempunyai fleksibiliti yang luar biasa dalam julat elasto-plastik. Merekabentuk struktur ini berasaskan kepada keadaan yang realistik adalah penting kerana kos yang tinggi bagi rekabentuk dan pembinaan. Beberapa kajian yang berdasarkan kajian berangka dan eksperimen telah dilakukan pada sambungan tiub dalam 2-dimensi. Dalam kajian ini, kaedah unsur terhingga (FE) bagi sambungan tiub dijalankan dalam 3-dimensi, bagi mengambil kira prestasi platform yang sebenar.

Didalam kajian ini sebuah model 3-D telah di bangunkan bagi pelantar keluli tegar yang telah sedia ada di Teluk Parsi menggunakan analisis tak terhingga tak linear. Sambungan dan anggota platform dimodelkan oleh unsur SHELL dan elemen PAIP masing-masing melalui perisian ANSYS. Selain itu, untuk menyiasat kesan fleksibiliti sendi pada model ini, analisis model tegar dan fleksibel bagi platform dan perbandingan tingkah laku mereka secara statik dan dinamik dibentangkan. Di samping itu, analisis push-over telah dijalankan bagi beberapa untuk sendi dengan dan tanpa ‘joint-can’ dan juga perbandingan lengkung $M-\theta$ dalam kedua-dua keadaan dilaporkan.

Hasil bagi analisis statik tak linear menunjukkan bahawa sambutan statik struktur jauh berubah disebabkan oleh kesan fleksibiliti sendi dalam julat tak linear. Ciri-ciri ragaman struktur dengan sendi fleksibel mempunyai perbezaan yang signifikan berbanding dengan sendi struktur tegar. Sebagai tambahan, analisis dinamik ‘time-history’ dan

kajian ke atas kesan fleksibiliti sendi menunjukkan bahawa nilai ricih asas bagi model fleksibel berkurangan kira-kira 30% berbanding dengan model tegar. Ia membuktikan bahawa kekangan pada sendi tempatan mempunyai kesan yang besar ke atas tingkah laku statik dan dinamik tak linear bagi struktur luar pesisir.

ACKNOWLEDGEMENTS

In the name of Allah, most gracious, most merciful, all praise and thanks are due to Allah, and peace and blessings be upon His Messenger and relations.

Foremost, I would like to express my sincere gratitude to my advisors, Dr. Zainah Ibrahim and Dr. Norhafizah Ramli@Sulong, for their continuous support during my study and research, for their patience, motivation, enthusiasm, and immense knowledge. Their guidance helped me throughout the time of the research and the writing of this thesis. I could not have imagined having better advisors and mentors for my study.

Besides my advisors, I would like to thank my parents for supporting me spiritually throughout my life.

CONTENTS

LIST OF FIGURES

LIST OF TABLES

LIST OF SYMBOLS

A	Sectional area
C	Shear area
C_1, C_2, C_3 , C_4	Integration constant
d	Brace diameter
D	Chord diameter
E	Modulus of elasticity
VP	Imposed punching shear
f	The nominal axial tension and in-plane and out-of-plane bending tension in the secondary member
Mu	Permissible capacity for the secondary member under the bending force
Qu	Ultimate resistance factor
P	Axial force
P	Force vector
Q	Matrix that converts end forces P to integration constants C
R	Discrepancy ratio
ρ	Water density
T	Brace wall thickness, time
T	Chord wall thickness
V	Shear force
v	Transverse displacement v(x,f)
Pa	Allowable capacity for brace axial load
Ma	Allowable capacity for brace bending moment
V_p	Punching shear stress

Z	Body force per unit volume in z direction
α	Non dimensional parameter 2L/D
β	Non dimensional parameter d/D
δ	Transverse displacement
x	Displacement vector
σ	Normal stress
τ	Shear stress

LIST OF ABBREVIATIONS

API	American Petroleum Institute
CPU	Central Processing Unit
CQC	Compound Perfect Square method
FE	Finite Element
FEM	Finite Element Method
FS	Factor of Safety
EI	Bending Rigidity
IBM	In-plane Bending Moment
IPB	In-plane Bending
LAT	Lowest Astronomical Tide
LRFD	Load & Resistance Factor Design
NF	Natural Frequency
OPB	Out of Plane Bending
PC	Personal Computer
PCG-Solver	Pre-conditioned Conjugate Gradient Solver
PEER	Pacific Earthquake Engineering Research
PSMD	PEER Strong Motion Database website
SPD	South Pars Oil and Gas Field
SRSS	Square Root Sum Of Squares method
TIN	Type Intersection Number

CHAPTER I

INTRODUCTION

1.1 Introduction

Oil production in the offshore fields has a long history. The oil industry started with drilling the first oil well from a wooden dock in offshore shallow waters in 1931 and has developed rapidly since then. The first steel offshore platform was built in the Gulf of Mexico in 1947 and soon this kind of offshore platform started to be used around the world.

Tubular elements have many applications in engineering structures. Elements with rounded and rectangular sections are used in onshore and offshore structures, space trusses, telecommunication and power transmission towers, the load carrying structure of cranes, and steel elevated tanks. The tubular sections are very economical and are considered superior to other sections for different reasons, such as high rotational strength (resistance), symmetry of section properties, the possibility of welding their connections, simplicity of shape, reduced painting area, good appearance and reduction of the area exposed to corrosion. Moreover, the tubular sections show the best behaviour against hydrodynamic and drag forces compared to other existing sections.

The rounded (circular) sections not only have high torsional stiffness, they also show a similar buckling strength in all section axes, and from a structural point of view are the most appropriate sections to form the spatial frame elements.

After World War II and the expansion of the oil industry offshore, the need to use tubular sections, which are the best option in building offshore platforms, has increased.

At that time, no knowledge existed about the role and performance of welded tubes as a structural connection. Thus, several studies were carried out on tubular structures and their connections, most of which were based on offshore platform design requirements. Meanwhile, one of the aspects that was taken into consideration was the flexibility of tubular joints.

In the computer analyses of structures with tubular elements, like offshore oil platforms, the connections between the elements were considered rigid using analytical methods. The ideal approach for making tubular joints is full-penetration welding the tubular elements, which causes the resulting joint to be classified as a rigid joint that is subject to axial loads as well as bending moments. This implies that the angle between the platform elements does not change after the structure is placed under loading. However, in real conditions, some local deflections are created in the connecting area of the main member under the imposed loads from the secondary member. This indicates that the tubular joints have a remarkable amount of flexibility in the elasto-plastic range. Therefore, the results of analyses based on joint rigidness differ to a great extent from the actual behaviour of the structure. These differences are observable in structure deformation, distribution of inner forces, the buckling forces of the members, and also the natural frequency of a structure, especially in the case of 3-D structures. Therefore, taking the flexibility effects into account appears crucial in terms of the overall analysis of a structure. As the high effect of joint flexibility on the results of tubular structure analysis was specified, it attracted the attention of many researchers and various studies and tests were carried out on tubular joints. The results obtained from the research studies can be generally categorised into two types. The first category is the formula and empirical equations obtained from the tests and observations, and the second one is the method for modelling the joints so that the flexibility effect is taken into account. These

methods can be divided into two main groups: modelling the joint as a structural member, or modelling by the finite element method.

1.2 Problem Statement

Generally, the tubular joints of a platform are considered rigid in offshore platform analyses and it is often assumed that the member deformations in the connecting areas are similar to each other. However, in actual conditions, the connecting points in members have significant elasto-plastic flexibility. Therefore, if a platform is modelled with rigid connections (joints), the results will be unrealistic. However, a finer estimation of the internal forces in a jacket type platform can be achieved by incorporating the flexibility of joints in the analysis.

Although several studies and experiments have been done on pipe connection platforms in 2-Dimensional states, modelling in 3-D is deemed important to obtain accurate results.

On the other hand, the development of offshore structures in deep waters and the high costs of designing and constructing these structures are further reasons for the need to design these structures based on realistic conditions. With regard to the fact that Iran is an oil-rich country and the significant role of offshore platforms in the oil industry, studying the behaviour of offshore platforms seems necessary.

1.3 Objectives

This study aimed at investigating the behaviour of offshore platforms using the finite element method (FEM) by considering the effect of the connections' flexibility in 3-dimensional states. The specific objectives are:

a) To investigate the effect of Joint-can on joint flexibility by comparing $M-\theta$ graphs using static analysis.

b) To perform nonlinear static analysis on a modelled platform considering joint flexibility and compare it with the rigid joints model.

c) To investigate the effect of joint flexibility on the two modelled platforms by performing modal analysis.

d) To carry out nonlinear dynamic analysis on a modelled platform considering joint flexibility and compare it with the rigid joints model.

1.4 Scope of Work

The purpose of the present study is to investigate offshore platform behaviour in respect of the flexibility effect of the joints in a 3-D condition using the finite element method. An attempt is made, firstly, to investigate the effect of Joint-can on the flexibility of three types of tubular joints by performing static analysis and $M-\theta$ curves are drawn in different conditions for comparison.

Secondly, to provide a 3-D model of one fixed steel platform existing in the Persian Gulf in which the joints are modelled using the SHELL element and the platform members are modelled using the PIPE element. The deck, piles and the Joint-can are taken into account in this modelling. Another platform is also modelled as 3-D with rigid joints and the modal, dynamic and static behaviour of the two platforms are compared.

In the current study, ANSYS software version 11 is used, which operates with finite element methods to analyse and design engineering systems.

1.5 The Organisation of The Thesis

The present thesis investigates the effect of the flexibility of tubular joints on the nonlinear responses of offshore platforms under the effect of earthquake loads. It is divided into 5 chapters.

Chapter 1 presents an introduction that provides a brief description of the history of offshore platforms, and the objectives and purpose of this study.

In chapter 2, which includes general information about offshore platforms and tubular structures, the previous research on tubular joints and also some information about different common analyses and code considerations in these structures is reviewed.

The modelling of a structure using flexible tubular joints and the analysis of platforms are explained in chapter 3. In this chapter, the definitions and relationships of finite elements, and the theories applied in modelling are investigated and the joints of a platform in the Persian Gulf are modelled with and without a Joint-can.

Chapter 4 concerns the analysis of rigid and flexible models of the platform and a comparison of their static and dynamic behaviours. It also obtains the dynamic properties and $M-\theta$ curves for several joints, with and without Joint-cans, and compares the flexibility of joints in these two conditions.

Finally, in chapter 5, the findings of the study are summarized and suggestions for future studies are presented. Chapter 5 thus concludes the study.

CHAPTER II

LITERATURE REVIEW

2.1 Introduction

Offshore platforms are built with the aim of producing oil and natural gas. The contribution of oil platforms to oil production in 1988 and 2000 was 9% and 24% of the world's total consumption, respectively. Today about 30% of the world's needed energy is supplied through offshore hydrocarbon resources. Using offshore oil and gas resources has been developing continually in recent years so that the installation of offshore platforms in deep waters and adverse environmental conditions is economically well justified these days.

Historically, the first offshore drilling was performed off the coast of California in 1896 using wooden posts. In the early 1930s, wooden platforms were used for building offshore platforms for the first time, and, in 1947, the first metal (steel) platform was installed 6 metres under water in the Gulf of Mexico. Iran, which is located on the coast of the Persian Gulf, the Oman Sea and the Caspian Sea, and possesses massive oil and gas resources in these areas, started to use these energy resources from the 1960s. Today the offshore platforms of the oil and gas industries are used for different purposes, such as exploration, drilling, production and accommodation. Regarding the huge costs of the construction, installation and promotion of these offshore platforms, an attempt has been underway during recent years to investigate the performance, analysis and design of these structures in terms of the lateral loads. Different types of offshore platform are shown in Figure 2.1. These platforms can be classified as: 1, 2) conventional fixed platforms; 3) compliant tower; 4, 5) vertically moored tension leg and mini-tension leg

platform; 6) spar; 7, 8) semi-submersibles; 9) floating production, storage, and offloading facility; and 10) sub-sea completion and tie-back to host facility.

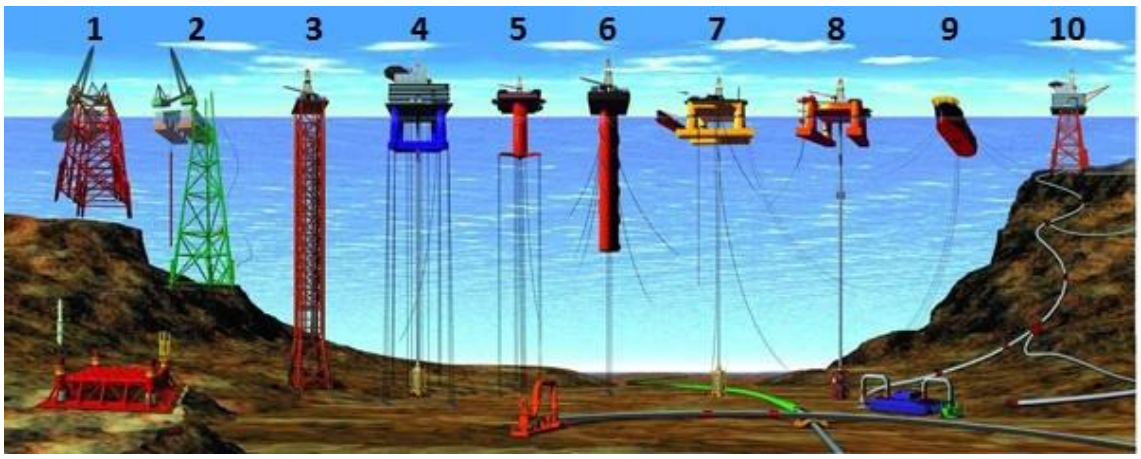

Figure 2.1: Types of oil platform and rig (Boland, 2013)

2.2 Fixed Platforms

Figure 2.2 illustrates a fixed extraction platform used in waters with a medium depth in the North Sea. These platforms consist of a structure made from steel tubes, which is fixed to the sea floor by some piers and the upper part of the platform includes drilling equipment, extraction, accommodation, cranes and other parts like a helicopter pad and rescue equipment. The crude oil and natural gas are transmitted to the upper part of the platform and after initial refinery treatment are transported to the carriers or onshore refinery or distribution units via pipes. The main elements can be connected together in K, T, Y or X shapes and the size (diameter) of the elements can vary in these types of joint. Some examples of the structures of such platforms will be shown in the following sections. The designer of the offshore platform should take into consideration the many limitations existing during the life of a platform. The lifespan of a platform includes different designing stages, building, launching, equipment installation, pile driving, and finally extraction and promotion stages. These stages usually last from 10 to 25 years and the platform should be well maintained during this time. Once the promotion stage has finished, the platform should be removed, thus respecting the natural ecology of the

sea so that it does not damage the natural environment. The complexity of each stage in a platform's lifespan can be perceived by studying its launching method.

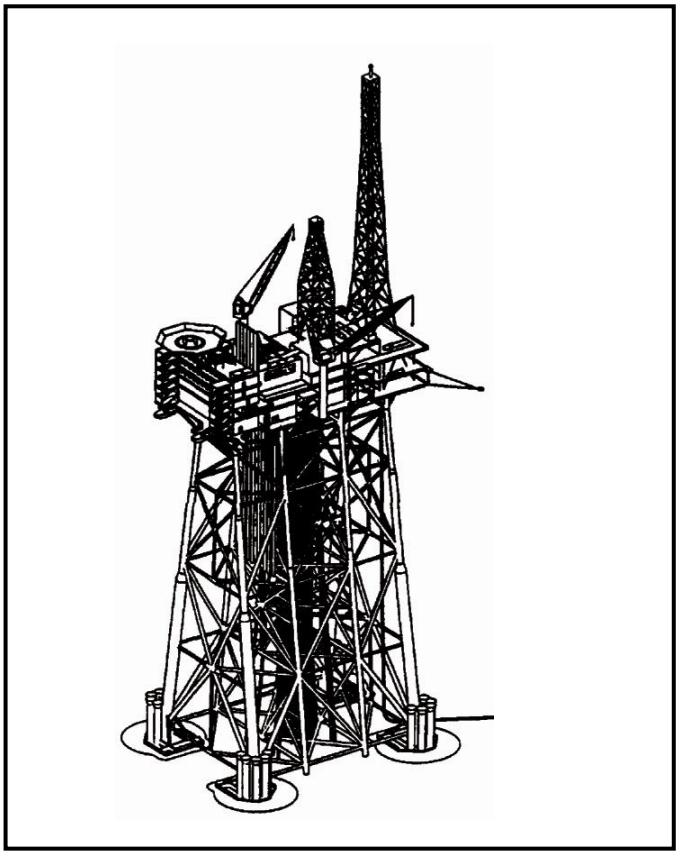

Figure 2.2: An example of a drilling platform (E.S.D.E.P, 1994)

The recent introduction of huge floating cranes, which are of the partially-submerged type and have a high capacity, has had a great impact on the common methods of launching and installing the platforms. The big size of these floating devices makes it possible for the cranes to have a jack-up power of around 12,000 tons. Therefore, it is possible to make many connections related to the construction and installation of the machinery on land and then install these bulky sections onto the platform using the above mentioned cranes. This results in reducing the cost and time of installation and eventually leads to faster production of oil in the fields.

The use of fixed production platforms in deep waters and adverse sea conditions requires the inspection and probable repair of the underwater parts of the platform. The

inspection and repairs are very costly and should be performed by special modern equipment (E.S.D.E.P, 1994).

The fixed platforms are usually installed in shallow waters. Today, although this type of platform has also been installed at a depth of 315.5 metres, it is usually used at depths of about 100 metres. The nomination of the platform as a template is because the legs of the platform are used as templates for installing the piles. This type of platform is also referred to as a ‘jacket platform’, which is shown in Figure 2.3, and consists of the following sections:

a. The deck of the platform: the deck is a 3-D space truss on which all the equipment and instruments above the surface of the water are installed.
b. The jacket of the platform: the jacket is a 3-D space truss consisting of steel (usually tubular) elements (members) under water. The main function of this section is to receive and transmit the environmental loads (such as waves and sea streams) to the foundation system, also as a template for conducting and covering the piles during pile driving, and sometimes for direct conducting and transmitting the deck loads to the foundation system of the structure.
c. The piles: the piles in fact form the foundation system of the platform. All deck and environmental loads imposed on the platform are finally transmitted to the ground through the piles. The foundation of the base (pier) of the platform is built using tubular steel piles that are open on one end and have a diameter of up to 2 metres. The piles are rammed (driven) 40-80 metres and in some cases up to 120 metres into the seabed.

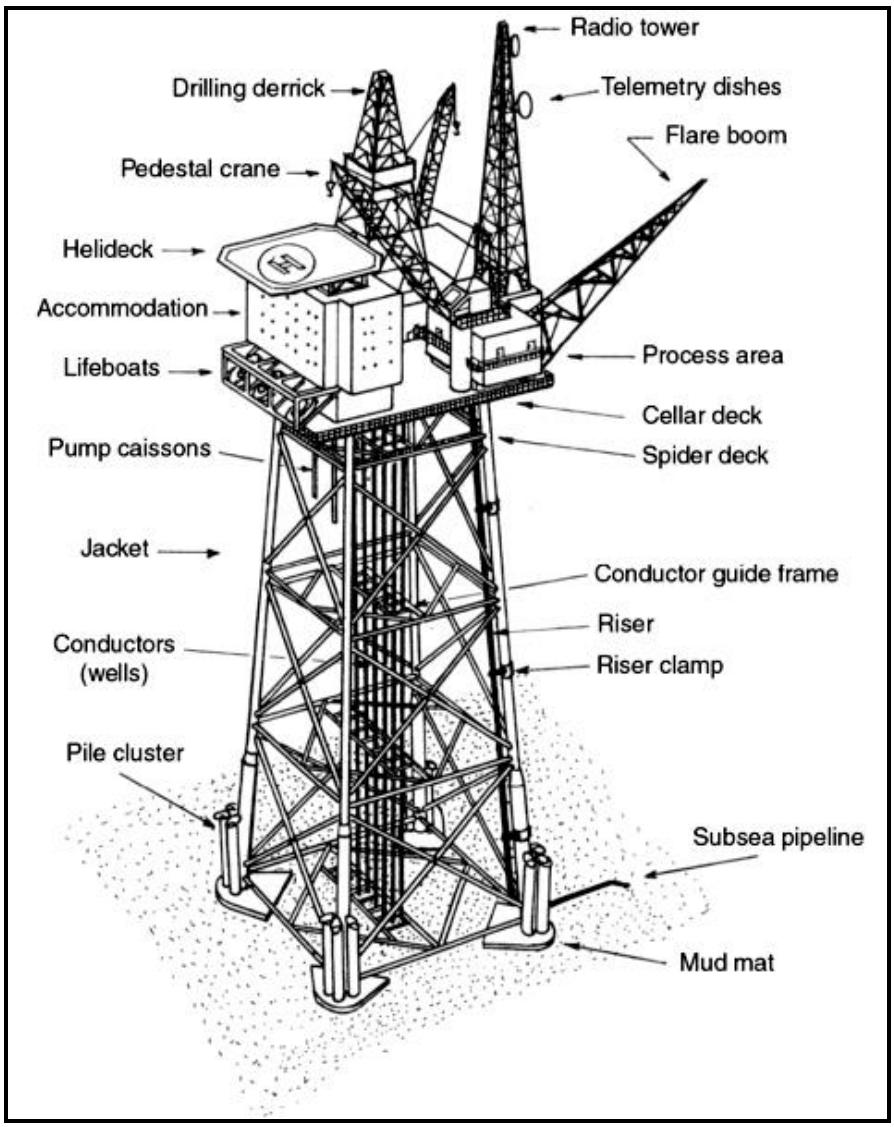

Figure 2.3: Jacket type platform sections (Arnold, 2007)

Most of the oil platforms are of the steel jacket type with piles in which the steel deck is installed on the jacket. The fixed offshore platforms possess a special advantage. The cost of installation of this type of platform is relatively low, they are stable and the drilling, production and other operations can be performed on them in the same way that they are done on land (Arnold, 2007).

The development of the drilling fleet around the world has been compatible with the increasing depths of water in which drilling has been carried out. This is depicted in Figure 2.4. In Figure 2.4, the first graph shows the maximum depths for drilling from

1940 to 2009. It can be seen that from 1964 to 2009, the achieved depths have increased rapidly, reaching from 100 m to 3047.9 m. Of course there have been some drillings in very deep waters just for geological study purposes.

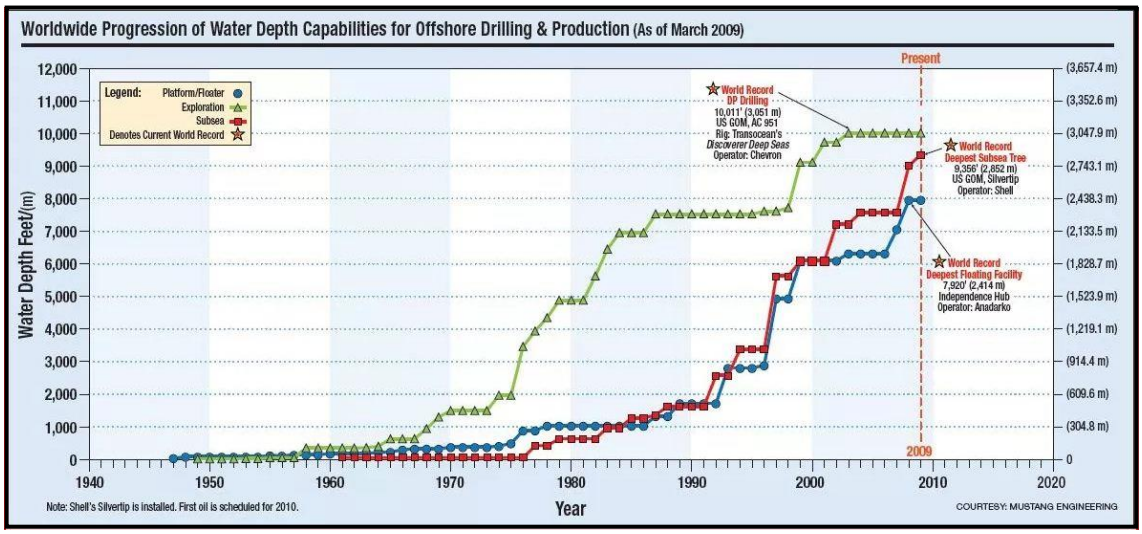

Figure 2.4: Worldwide progression of water depth capabilities for offshore drilling and production (Carlyle, 2012)

The depth of waters in which drilling has been performed indicates the needs of oil production in the future. The oil platforms should be capable of developing drilling and separating crude oil from gas, water and sand and also in cases where there is insufficient pressure in the reservoir (tank) to push up (jack up) the crude oil, a gas jack-up is needed. Water injection might also be necessary to increase the pressure in the reservoir and produce more oil. With the creation of side wells (slanting/inclined), it is possible for platforms to use a bigger reservoir. All these issues and other requirements make the equipment installed on a platform so complex that we can regard it as a small-scale refinery. Therefore, the production depth is always slightly less than the drillable depth. Finally, because of the need for installing modern engineering devices on the platforms in deeper areas, the extractable depths have not increased as fast as the drillable depths. This can be seen in Figure 2.5, which illustrates the evolution of oil

platforms. These types of fixed platform are called jacket platforms. The Figure also shows the development of extractable depths from 1947 to 1978.

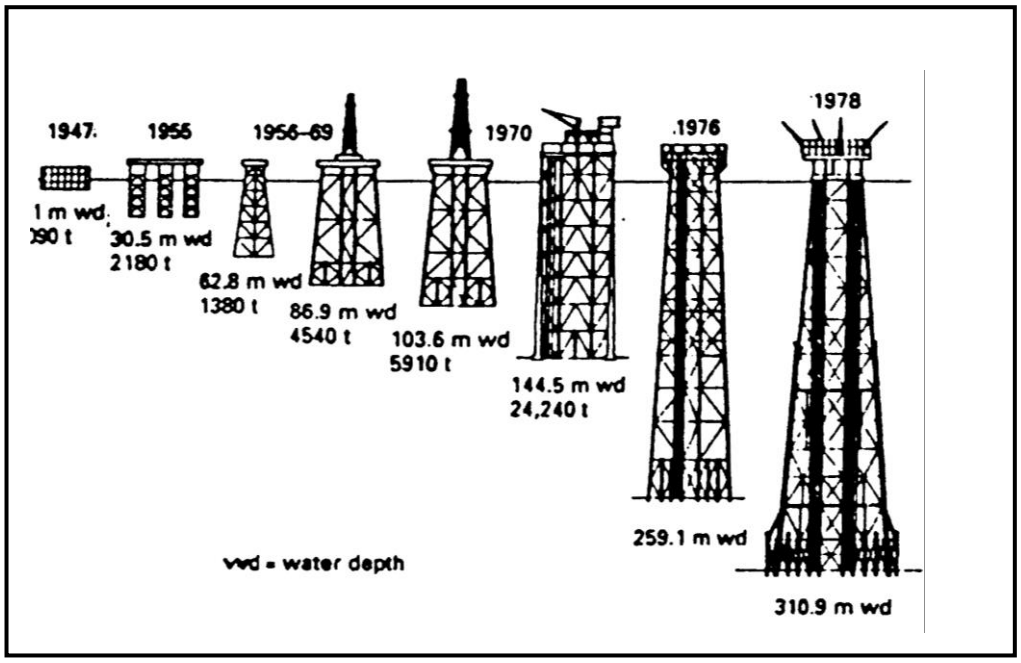

Figure 2.5: The evolution of oil platforms (Arnold, 2007)

2.3 Selecting an Appropriate Platform to be Installed in the Persian Gulf

Basically, the depth of water in the Persian Gulf is relatively low and the water column in which the platforms are currently installed is from a depth of 25 metres to a maximum of 72 metres. Overall, the average water depth in the Persian Gulf is about 45 metres. This is about 70 metres in the deeper areas and strip, and even deeper areas mostly with depths of about 80 metres hardly exist.

The fixed-type platforms have been recognised as the most appropriate platforms to be used in the Persian Gulf for the following reasons:

- Availability of the technology for their construction, transportation and installation
- Cost effective installation in depths of less than 100 m

- Low cost of installation
- Stability against the waves and no significant displacement or vibration in the deck during the production period
- Capability of being maintained well regarding the atmospheric and water conditions in the Persian Gulf
- Platform manufacturing sites in the area

2.4 Tubular Elements

Tubular elements have many applications in different structures. Elements with circular and rectangular sections are used in coastal and offshore structures, space trusses, telecommunication and power transmission towers, the load-bearing structure in cranes, and circular recreational structures in parks, etc. Tubes are very economical and are superior to other existing sections for different reasons, such as their high rotational resistance (strength), symmetry of section properties, welding capability of the joints, simple shape, less area to paint, more attractive appearance, and less area exposed to corrosion. Moreover, tubular elements show the best behaviour against hydrodynamic and drag forces compared to other sections. The rounded (circular) sections, besides having high torsional stiffness, have an equal axial flexural strength throughout the whole section and are structurally the most appropriate sections to be used as space frame elements.

Such elements with circular (rounded) sections are usually used in coastal structures, especially in offshore platforms. These kinds of platform are utilised for different oil production purposes. Their applications range from oil exploration and production to personnel housing in the oil industry. One type of platform is called the fixed steel platform, which is extensively used by Iran and other Gulf States in oil production facilities in the Persian Gulf.

This fixed platform is composed of three major parts. The first part, which is built at the top of the structure, is known as the deck of the platform. The second part is the jacket or the base, which is composed of tubular elements and a wind brace (bracing). The last part of the platform is the piles through which the imposed load to the platform is transferred into the ground.

Tubular joints are used in single- and double-plate forms in different structures. Tubular joints refer to the connections in which the elements and the imposed loads are placed on the same plate, and multi-plate joints are the connections in which the connection elements and imposed loads are not located on the same plate. In the joints, those elements that are connected are referred to as secondary members or ‘braces’ and the main member is called the ‘leg’. As shown in Figure 2.6, these joints are categorised for any kind of loading based on the shape of the secondary member and the loading pattern.

For instance, in a K joint the punching force in a secondary member must be in balance with the loads of the other secondary members on the same plate and the same point of the connection. In addition, in the T and Y joints, the punching forces must be equal to the shearing force in the main member. In the X joints, the shearing force is transferred from one part of the main member to a secondary member on the other side of the joint. These joints can also be combined to form other joints (API, 2000).

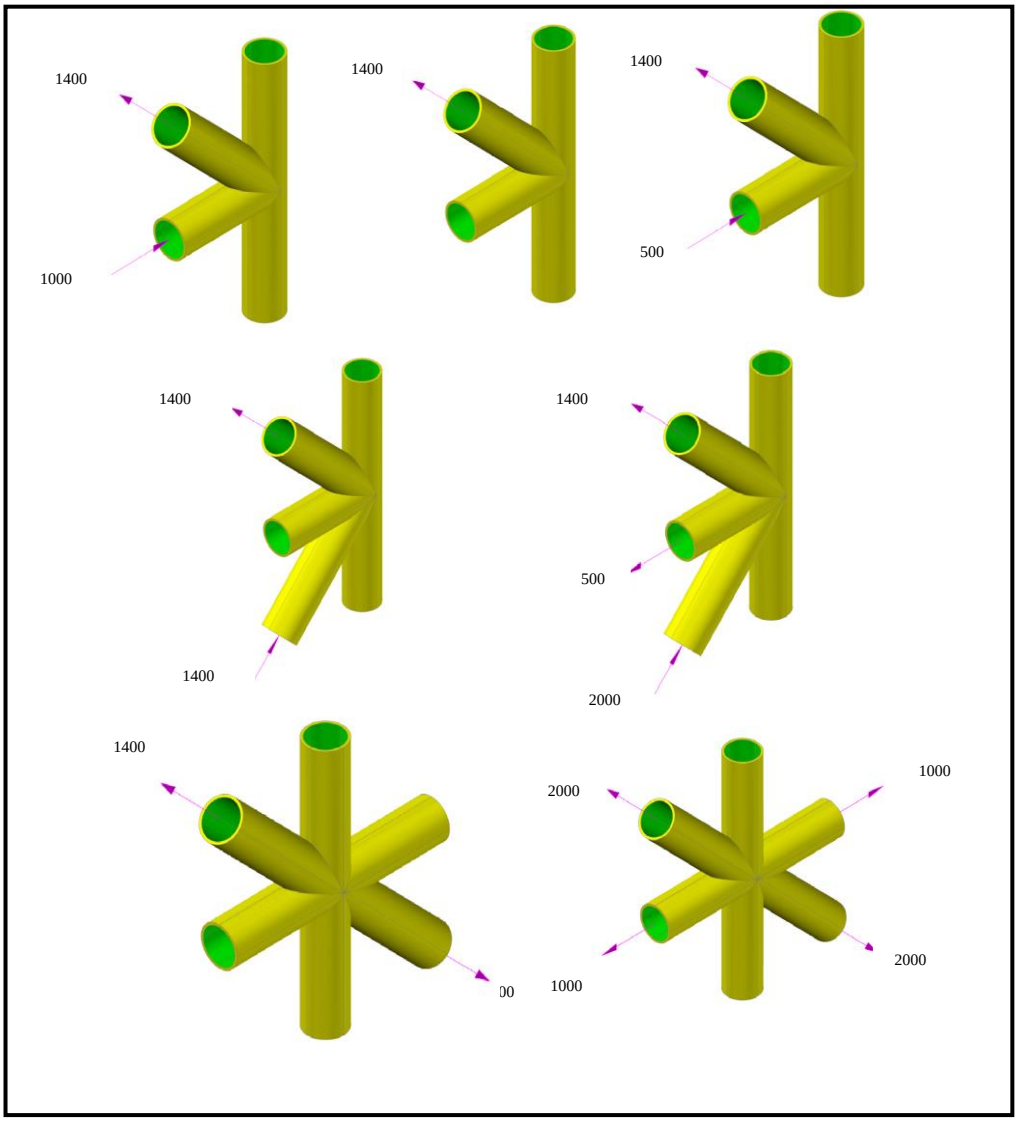

Figure 2.6: Different types of tubular joint (API, 2000)

Dimensionless parameters, which are specified and calculated according to the geometry of the joint, play an important role in the calculation of joint strength (resistance) and specifications. These parameters include β (diameter coefficient), γ (member slenderness ratio), τ (Thickness coefficient). As illustrated in Figure 2.7, the parameters for rounded (circular) and tube sections depend on the geometric properties, such as D (main member diameter), d (secondary member diameter), T (main member thickness), t (secondary member thickness**)**, θ (the angle between the main and secondary member), l (length of secondary member), L (length of main member), and g (the gap between the main and secondary member).

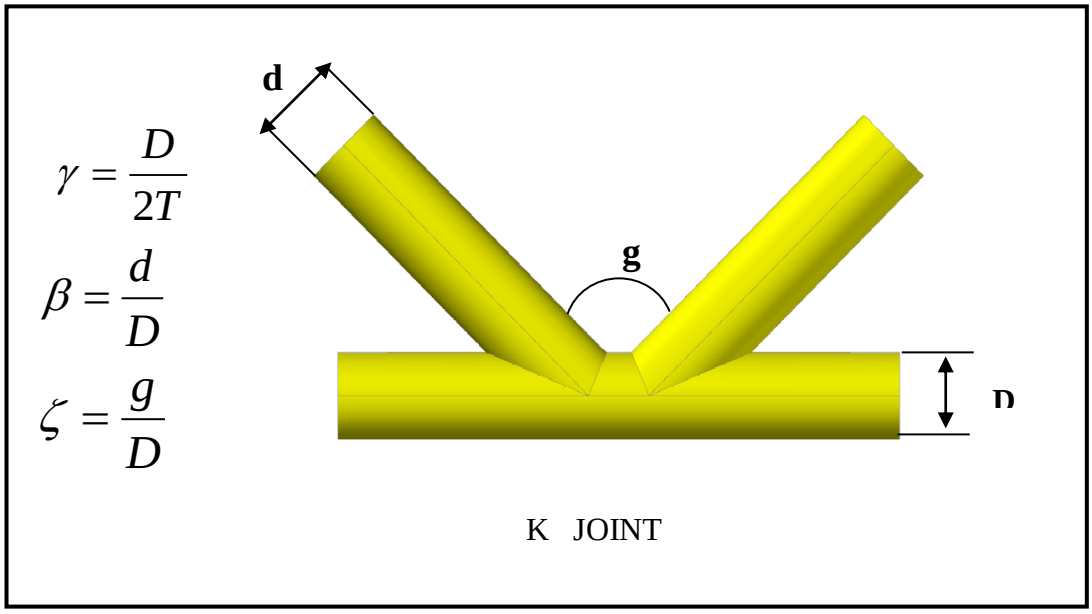

Figure 2.7: Geometric parameters specifying tubular joints: K joint (API, 2000)

Tubular joints are classified into four categories as follows (UEG, 1984):

1) Simple welded joints,

2) Complex welded joints,

3) Cast steel joints, and

4) Composite joints.

This classification is not firm, but is generally accepted. Simple joints are those without any stiffener, gusset plate, diaphragm or grout. In multi-braced simple joints the braces do not overlap. To strengthen a simple joint, the chord section is typically thickened in the connection zone. This section with higher strength is named the Joint-can.

The term complex is assigned to the following joints:

1) Joints with uniplanar or multiplanar overlapping brace members,

2) Joints with internal stiffeners or diaphragms, and

3) Joints with external stiffeners.

Simple joints have lower strength and stiffness than complex joints. Some examples of complex joints are shown in Figure 2.8.

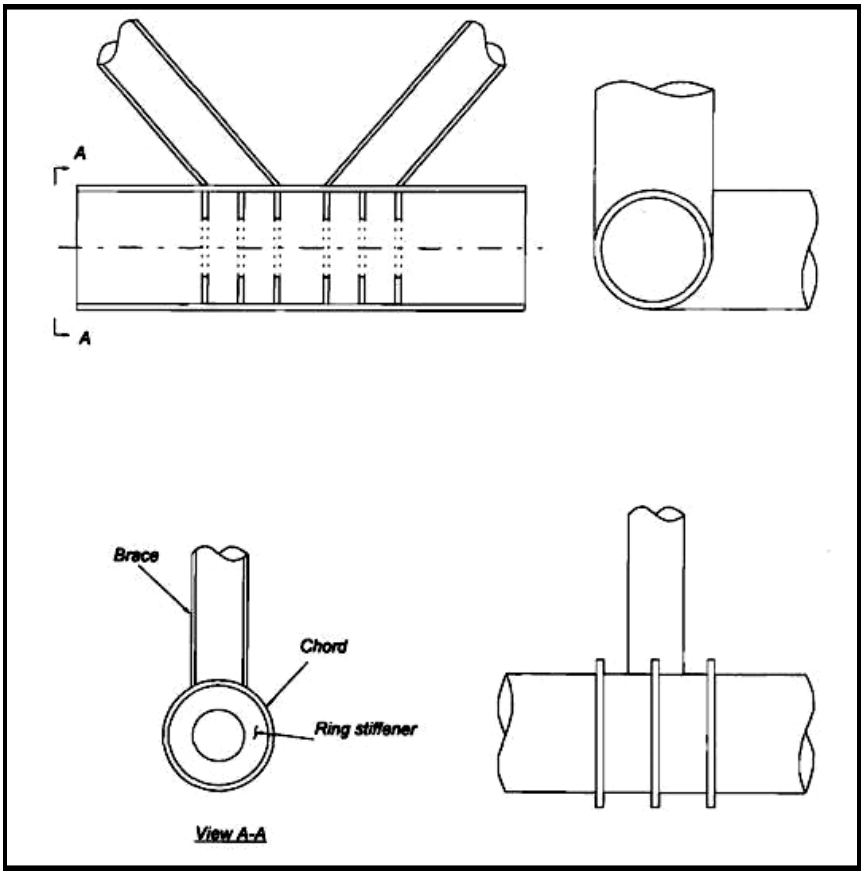

Figure 2.8: Complex joint examples (UEG, 1984)

Cast joints are made by a casting process in which the brace and chord are cast together. Therefore, there is no welded connection between the brace and chord, creating better shapes of fillet. Cast joints are potentially stronger than the welded joints.

Composite joints are those filled fully or partially between the leg and the pile passing through the leg, with concrete. A double-skin grout reinforced joint, which is placed in the latter group of grouted joints is shown in Figure 2.9.

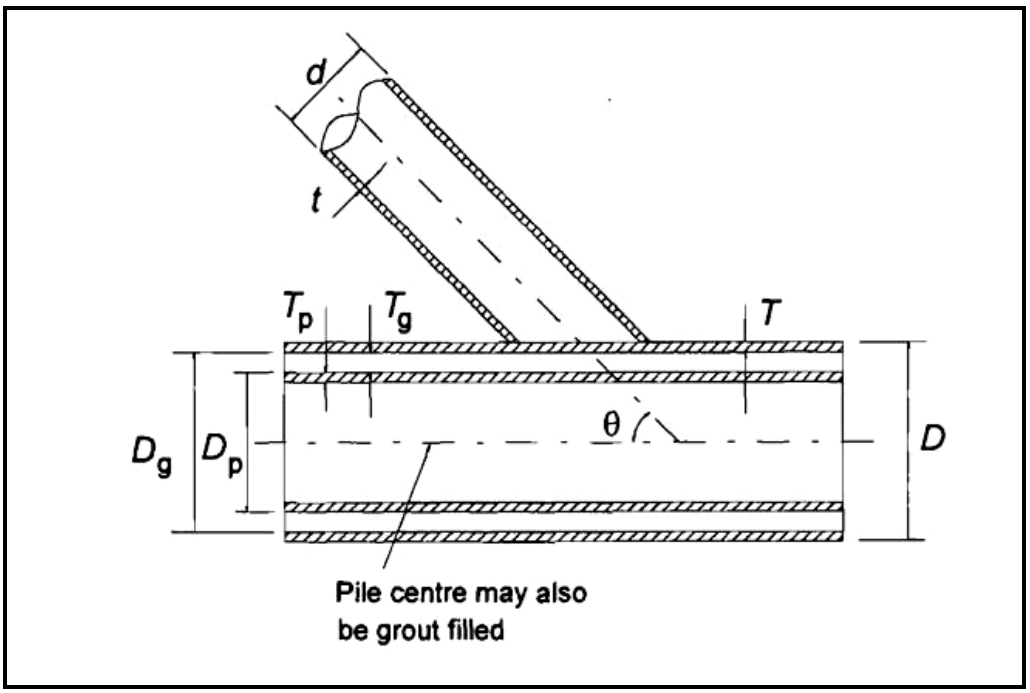

Figure 2.9: Concrete grouted joint (UEG, 1984)

2.5 Tubular Joint Failure

Since tubular joints used are of geometrically various types, their responses to axial loads and bending moments also vary to a great extent. In fact, the form of the joint failure depends on the joint type, the geometric parameters specifying that joint, and the loading conditions.

As shown in Figure 2.10, the tested joints are very simple ones, i.e. T and DT types only. In addition, although the loads are only imposed axially (tensile and compressive), the joints respond differently to different loads. The typical trend of failure of a tubular joint under tensile loading includes the main member's yielding around the secondary member, and, finally, the deflection of member sections (Skallerud & Amdahl, 2002) (Skallerud et al., 2002).

Imposing a tensile load on the joint brings about stress in the joint section. As the load increases, the first crack is caused on the host point, which, eventually, results in the total separation of the main member from the secondary member.

Failure under compressive loadings in Y/T joints and also in the Y/DT joints usually happens in the form of buckling and deflection in the plastic of the main member walls. The stiffness and capacity of the DT/X joints are less than those of the Y/T joints but the deflection form is similar in all these joints (Skallerud & Amdahl, 2002)

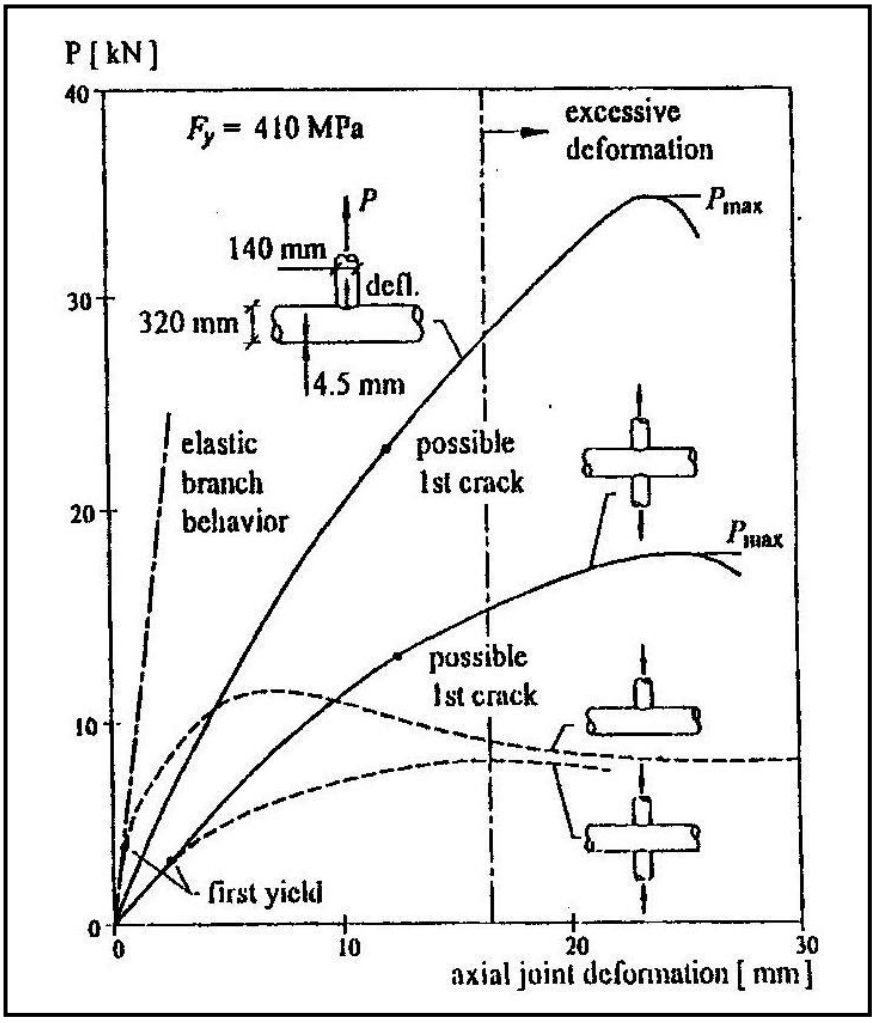

Figure 2.10: Tubular joint response to axial loads (Skallerud & Amdahl, 2002)

The failure mechanism of K joints under axial loading, as one secondary member is under tension and the other one is compressed, depends mostly on the gap between the two secondary members. In the case of large gaps, each member acts as two simple Y/T joints. As the gap becomes smaller, the joint resistance increases because the flexural stiffness of the main member in the gap between the two secondary members also increases.

Plastic deflection and failure in the main member resulting from the punching shear are the two main types of failure in these kinds of joint. For high β values, the main member section failure (shear failure) can take place in the gap between the two secondary members (Skallerud & Amdahl, 2002). However the punching shear clause has been removed from API since 2007 (API, 2007).

Overall, in different joints under flexural loading inside the plate, failure is caused by the rupture of the main member's wall in the section under tension from the secondary member, plastic bending and buckling in the wall of the main member under pressure.

The form of joint behaviour and failure differ under different loading patterns as reported by The European Steel Design Education Programme (E.S.D.E.P, 1994), and is given as follows:

1. Plastic failure in the main member section: in this case the section is broken on the plastic hinges or yielding lines (Figure 2.11).

2. Failure as a result of the plasticisation of the main member's surface for the K type joint when one member is under pressure while the other one is under tension (Figure 2.12 Mode A).

3. Punching shear failure on the main member's surface (Figure 2.12 Mode B).

4. Secondary member failure on the welded point (Figure 2.12 Mode C).

5. Failure caused by local buckling of the compressive secondary member (Figure 2.12 Mode D).

6. Shear failure of the chord (Figure 2.12 Mode E).

7. Failure caused by the yielding of the main member's wall (Figure 2.12 Mode F).

8. Failure as a result of the main member buckling close to the secondary member under tension (Figure 2.12 Mode G).

Failure type 2 is the most common mode of failure in K joints with low to medium β values, where the β value ranges from 0.6 to 0.8. Failure type 9 is common in overlap joints. Failure type 5 usually occurs in K joints with the β value approximating unity (1). Failure types 3 and 4 are common in K joints that have a bigger width ratio compared to their thickness (high $\frac{h_0}{t_0}$ or $\frac{b_0}{t_0}$). Failure type 1 usually occurs in rounded sections.

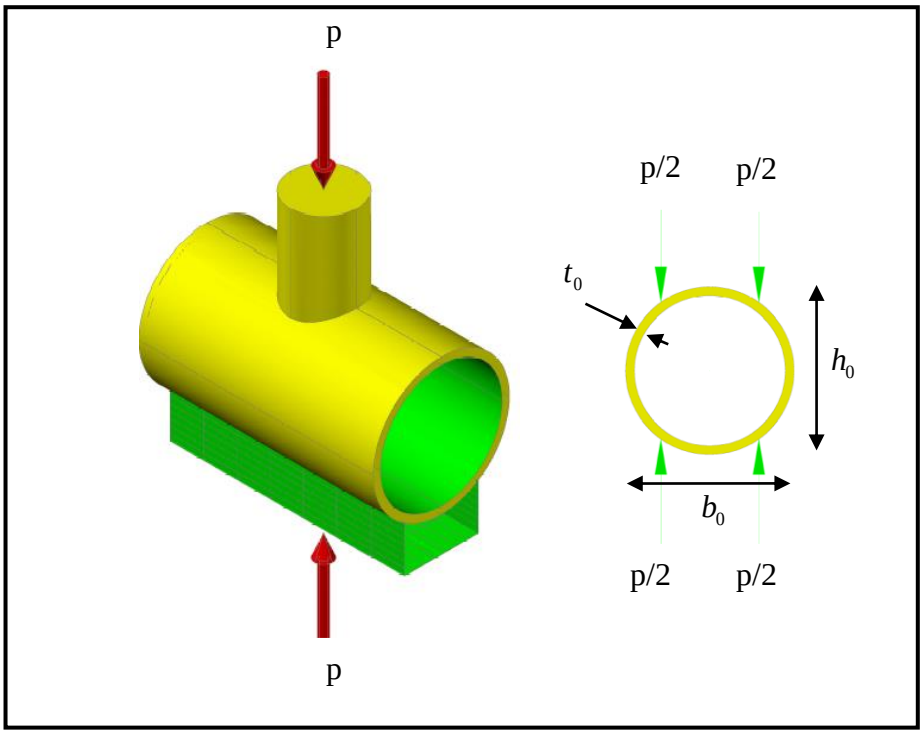

Figure 2.11: Failure in the plastic part of the main member (E.S.D.E.P, 1994)

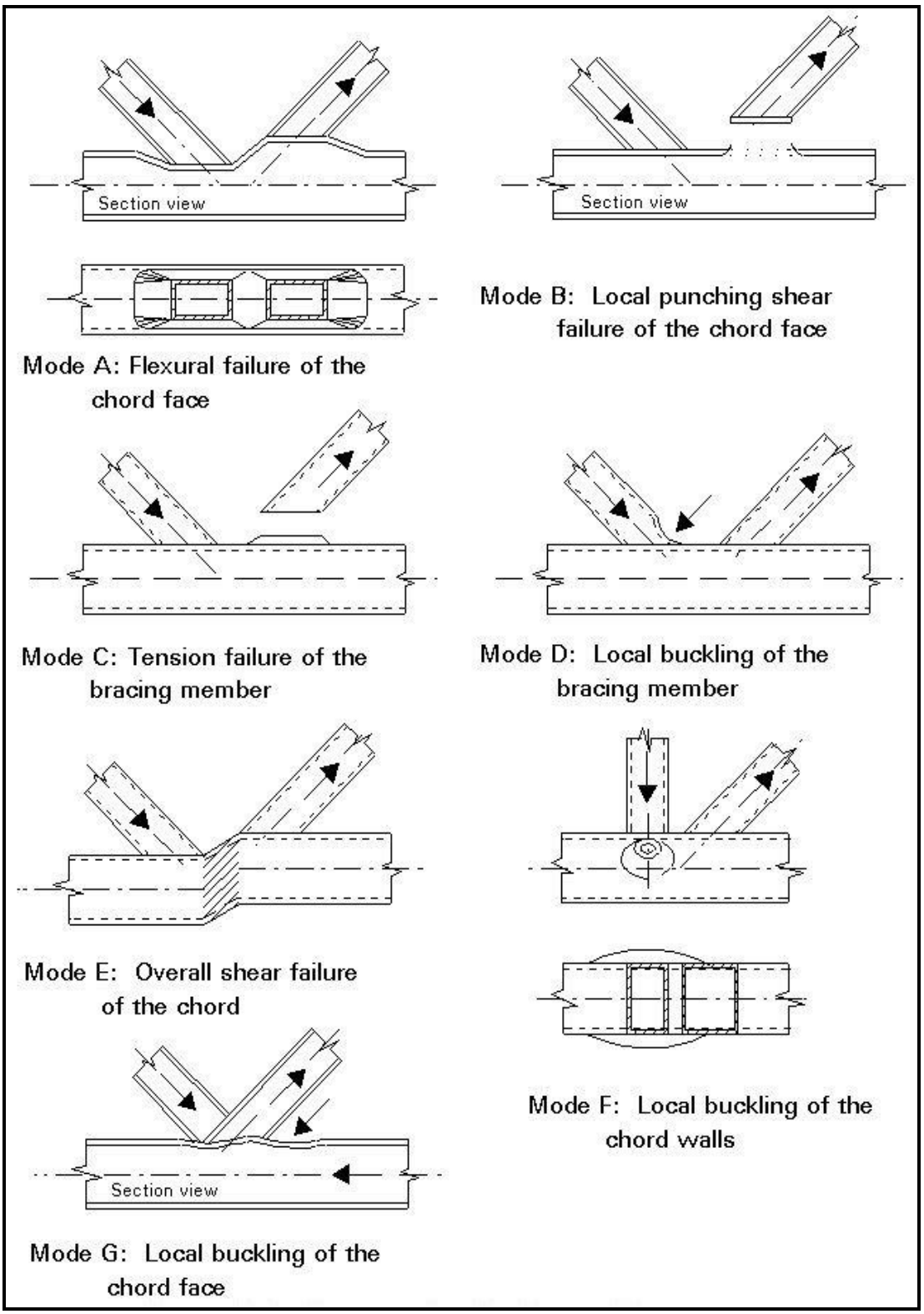

Figure 2.12: Failure modes for K and N type connections (E.S.D.E.P, 1994)

2.6 Codes on Ultimate Resistance and Designing Tubular Joints

The findings of the tests carried out on the failure in tubular joints indicate that a joint collapses under a force several times bigger than the force causing yielding in the first point. Regarding this, the ultimate resistance equations have been discussed in the API (2008), DNV (1977), AWS (1996), CIDECT (Kurobane et al., 2004) codes and HSE (1999) report. In the static strength method, the permissible loads are obtained based on interpreting the result of the ultimate load test and considering a sufficient safety factor. According to these codes, the imposed loads should not exceed the maximum permissible load. In the following section, the API code will be described. For a detailed description of the other design codes, source API 2A-WSD is recommended.

2.6.1 The API Code on Tubular Joints

According to these regulations, designing tubular joints is done based on the force values and the moments that exist in the bracing and main member's connecting point. The tubular joint resistance formula presented in this code is based on an interpolation of the ultimate resistance test results that are eventually an estimation of the minimum extreme. In the 18th publication of API in 1989, the joint members were designed according to the permissible stresses and in the 20th publication in 1993, the design based on LRFD was also authorised (API, 1993).

The geometric parameters affecting a simple tubular joint are shown in Figure 2.13.

A) According to API (1993), a joint should be controlled by either punching shear or nominal loads. They are calculated as follows: punching shear:

The imposed punching shear can be calculated by the following equation:

$$VP = \tau f \sin\theta \qquad (2.1)$$

in which f is the nominal axial tension and in-plate and out-of-plate bending tension in the secondary member. The permissible punching shear tension (stress) in the main member's wall is obtained through the following equation:

$$VP = Qq.Qf.\frac{F_{yc}}{0.6\gamma} \tag{2. 2}$$

This is a factor depending on the type of loading and geometry of the joint. The value of this parameter is given in Table 2.1, but it is also obtained as follows:

$$Qf = 1.0 - \lambda\gamma\beta^2 \tag{2. 3}$$

In which λ in the case of axial tension and bending in – and out of plane equals 0.03, 0.045, and 0.021, respectively.

$$A = \frac{\sqrt{\bar{f}Ax^2 + \bar{f}_{IPB}^{\,2} + \bar{f}_{OPB}^{\,2}}}{0.6F_y} \tag{2. 4}$$

So that $\bar{f}_{OPB}, \bar{f}_{IPB}, \bar{f}_{Ax}$ are the in-plane and out-plane nominal axial tensions and bending tensions in the main member in the condition of also having a combination of bending and axial tensions in the secondary member. Therefore, the following equation will apply:

$$\left(\frac{VP}{VPa}\right)^2 IPB + \left(\frac{VP}{VPa}\right) OPB \le 1.0 \tag{2. 5}$$

$$\left|\frac{VP}{VPa}\right|_{Ax} + \frac{2}{\pi} arcSin\sqrt{\left(\frac{VP}{VPa}\right)^2 IPB + \left(\frac{VP}{VPa}\right)^2 OPB} \le 1.0 \tag{2. 6}$$

B) The Nominal loads

The permissible capacity of a joint in terms of the existing nominal loads is calculated as follows:

$$Pa = Qu.Qf.\frac{F_{yc}.T^2}{1.7Sin\theta} \tag{2. 7}$$

$$Mu = Qu.Qf.\frac{F_{yc}.T^2}{1.7Sin\theta}(0.8d) \tag{2. 8}$$

Where pa is the permissible capacity of the secondary member under the axial force.

Mu is the permissible capacity for the secondary member under the bending force.

Qu is the ultimate resistance factor, which depends on the type of the joint.

The Qu value has been given in Table 2.2. A safety factor (coefficient of safety) equal to 1.7 for the joint static failure condition and 1.28 (coefficient of safety) in the excessive loading condition have been considered. One example is the storm load; in the case of having a combination of axial and bending loads on the secondary member, the following equation will apply:

$$\left(\frac{M}{Ma}\right)^2 IPB + \left(\frac{M}{Mu}\right)^2 OPB \le 1.0 \tag{2. 9}$$

$$\left|\frac{P}{Pa}\right|_{Ax} + \frac{2}{\pi} arcSin\sqrt{\left(\frac{M}{Ma}\right)^2 IPB + \left(\frac{M}{Ma}\right)^2 OPB} \le 1.0 \tag{2. 10}$$

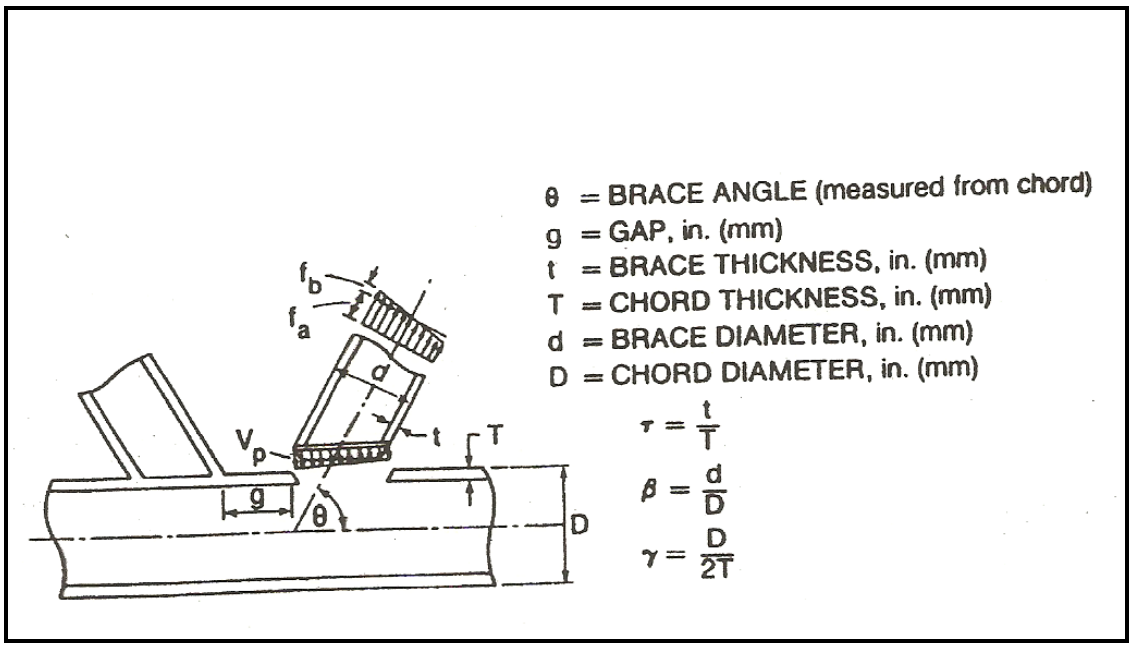

Figure 2.13: Parameters needed for designing API (1993)

Table 2.1: Calculation of Qg facto (API, 1993)

$Q_\beta = \frac{0.3}{\beta(1-0.833\beta)}$ for $\beta > 0.6$ $Q_\beta = 1.0$ for $\beta > 0.6$	$Q_g = 1.8 - 0.1\ g/T$ for $\gamma \leq 20$ $Q_g = 1.8 - 4\ g/T$ for $\gamma > 20$ but in no case shall Q_g be taken as less than 1.0

TYPE OF JOINT & GEOMETRY		TYPE OF LOAD IN BRACE MEMBER			
		Axial Tension	Axial Compression	In-Plane Bending	Out-of-Plane Bending
	Overlap **K** Gap	1.8 plus see 4.3.2 (1.10 + 0.20/β) Q_g		(3.72 + 0.67/β)	(1.37 + 0.67/β)Q_β
	T & Y	(1.10 + 0.20/β)			
	w/o diaphragms **CROSS** w/ diaphragms per 2.5.5c.4	(1.10 + 0.20/β) (0.75 + 0.20/β)Qβ (1.10 + 0.20/β)			

Table 2.2: Calculation of Qu factor (API,1993)

TYPE OF JOINT & GEOMETRY		TYPE OF LOAD IN BRACE MEMBER			
		Axial Tension	Axial Compression	In-Plane Bending	Out-of-Plane Bending
	K	(3.4 + 19β)Qg		(3.4 + 19β)	(3.4 + 7β)Qβ
	T & Y	(3.4 + 19β)			
	w/o diaphragms **CROSS** w/ diaphragms per 4.3.4	$Pa = Qu.Qf \frac{F_{yc}.T^2}{FS\ Sin\theta}$ (3 (2. 11).4 + 19β) (3.4 + 13β)Qβ (3.4 + 19β)			

2.6.2 Changes in API (2007)

According to API (2007), tubular joints without the overlap of principal braces and having no gussets, diaphragms, grout or stiffeners should be designed using the following guidelines:

$$Pa = Qu.Qf \frac{F_{yc}.T^2}{FS\ Sin\theta} \qquad (2.\ 11)$$

$$Ma = Qu.Qf \frac{F_{yc}.T^2 d}{FS\ Sin\theta} \qquad (2.\ 12)$$

where: Pa = allowable capacity for brace axial load, Ma = allowable capacity for brace bending moment,

Fyc = the yield stress of the chord member at the joint (or 0.8 of the tensile strength, if less), ksi (MPa),

FS = safety factor = 1.60. For joints with thickened cans, Pa shall not exceed the capacity limits defined in 4.3.5. For axially loaded braces with a classification that is a mixture of K, Y and X joints, take a weighted average of Pa based on the portion of each in the total load.

The update for Chord Load Factor Qf is:

$$Qf = \left[1 + C_1\left(\frac{FSP_C}{P_y}\right) - C_2\left(\frac{FSM_{ipb}}{M_p}\right) - C_3 A^2\right] \quad (2.13)$$

The parameter A is defined as follows:

$$A = \left[\left(\frac{FSP_C}{P_y}\right)^2 + \left(\frac{FSM_c}{M_p}\right)^2\right]^{0.5} \quad (2.14)$$

Where Pc and Mc are the nominal axial load and bending resultant in the chord, Py is the yield axial capacity of the chord, Mp is the plastic moment capacity of the chord, and C1, C2 and C3 are coefficients depending on the joint and load type as given in Table 2.3 and FS = 1.20.

Table 2.3: Values for C1, C2, C3 (API, 2007)

Joint Type	C1	C2	C3
K joints under brace axial loading	0.2	0.2	0.3
T/Y joints under brace axial loading	0.3	0	0.8
X joints under brace axial loading*			
β≤0.9	0.2	0	0.5
B=1.0	-0.2	0	0.2
All joints under brace moment loading	0.2	0	0.4
*Linearly interpolated values between β = 0.9 and β = 1.0 for X joints under brace axial loading.			

API (2007) has considered a new Qu value, which is given in Table 2.4.

Table 2.4: Values for Qu (API, 2007)

Joint Classification	**Brace Load**			
	Axial Tension	Axial Compression	In-Plane Bending	Out-of-Plane Bending
K	$(16 + 1.2\gamma)\,\beta^{1.2} Qg$ but $\leq 40\,\beta^{1.2} Qg$		$(5 + 0.7\gamma)\beta^{1.2}$	$2.5 + (4.5 + 0.2\gamma)\beta^{2.6}$
T & Y	30β	$2.8 + (20 + 0.8\gamma)\beta^{1.6}$ but $\leq 2.8 + 36\,\beta^{1.6}$		
X	23β for $\beta \leq 0.9$ $20.7 + (\beta - 0.9)(17\gamma - 220)$ for $\beta > 0.9$	$[2.8 + (12 + 0.1\gamma)\beta]Q\beta$		

2.7 Flexibility of Tubular Joints

In the computer analyses of the structures with tubular elements in traditional methods, the connections between the elements are considered rigid. In fact, the joint is considered a dimensionless point on which the elements are rigidly connected and it is not modelled as a structural element. This assumption implies that there is no rotational or axial deformation at the end of the secondary member against the primary member's axis. In reality, however, some local deflections occur in the circular section of the primary member under the forces exerted by the secondary member. This suggests that tubular joints have a remarkable level of flexibility in the elasto-plastic range. Therefore, the results of analyses based on the rigid-joint assumption are different to a great extent from the actual behaviour of the structure, which is obvious in instances such as structural deflections, distribution of internal forces, the buckling forces of the elements, as well as the natural structure frequency, especially in the case of 3-D structures. Hence, taking into consideration the flexibility effects in the overall structure analysis is very significant. Many researchers have been attracted to studying the effects of joint flexibility on structural analysis results as the effects have been shown to be high. Several research studies, and tests have been conducted on tubular joints so far, the results of which can be classified as follows:

1) Analytical methods,

2) Experimental and semi-experimental methods, and

3) Numerical methods.

Each of the above approaches has some advantages and deficiencies, however experimental techniques can produce the most accurate results provided the test set-up is made according to the assumptions adopted for the tests. The experimental accuracy and realisation of actual conditions are very important for interpreting the experimental

results. Analytical methods based on plate and shell theory become very complicated when dealing with tubular joints. They can, however, produce fast and relatively accurate results where applicable.

Numerical methods are those procedures that attempt to reach the solution of a problem by somehow discretizing the domain of the function being studied. It is tried here to differentiate between an analytical and a numerical method. Analytical procedures are based on the theories of continuum mechanics and aim at the exact solution. However, numerical methods approximate the exact solution. The Finite Element method is one of the most powerful numerical methods for studying the behaviour of structures. However, the complicated behaviour of tubular joints creates some inaccuracy and difficulty when the Finite Element method is applied to the joints.

2.7.1 Analytical Methods

Different researchers have proposed equations for the flexibility coefficient of joints, through conducting tests on different types of joint, which are presented below.

It must be noted that tubular joints vary significantly in terms of their geometrical parameters and loading patterns, thus it is very difficult to obtain empirical equations for these joints and it would be costly to do so. Therefore, researchers have tried to solve the issue by applying simplifying assumptions for various loading cases and the presented equations are specifically for simple tubular joints.

Kellogg (1956) replaced the brace load with an equivalent distributed load shown in Figure 2.14. Based on the theory of beam on an elastic foundation, Kellogg derived the maximum stress under the equivalent load. This method only considers the axial load and/or in-plane bending moment on the brace. It gives approximate stress values for the chord and does not have any reference to the brace (UEG, 1984).

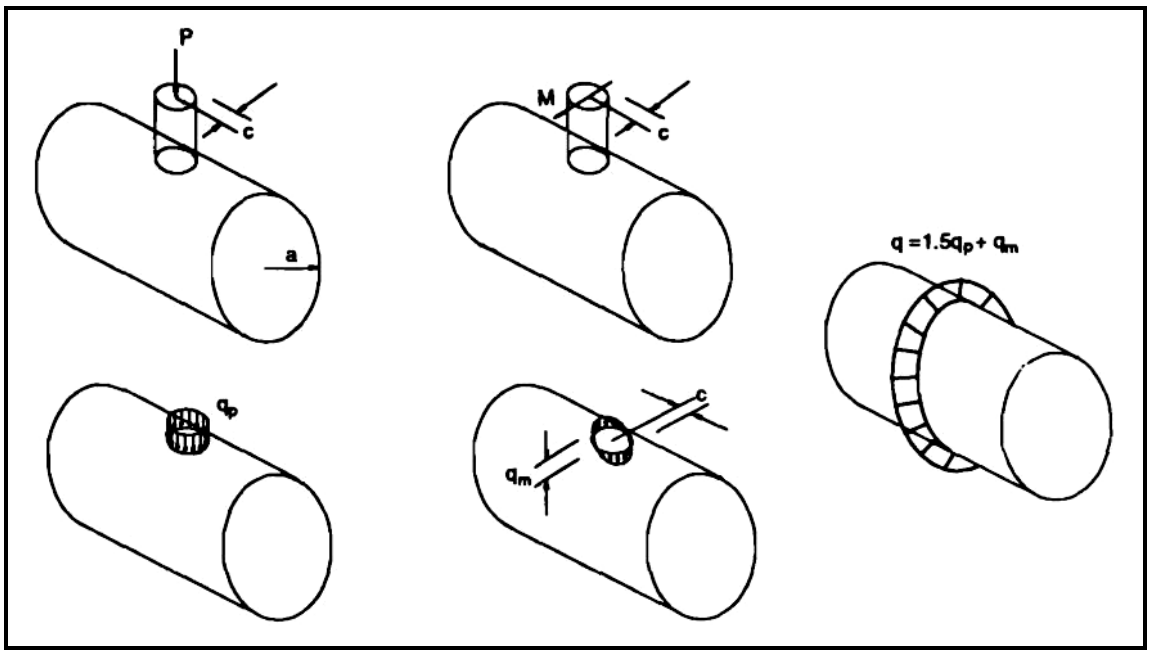

Figure 2.14: Kellogg's tubular joint models (UEG, 1984)

Another example of this type of analysis is Bijlaard's method (1955), which used a double Fourier series to show the displacement field of a cylinder subjected to a rectangular distributed load. Although the moment and deflections were computed for point O in the model shown in Figure 2.15, equations were introduced for obtaining the moments at the edges of the loaded area. The method needs to take into account a large number of terms in the Fourier series to give a relatively accurate result. For example, Rodabaugh (1980) used 21 terms in the hoop direction and 81 terms in the axial direction to determine the behaviour of K-joints (UEG, 1984).

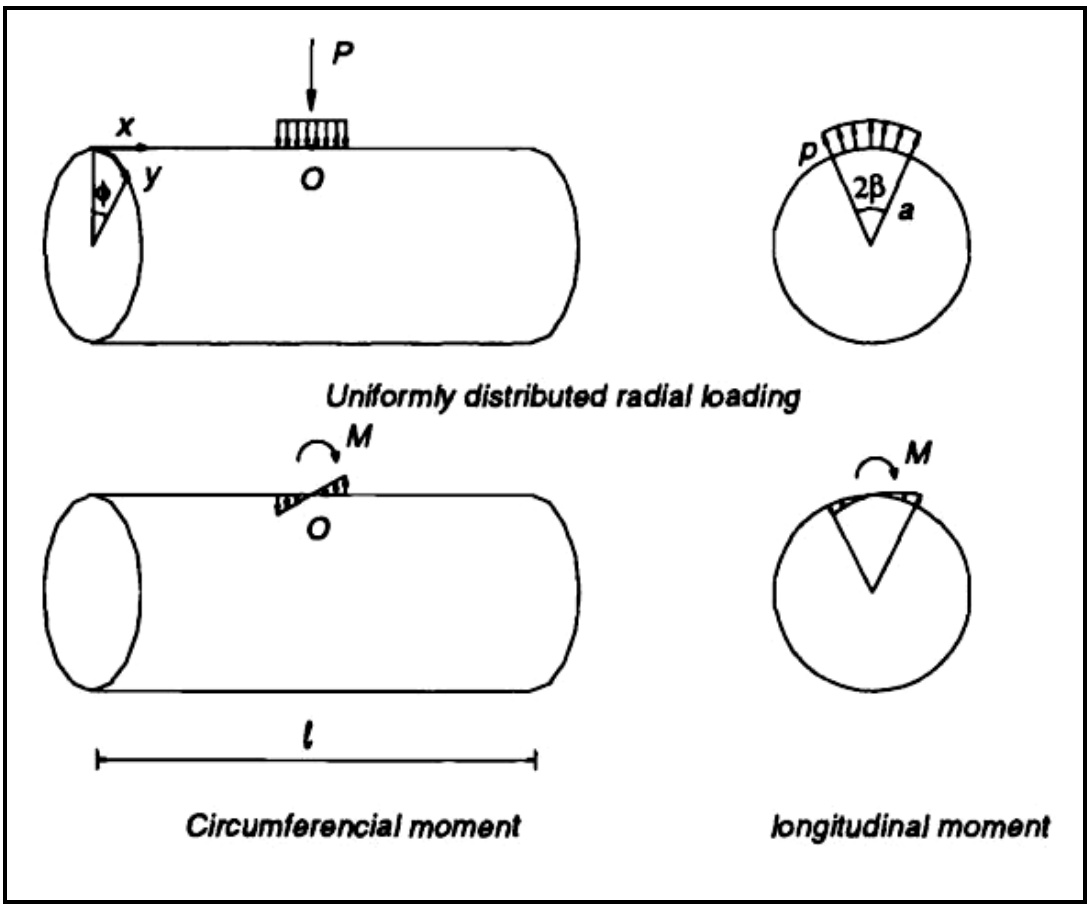

Figure 2.15: Cylindrical vessel model used by Bijlaard (UEG, 1984)

Despite the agreement between experimental data and Bijlaard's results, the method is too simplified for tubular joints. It may, however, be applied to the joints with small β ratio for preliminary design purposes.

Dundrova (1965) presented one of the most complete theoretical studies. She analysed a T-joint under axial load based on the classical theory of cylindrical shells. Her solution finds the distribution of the forces acting on the chord wall by imposing a compatibility condition between the brace axial displacement and chord wall deformation. However, brace bending stiffness is not considered in Dundrova's solution. She was the first one who considered the brace explicitly in the analysis (UEG, 1984).

Tubular joint flexibility was studied in a report by Holmas et al. (1985) using the classical shell theory. The range of β considered by Holmas is between 0.1 to 0.5. The

Donnell form was used to express the forces and moments on a shell element, as shown in Figure 2.16. The bending moment and axial force in the brace were replaced by the equivalent forces, as shown in Figure 2.17.

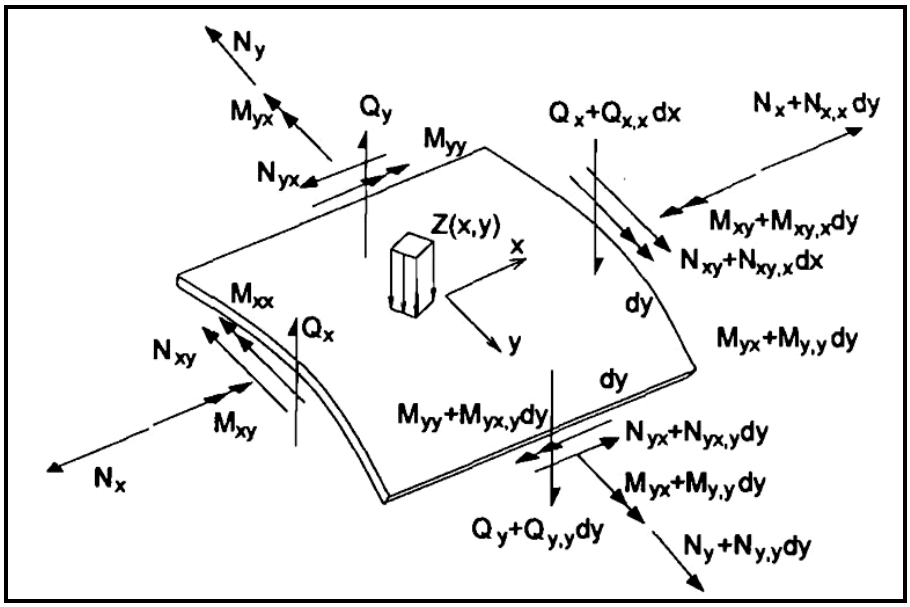

Figure 2.16: Shell element used by Holmas (Holmås et al., 1985)

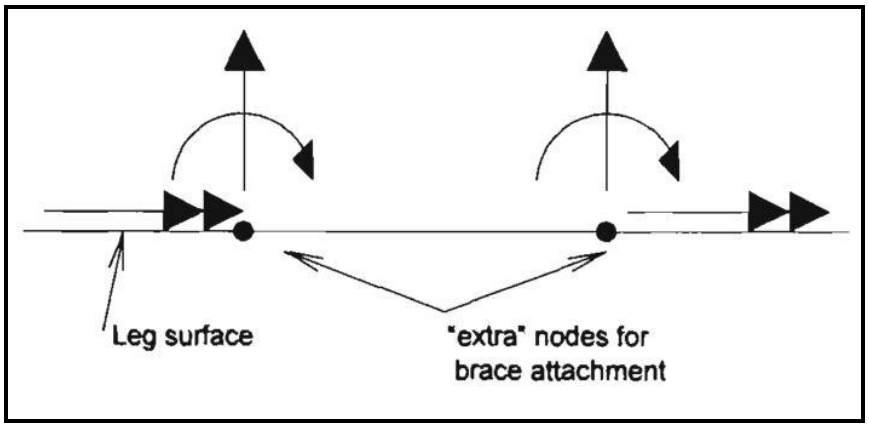

Figure 2.17: Extra DOF to express local joint behaviour used by Holmas (Holmås et al., 1985)

It seems that the model by Holmas is similar to Dundrova's model, in that it recommends three extra degrees of freedom for every brace attachment, which are one translational, and two in-plane and out-plane bending degrees of freedom. The report

shows the variation of the axial and IPB stiffness of a T-joint for various D/T ratios and β values. A model was suggested by Holmas for considering the high axial stiffness of the brace based on the collocation method, but the bending stiffness of the brace was not taken into account in this model.

B. Chen et al. (1990) investigated the local joint flexibility of simple T, Y and symmetrical K-joints for axial and in-plane bending loads. They used the classical theory of thin shells and the Finite Element method to analyse tubular joints with the chord and braces treated as substructures of thin shells while the intersection curve between any two substructures is discretized into finite elements. Chen et al. (1990) recommended a formula for the stiffness matrix of a symmetrical simple K-joint. They reached a good agreement with other formulae by DNV (1977), Fessler (1986) and Ueda (1990) and some experimental results by Tebbett (1982).

T. Chen et al. (1990) introduced a similar analytical method to the method by B. Chen (1990), using the two models by Holmas (1985), and Ueda & Rashed (1986) for definition of joint flexibility. These two models were based on the solutions of shell equations and Finite Element analysis, respectively. The model by T. Chen has the features of simple computations and low CPU time. T. Chen studied the axial and in-plane bending flexibility of T, Y and TY- joints.

2.7.2 Experimental and Semi-Experimental Methods

2.7.2.1 Experimental Methods

The theories of structures and continuous media are not used in these procedures. A physical model, which can range from small to full scale in size, is tested under the conditions similar to the real structure. The model can represent the whole structure or a component thereof.

In the study of tubular joints, the test specimens selected earlier were from steel. Synthetic materials, such as acrylic and epoxy resin, were used later as substitutes for steel since they are cheaper, easier to handle and more flexible. Experiments are usually carried out by loading the joints through static forces and measuring the desired quantity, which can be a strain in any direction or displacement of a location with respect to a datum. Test specimens from synthetic materials are on a small scale, whereas those from steel could be the same scale as the prototype. Numerical methods are usually employed for curve fitting of the test results, where, generally, an equation or formula is established to be used for analysis and design. Parametric formulae for stress concentration factors is a popular example of the application of experimental methods to tubular joints.

The photoelasticity method is also an experimental technique involved in the experimental stress analysis of tubular joints, where three-dimensional stress distribution can be determined. The method is restricted to stress analysis, and, unless a relationship between flexibility and stress is employed, it cannot be used for the study of joint flexibility.

Fessler et al. (1981) developed a procedure to define and measure the flexibility of tubular joints. Three loading modes were considered: 1) axial tension, 2) in-plane bending moment, and 3) out-plane bending moment. Fessler et al. (1981) only considered T and non-overlapping Y joints by testing 25 joints made of precision-cast epoxy resin tubes. Methods based on the experimental results were proposed to determine the joint flexibilities of the different deformation modes. An equivalent brace length was proposed to consider the flexibility of typical joints when the customary line model was used. A line model is constructed of one-dimensional beam elements being connected at the joints.

Fessler & Spooner, (1981) concluded that further work should include an analysis of simple frames of typical structures. It appears that the experimental method proposed by Fessler & Spooner, (1981) includes a relatively time-consuming procedure and can be costly in terms of test equipment. Figure 2.18 shows the rig used for loading the test specimens. Deflections were directly measured at various locations.

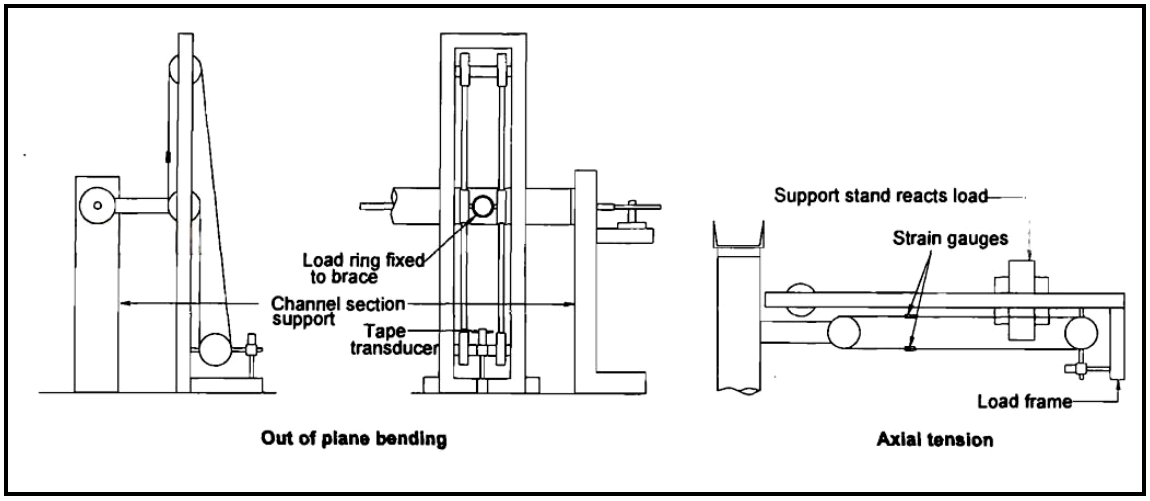

Figure 2.18: Test rig used by Fessler (Fessler & Spooner, 1981)

In another work, Fessler et al. (1986a) developed a set of parametric formulae for IPB, OPB and axial deformation of the brace in single brace tubular joints, using the same method as in the 1981 paper. There were 27 tests on araldite models covering the common range of parameters in offshore structures. In comparison with the experimental results, Fessler's formulae overestimated the bending stiffness of the T- and Y-joints.

In a companion paper, Fessler et al. (1986) presented a set of equations for the cross-flexibility between any two braces that may be in any orthogonal plane at a joint. This work was also based on the same experimental procedures and actually on the same test specimens as the other paper (1986) by the same authors. The measurements on the end of fictitious unloaded braces were determined from the measurements of the single

brace joint models. In both papers, the effect of the variations in brace wall thickness on joint flexibility were ignored. For non-overlapping joints, the proposed parametric equations may overestimate the flexibility by up to 70% compared to the measured data when the flexibility is significant.

2.7.2.2 Semi-Experimental Methods

When compared with the experimental methods, semi-experimental procedures also benefit from the analytical methods of structural analysis. In these procedures, a mathematical model is employed and tuned using the test results. The punching shear model, shown in Figure 2.19, is an example of this method. The punching shear stress, V_p, is assumed to be uniformly distributed. So it can be written as:

$$V_P = \frac{N}{\pi dt} \tag{2. 15}$$

in which N, d and t are the axial force, diameter and thickness of the brace, respectively. The axial force in terms of shear stress would be:

$$N = V_P \pi dt \tag{2. 16}$$

Design codes give the allowable values of the punching shear stress for different geometrical parameters. The values have been derived from experiments on various test models and then stated in the analytical form of punching shear stress formula.

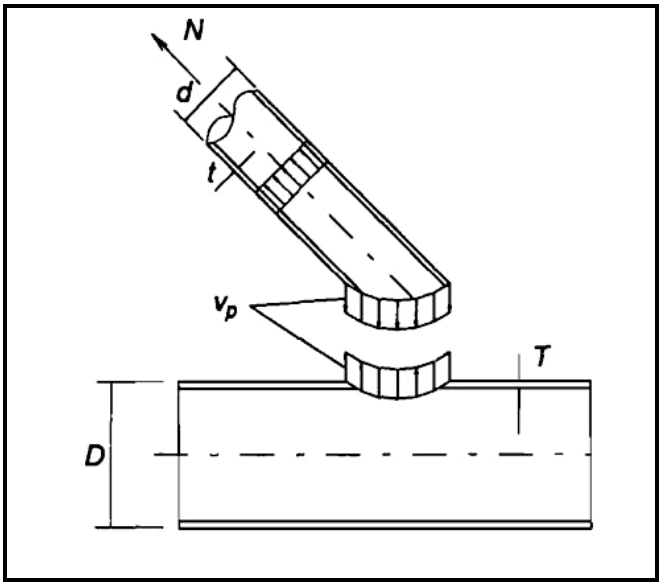

Figure 2.19: Stress distribution assumed in Punching Shear Model (Springfield & Brunair, 1989)

The method used in this study is a semi-experimental technique in which an unknown analytical parameter is determined by experiment. A work on the support flexibility of pre-tensioned cables was carried out by Springfield and Brunair (1989). The end fixity, as the main objective, and the bending stiffness (EI) of an electrical transmission line were determined by measurement of the displacements at certain locations of the line when it was vibrating under a certain natural frequency. The theoretical model used by Springfield and Brunair (1989) is an axially loaded, transversely vibrating beam supported at the ends through rotational springs. Springfield and Brunair (1989) concluded that consideration of end fixity leads to a conductor bending stress of approximately one-third the value given by assuming a rigid end.

Alanjari et al. (2011) selected two sample tubular-framed structures which is shown in Figure 2.20. They studied the impact of joint flexibility and failure on the overall behaviour of jacket frames. The first frame was modelled analytically, which was experimentally tested by Zayas et al. (1980). Cyclic inelastic loading was applied and the results were presented through hysteretic base-shear deck displacement graphs. The

second frame was modelled by a plane or space frame having tubular members rigidly interconnected to each other at nodal points. The element takes advantage of empirical formulae to model joint flexibility and failure.

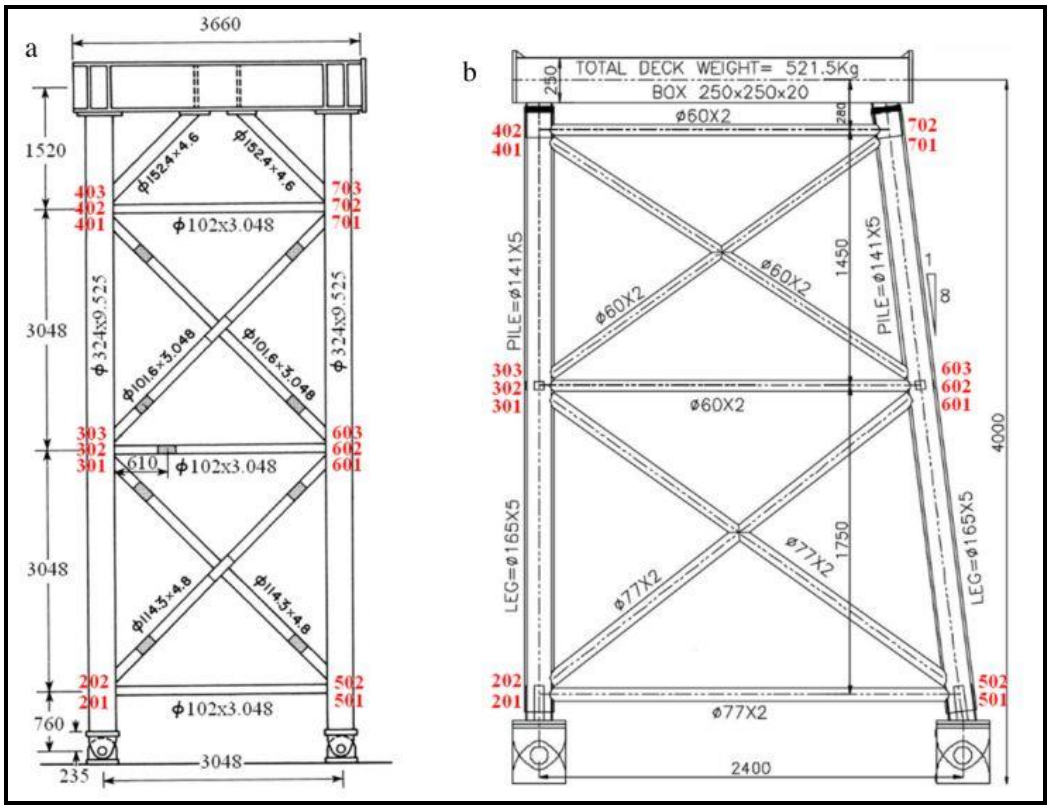

Figure 2. 20: Alanjari sample planar offshore frames (Alanjari et al., 2011)

The element is formulated using the physical interpretation of the chord shell behaviour in the vicinity of the joint. It is formulated on the basis of the equilibrium of a two-node element, which is connected to the brace and chord uniaxial elements.

Despite its simplicity, the element is capable of simulating fairly well the real response of the actual tubular connections upon the axial and In-plane Bending Moment (IBM) loadings. It should be noted that yielding of the element is accounted for by using empirical formulae. Several other empirical formulae and codes recommend various limit state relationships, which vary from one another in terms of joint strength. Even

so, the presented formulation by Fessler et al. (1986b) and Billington et al. (1982) seems to be in fair agreement with observations from the experimental tests and results of finite element analyses that take advantage of sophisticated three-dimensional models.

Conventional centre-to-centre modelling fails to predict the real lateral elastic stiffness of the structure, since it does not contain local joint flexibility as an inherent characteristic of tubular joints.

Figure 2.21 shows that the Alanjari model exhibits less stiffness compared to the centre-to-centre and rigid models, due to the presence of joint flexibility. However, all the structures have almost the same maximum lateral load-carrying capacity, showing that joint yielding has almost no effect on the capacity of the structures.

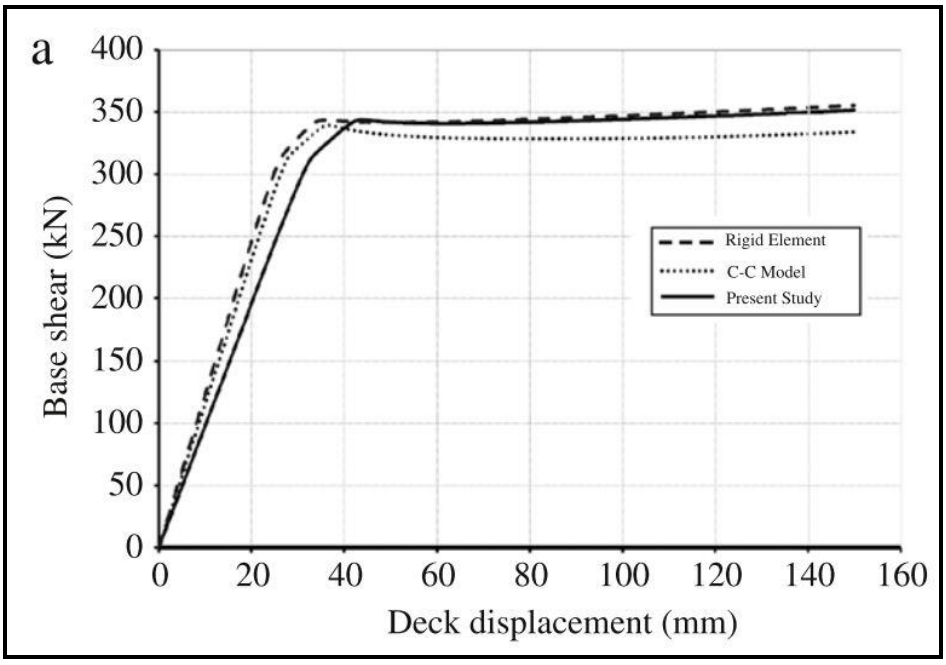

Figure 2.21: Push-over curves comparison between the rigid model, the centre-to-centre model and the Alanjari model (Alanjari et al., 2011)

Figure 2.22 describes the comparison between the model platform using the nonlinear joint element model and the spring model. The spring model contains joint flexibility

and yielding in both the axial and in-plane bending directions. It is clear that, in both models, joint yielding occurs prior to brace buckling, which reduces the platform lateral load-carrying strength by up to 20%.

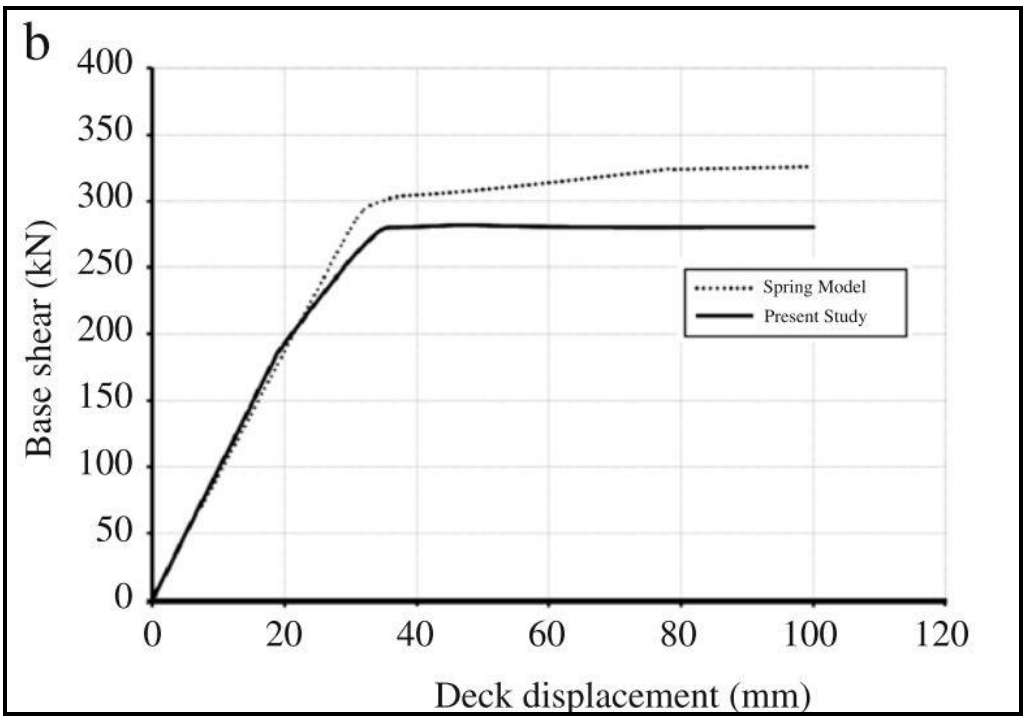

Figure 2.22: Push-over curves comparison between spring and Alanjari models having 50% weakened joints (Alanjari et al., 2011)

The buckling of the braces is normally encountered prior to joint failure due to the significantly greater strength of the joints compared to the critical buckling load of the braces. This depends greatly on the chord thickness in the vicinity of the joints, which emphasises the role of the Joint-cans. However, in numerous existing platforms, which were installed several years ago, reassessment programmes have revealed considerable damage to the joints in the form of fatigue cracks and corrosion. This might lead to considerable strength loss in the joints, which might have catastrophic consequences for structural safety.

The proposed element is fully capable of incorporating axial load and IBM interactions in tubular joints. Verification studies emphasise the marked axial strength-deteriorating role of the IBM in the joints. However, the current element is able to consider this deterioration regardless of the magnitude of the IBM. In the case of an offshore structure as a whole, a model capable of considering the interaction between the axial loads and the IBMs can predict the actual lateral-load response of the platform whose joints are vulnerable in comparison with its braces.

2.7.3 Numerical Methods

Numerical and analytical methods were facilitated with the advent of computers, resulting in the development of the analysis procedures in the theory of structures. The Finite Element method, the dynamic deformation method and the flexibility method are some examples. The dynamic deformation method is an improved version of the slope deflection method where the inertia forces are also considered (Koloušek et al., 1973).

Bouwkamp et al. (1980) developed a new procedure involving a modified three dimensional Finite Element formulation for the modelling of a tubular joint substructure and its subsequent insertion into a complete offshore platform computer model. The sub-structuring technique used by Bouwkamp allows fast modelling of the tower frame without having to do finite element modelling of each joint, when the super-element is available. The technique is based on the results of the Finite Element analysis. There are also some simplifications to easily model the super-element. Figure 2.23 shows a typical substructure of a joint used by Bouwkamp.

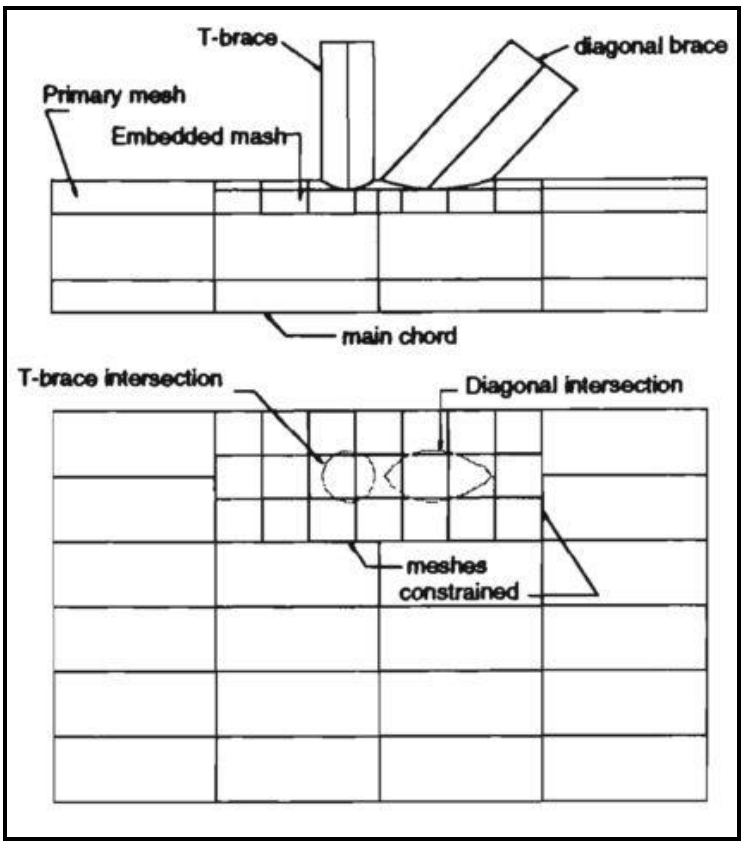

Figure 2.23: Model of joint substructure used by Bouwkamp (Bouwkamp, 1980)

Efthymiou (1985) reported a Finite Element study on the local stiffness of unstiffened tubular T, Y and K-joints subjected to in-plane and out-plane bending. He defined the local joint stiffness as the applied moment at the brace divided by the local joint rotation. The rotation of the brace end due to the joint flexibility was calculated by deducting the beam type rotation from the total rotation of the brace end. He measured the rotation at the end of the brace, as shown in Figure 2.24. This is different from the other methods in which the measurements are usually made on the chord wall.

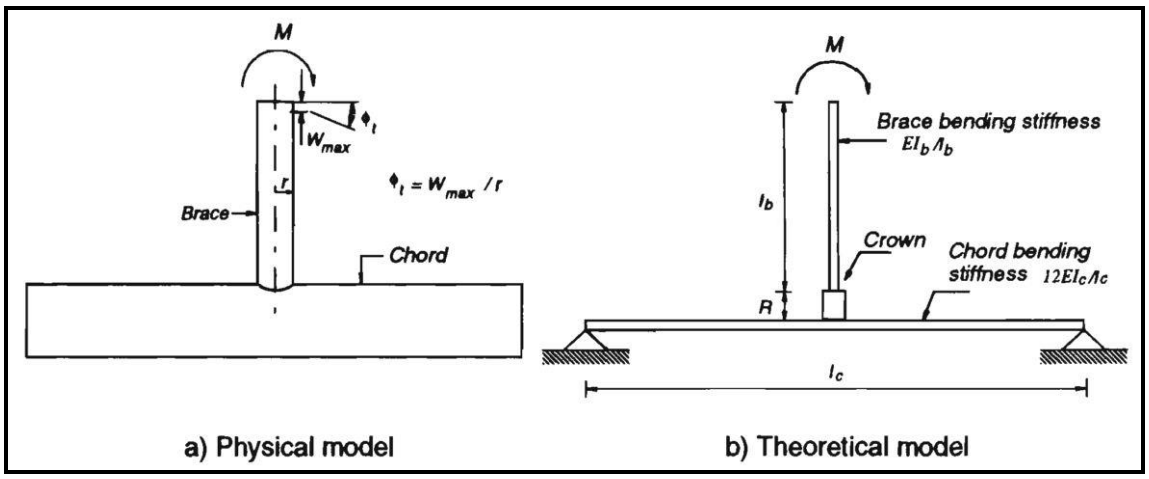

Figure 2.24: Rotations measured for calculation of joint flexibility (Efthymiou, 1985)

The FE program used by Efthymiou (1985) was PMBSHELL, which had a thin shell element implemented. To verify the performance of PMBSHELL, Efthymiou (1985) reanalysed one geometry using another program called SATE, which had a combination of plate and membrane elements. The results of these two analyses showed very good agreement. He established a set of parametric formulae based on 24 FE analyses for T-, Y-, and K-joints. Efthymiou's (1985) equations for the T- and Y-joints predict local stiffness to within 15% of the stiffness values used for curve fitting. The equations for K-joints are somewhat less accurate. Their predictions are expected to be within 30% of the measured stiffness. The parameters considered by Efthymiou (1985) were β and γ. His equations are inclusive of common joint types used in offshore structures, but the database that he used to establish the equations does not seem to have adequate data. Furthermore, Efthymiou's (1985) study was only based on the FE analysis results and does not have any comparison with experimental findings.

Ueda et al. (1986) developed a model for tubular joints. The model takes account of joint flexibility in elastic as well as elastic-plastic ranges based on elastic fully-plastic load-displacement relationship. It is stated by Ueda that the geometry of tubular joints makes it difficult to obtain closed form analytical solutions to evaluate load

displacement relationships. In this respect, the method that is chosen in this thesis has a highly theoretical base. It determines the natural frequency of a tubular joint from the measurement and then employs it in the analytical model to produce a relationship between load and displacement.

Ueda has proposed line elements for modelling the joint local behaviour, as shown in Figure 2.25. Elements 'c' represents the local behaviour of the chord wall in Ueda's model. The stiffness matrices for the elements are taken from another reference by the same authors. The method is used for both elastic as well as plastic zones (Ueda et al., 1986).

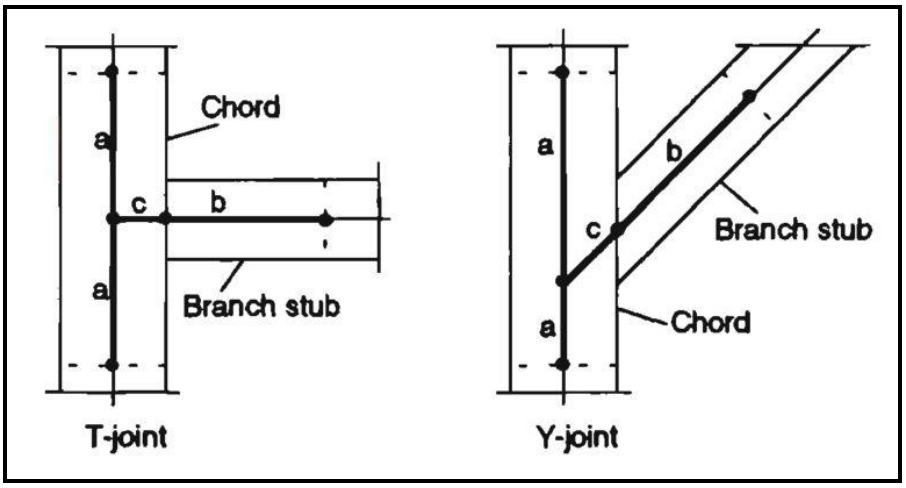

Figure 2.25: Joint model proposed by Ueda (Ueda & Rashed, 1986)

The proposed method by Ueda for considering local joint behaviour is computationally simple and does not need a great deal of computer memory. However, it is still based on preliminary analysis by the Finite Element method to obtain the stiffness of the joints. The method actually implements the stiffness results of a finite element analysis into a simpler line model. In addition, the computational nature of the method allows no modification in the joint model due to imperfections and other complicating factors involved in manufacturing and fabrication. Such an ability could remove the

approximations introduced by the Finite Element and generally correct the FE model using experimental data (Ueda & Rashed, 1986).

In another paper, Ueda et al. (1990) developed a set of formulae for the stiffness of the T- and Y-joints. The database used for establishing the formulae was taken from FE analysis and included 11 samples for IPB mode and 7 samples for axial deformation of brace.

The relationships between the stiffness of T- and Y-joints used by Ueda et al. (1990), especially axial stiffness, do not appear to be consistent with the results of others. For example, Fessler (1986) showed that:

$$K_Y(axial) = K_T Sin^{-2.19}\theta \text{ , and } K_Y(IPB) = K_T Sin^{-1.22}\theta \qquad (2.17)$$

in which K_Y and K_T are the stiffness of Y- and T-joints, respectively. θ is the brace angle in a Y-joint. Efthymiou obtained the following relation:

$$K_Y(IPB) = K_T \sin^{-(\beta+0.4)}\theta \qquad (2.18)$$

Whereas, Ueda used the same axial stiffness for the T- and Y-joints. To determine the IPB stiffness of a Y-joint, Ueda used the stiffness value of a T-joint divided by sinθ, where θ is the angle of the diagonal brace.

Souissi (1990) carried out a study on the flexibility of tubular T-joints using the Finite Element Method. He established a super-element to model a joint and attributed its property to the fictitious centre nodes that were at the end of each tube, chord and brace (Figure 2.26).

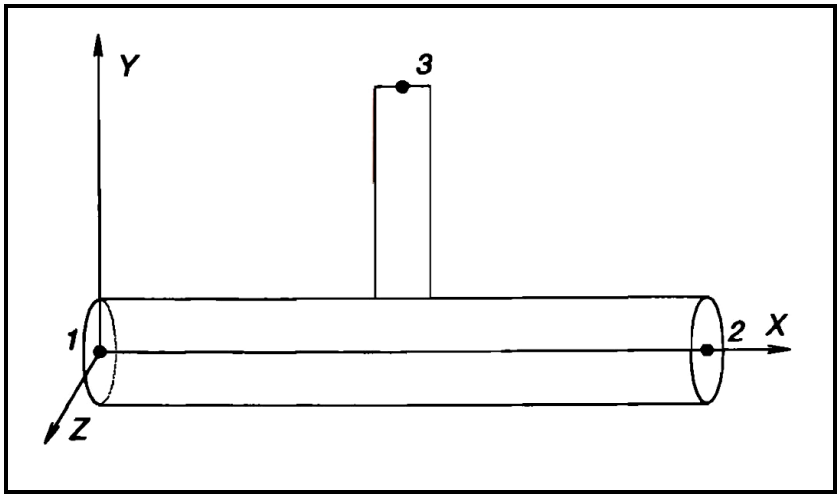

Figure 2.26: Joint super-element used by Souissi (1990)

Souissi (1990) considered in-plane bending, out-plane bending and axial loading, and performed 18 analyses for each case. His results showed good agreement with Efthymiou's (1985) results. He recommended that corrective factors could be applied for each loading case to consider the effects of τ on joint flexibility.

2.8 Joint Flexibility Models Based on Finite Element Methods

In finite-element methods, sub-structures are used to model the whole structure so that structural elements are divided into smaller components, thus the slight changes in movement of different points can be easily observed.

The use of finite element methods makes it possible to ensure the correctness of the work done without relying on the results of experiments. In addition, these methods are not cost effective and they must only be used for limited research purposes and the precision assessment of the methods that model the joints with structural elements.

A great deal of research has been done in this area, some of which will be briefly discussed here. Tebbett (1982) showed the effectiveness of grouting the legs of fixed jacket offshore platforms, which has become important with regard to the reappraisal of

steel jacket structures. To do so, he placed emphasis on considering the flexibility of tubular joints in the analysis of the jacket structures. Tebbett (1982) concluded that the effects of local joint flexibility can be significant and, if possible, should be included in the structural analysis during the reappraisal of jacket structures. Furthermore, if grouting is being considered, the reduced local joint flexibility should be accounted for in the analysis. Kawashima & Fujimoto (1984) checked their model by testing an L-frame and a portal frame. Kawashima only studied the effects of flexibility on the mode shapes and natural frequencies by conducting dynamic analysis. They obtained a good agreement between the analytical results of the joint model and experimental results, especially for the lower natural frequencies. The effect of flexibility consideration on the natural frequencies showed a variation from -25% to 0% between the calculated results. The -25% change occurred for the first natural frequency of the portal frame. Joint stiffness introduced a maximum change of 10% to the calculated natural frequencies of the L-frame. Matsui et al. (1984) studied the behaviour of truss beam columns composed of tubular sections. Matsui considered the effect of joint flexibility on the buckling behaviour of the web members with a large diameter-thickness ratio. The flexibility analysis of Matsui is based on a spring model from Sakamoto & Minoshima (1979). The results of Matsui's analysis indicate a maximum of 10% difference in the buckling strength of a truss when only the bending moment is applied to the chords. Van der Vegte et al. (1991), and Cofer & Will (1992) reported several non-linear analyses of the ultimate strength of tubular joints and provide an important affirmation that the finite element method can accurately predict the behaviour of tubular joints. Van der Vegte (1995) studied the ultimate strength of uniplanar X- and T-joints, and developed limit state equations through regression analyses over the results of carefully verified finite element models. Dier (2005) described the recent developments that have taken place in offshore tubular joint technology. The static

loading performance of tubular joints in multi-column composite bridge piers was studied by Lee et al. (2002). Lee and Parry (2004) conducted research on strength prediction for ring-stiffened DT-joints in offshore jacket structures. Wang and Chen (2007) examined the cyclic performance of the circular hollow section joints used in steel tubular structures, and performed quasi-static experimental tests to study the response of eight T-joint specimens. Honarvar et al. (2008) studied the cyclic behaviour of two small-scale models, representative of a jacket type offshore platform located in the Persian Gulf, with two different pile-leg interactions. They also presented the analytical modelling of pile-leg interactions as well as brittle joint behaviour, and concluded that joint rupture is encountered in the grouted model prior to the ungrouted frame due to the greater stiffness and strength of grouted legs.

2.8.1 Bouwkamp Model

Bouwkamp et al. (1980) summarised the results of a limited study into the effects of tubular joint flexibility on the structural behaviour of deep water fixed offshore towers (Figure 2.27). Bouwkamp produced a model, using Finite Element analysis results, to incorporate the joint flexibility into the structural analysis. In order to illustrate the procedures used to assess the effect of flexible joints, a two-dimensional 330 m high tower frame was analysed under dead and wave loads, using the developed joint model as well as the so-called line model. In the latter model, the joint effects were neglected. It was concluded that the effects of joint flexibility on the structural behaviour of offshore towers could be significant. The nature and magnitude of these effects are dependent not only on the tower height, but also on its geometrical and structural configuration. The effects were noted in the higher modes of vibration and in the deflected shape of the tower under static loads. It was observed that joint flexibility effects are more pronounced when stiffness of the member intersecting at a joint is relatively high.

The effect of joint flexibility on the deflected shape was seen to be very small for the nodes at the top of the tower. However, larger displacements were observed for the joint model at -170m below water level, with a maximum increase of 50% over the line model at -300m. Regarding the member forces and moments, Bouwkamp showed:

1) A slight increase in calculated leg axial forces (up to 2% higher) and a considerable reduction in calculated brace axial forces (up to 20%);

2) A modified distribution of pile loads with the load transferred to the piles through the main legs; and

3) An increase of up to five fold in leg moments.

Joint flexibility consideration in dynamic analysis was shown to lead to lengthening of the fundamental periods particularly for higher modes, where changes in order of the mode shapes were also observed.

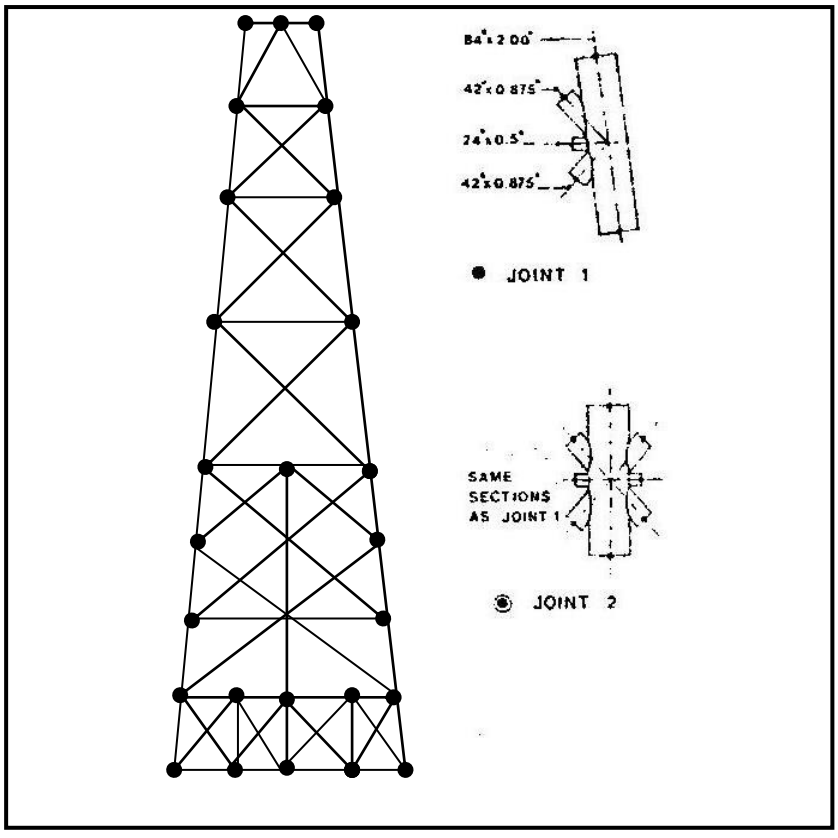

Figure 2.27: Frame models analysed by Bouwkamp (1980)

2.8.2 UEG Report, Node Flexibility and its Effects on |Jacket Structures (1984, UR22)

This report presents an investigation into the effects of chord wall flexibility at brace connections on the behaviour of oil production jacket structures. It considered the effects of joint flexibility on the in-plane deflections, axial forces, bending moments, brace buckling and natural frequencies of three different 100 m tall vertical plane frames. The overall geometry of the frames is shown in Figure 2.28. They have been modelled using two-dimensional beam elements with three in-plane degrees of freedom at each end, two translations and one rotation.

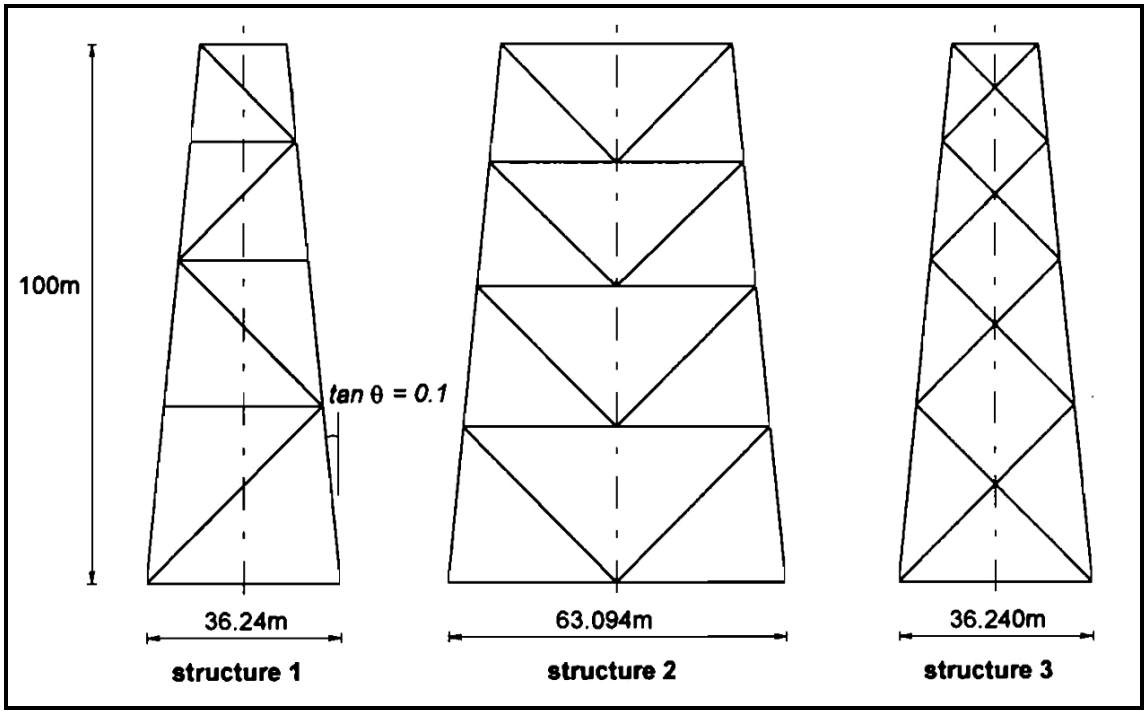

Figure 2.28: Frame models analysed in UR22 report by UEG (1984)

A simple representation of the joints was selected in the study. One nodal point was provided on the chord and one on each brace at the brace to chord wall intersection, as shown in Figure 2.29. The nodal points 2, 3 or 4 were then all connected by a stiffness matrix derived from the flexibility matrices provided by Fessler (1981).

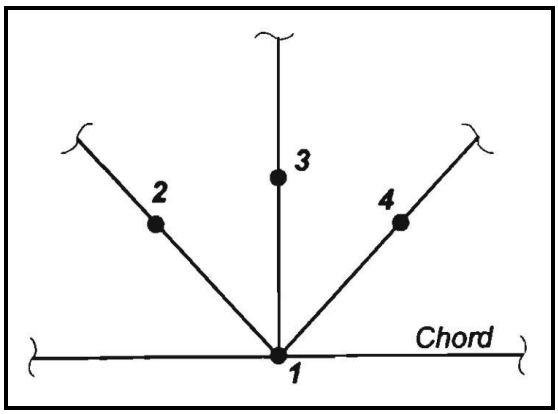

Figure 2.29: Nodal points considered in UR22 Study to represent a joint (UEG, 1984)

Two types of analysis were carried out, one incorporated flexibility of the joints based on Fessler's model, and the other did not consider flexibility, which was called conventional analysis, as the braces were extended to the chord centre lines.

The various joints used were identified by three characters TIN (Type Intersection Number). Type may be C-Conventional or M-matrix. T describes the intersection of the braces and chords, which is P-intersect at Point or E as Eccentric. 'N' is the joint Number corresponding to the geometrical ratios characterising the joint geometry. The joint numbers of the different geometrical parameters are shown in Table 2.5.

Table 2.5: Joint parameters used in UR22 (UEG, 1984)

Joint No.	D/T	d/D
1	25.3	0.53
2	50.6	0.53
3	25.3	0.33
4	25.3	0.75

For example MP3 refers to the analysis, using matrix formulation for the joints, where the braces are intersecting at a point having D/T=25.3 and d/D=0.33. Four load cases were applied to each structure. The first load case was a point load applied at the top of the frame. The other three were distributed wave load cases derived from a

representative 100-year storm wave with different phase angles: 0°, 90°, and 45°. The following results were obtained from the analyses:

1) Global Deflections

The introduction of the joint flexibility into the analysis, made differences of up to 13% to the overall sway of the structures analysed. A comparison of the deflections for the structures with different joint types is given in Table 2.5.

2) Effect of Flexibility on Axial Forces

This effect was found to be negligible. The biggest change between the conventional and flexible analysis was 1.5%. The maximum axial stress change was less than $1N/mm^2$.

3) Effect of Flexibility on Bending Moments

The largest change in brace end moment found was in structure 1 with joints MP2, where a horizontal brace moment increased to about three times the conventional rigid frame analysis value implying a 200% change. The largest variation of bending stress for structure 2 was 60%. Structure 3 had the largest change of about 50%. These changes correspond to a combination of the analysis results of load case 2 and load case 3. The bending stress changes for all the various structures and joints, under the wave load with a 45° phase angle, are shown in Table 2.6. The largest stress changes in the structures under the same loading were:

Structure 1: $30N/mm^2$,

Structure 2: $29N/mm^2$,

Structure 3: $4N/mm^2$.

Table 2.6: Summary of changes from UEG report on joint flexibility (UEG, 1984)

Change from Conventional Analysis		Structure 1				Structure 2				Structure 3			
		MP1	MP2	MP3	MP4	MP1	MP2	MP3	MP4	MP1	MP2	MP3	MP4
Deflection change %		0	5	2	-1	3	13	5	-1	1	5	1	-1
	Chord	0	0	0	0	0	0	--	--	0	0	--	--
Axial stress	45 brace	0	0.5	0	0	0	0	--	--	0	0	--	--
Change(N mm^{-2})	90 brace	0	0	0	0	0	0	--	--	--	--	--	--
	Chord	4	7	7	4	7	14	14	14	5	5	5	9
Bending stress	45 brace	15	20	15	15	11	-25	-29	13	13	6	6	6
Change %	90 brace	44	94	50	22	8	14	14	6	--	--	--	--
Bucking load	45 brace	4	-9	--	--	--	-10	--	--	--	-12	--	--
Change %	90 brace	--	--	--	--	--	-13	--	--	--	--	--	--
	1	--	2	--	--	--	6	--	--	--	2	--	--
	2	--	3	--	--	--	9	--	--	--	1	--	--
	3	--	1	--	--	--	3	--	--	--	3	--	--
	4	--	N	--	--	--	26	--	--	--	82	--	--
	5	--	3	--	--	--	3	--	--	--	13	--	--
Natural frequency	6	--	3	--	--	--	4	--	--	--	8	--	--
Change %	7	--	1	--	--	--	3	--	--	--	1	--	--
(rigid/semi-rigid)	8	--	5	--	--	--	N	--	--	--	3	--	--
	9	--	15	--	--	--	17	--	--	--	2	--	--
	10	--	0	--	--	--	15	--	--	--	0	--	--
	11	--	N	--	--	--	26	--	--	--	N	--	--
	12	--	6	--	--	--	24	--	--	--	15	--	--
	13	--	4	--	--	--	N	--	--	--	N	--	--

4) Effect of Joint Flexibility on Brace Buckling

The effect of joint flexibility on the buckling load of the braces was determined in the study. The results are shown in Table 2.6. The buckling load was reduced by about 10% between the conventional CP1 and the most flexible MP2 analysis. This was caused by the flexible joints increasing the effective length of the brace.

5) Effect of Joint Flexibility on the Vibration Characteristics of Jacket Structures

The first few natural frequencies and their corresponding mode shapes were calculated for each structure with the conventional CP1 and the most flexible MP2 joints. The natural frequencies of similar mode shapes were compared. Table 2.6 summarises the

natural frequencies and reports the proportional changes. The changes in the natural frequencies of corresponding modes were on average 4%, 12% and 11% for structures 1, 2 and 3, shown in Figure 2.28, respectively. The greatest change in natural frequency of similar modes was 82% and occurred for mode shape 5 in structure 3.

The study showed that the increase in bending stress caused by incorporating joint eccentricity of D/4 in the conventional analysis was similar to that caused by joint flexibility. It was concluded that the effects of joint eccentricity coupled with those of joint flexibility could therefore be significant.

Report UR22 indicates the significance of incorporating joint flexibility of tubular joints into the analysis of offshore towers. This report only considers one joint modelling technique; that is, using the joint stiffness matrices provided by Fessler. Other simulation techniques could produce different results. Furthermore, it only focuses on the different aspects of joint flexibility in the structural analysis, whereas an analysis of fatigue life seems to show the significance of joint flexibility consideration more clearly.

Ueda Model (Ueda et al., 1986)

Ueda et al. (1986) carried out a parametric study on five K-braced, five-storeyed two dimensional tubular frames, as shown in Figure 2.30. Three horizontal point loads were considered in Ueda's analyses.

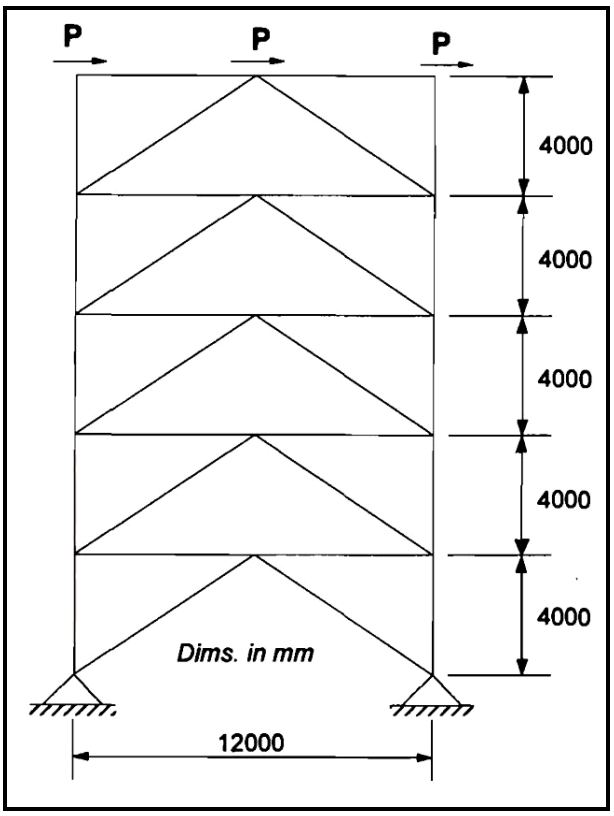

Figure 2.30: K-braced frame analysed by Ueda and its load cases (Ueda et al., 1986)

Table 2.7: Joint specification in Ueda's analyses (Ueda, 1986)

Model NO.	Model type	D	T	Initial load (Kgf)
R15			64	1410000
R20			50	1100000
R30			33	730000
R40	R	1000	25	550000
R50			20	440000
R59			17	374000
R67			15	330000
F15			64	1410000
F20			50	1100000
F30			33	730000
F40	F	1000	25	550000
F50			20	440000
F30D			33	730000
F40D			25	550000
R:Rigid Joints F: Flexible Joints				
Chord	D×T (Table2.2)			
Horizontal Brace:	400×25 mm			
Diagonal Brace:	400×25 mm			
Yield Stress:	70kgf/mm^2			

Ueda investigated the effects of the joint flexibility and strength on the structural behaviour and collapse loads of the K-braced frames. It was found that joint flexibility might only have a little effect on buckling of braces, whereas joint strength may have a great influence upon the collapse modes and strength. The lateral stiffness of the K-frame with D/T = 50 decreased by up to 46% when joint stiffness was considered in the analysis. There was, however, less reduction of lateral stiffness when lower D/T ratios were assumed in the analysis (Ueda et al., 1986).

The significance of Ueda's study is that it investigated the effects of tubular joints on the ultimate strength of tubular frames. However, the three point loads considered by Ueda in his study do not simulate the loading from waves, current, etc., which exist in the sea environment. The results of Ueda's study could be more applicable to the offshore structures if different loadings were used (Ueda et al., 1986).

2.8.3 **Chen Model** (T. Chen et al., 1990)

T. Chen et al. (1990) analysed a 5-storey tower, as shown in Figure 2.31, considering flexible tubular joints based on the data by Holmas and Ueda. The results of Chen's analyses are reported in Table 2.8.

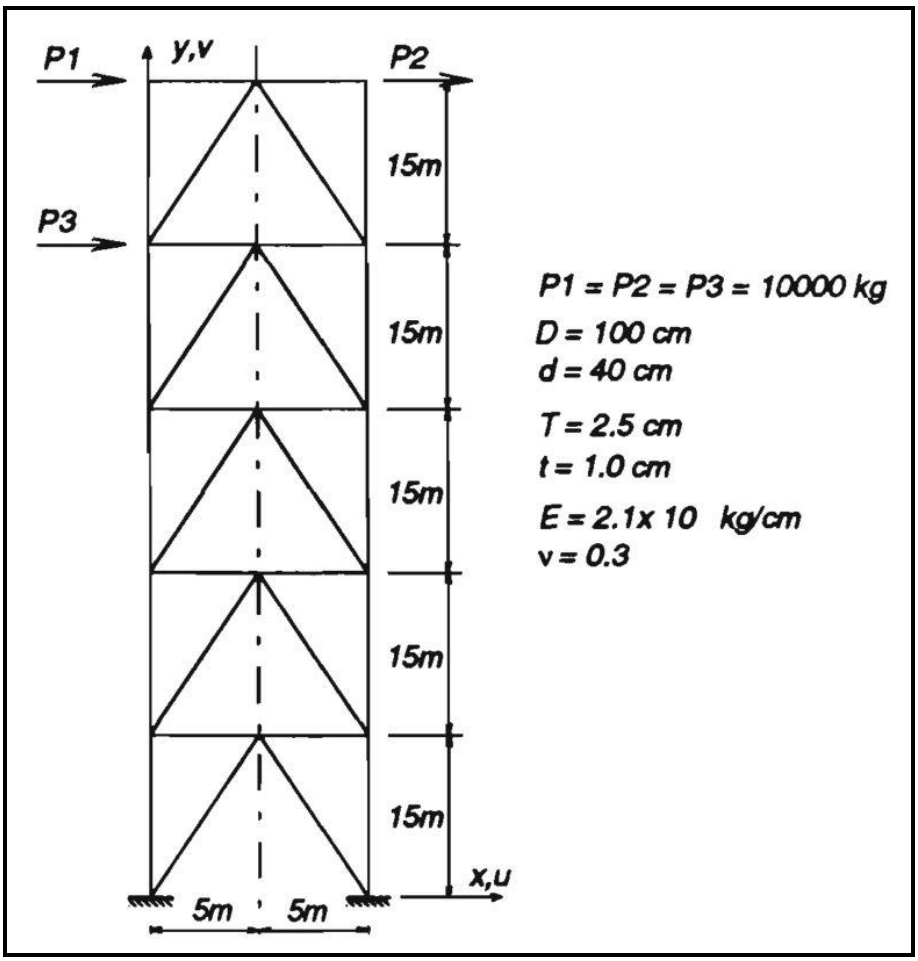

Figure 2.31: Tower analysed by T. Chen (1990)

Table 2.8: Effect of flexibility consideration in analysis T. Chen (1990)

	Computed results based on **Rigid Joints**	Computed results based on **Holmas' Joints**	Computed results based on **Udea's Joints**
u_{max} (cm)	7.198	8.784	8.722
υ_{max} (cm)	0.365	0.389	0.379
θ_{max} (rad)	-1.09E-3	-1.20E-3	-1.21E-3
N_{max} (kg)	3.4E5	4.27E5	4.23E5
Q_{max} (kg)	1.26E5	1.54E5	1.53E5
M_{max} (kg-cm)	1.99E6	1.71E6	1.92E6

Chen's results show good agreement between the two methods by Holmas and Ueda. The biggest difference was between the maximum bending moments calculated by the two methods. The model of Holmas produced a 14% change in bending moment whereas Ueda's model only caused a 4% change.

According to Chen's results, there was a maximum change of about 20% in the horizontal displacements, a 23% change in axial forces and a 10% change in bending moments when semi-rigid joints were employed in the analysis.

Chen's results are due to a loading composed of three point loads, as shown in Figure 2.38. This type of loading does not occur as frequently as wave loading in the sea environment. Therefore, the results are not very applicable to the offshore structures. However, generally, Chen's results show the effects of joint stiffness on the behaviour of structures.

2.8.4 **Souissi Model** (Souissi, 1990)

Souissi (1990) also compared the results of the analysis of two frames (Figure 2.32), one with flexible and the other with rigid joints (conventional analysis).

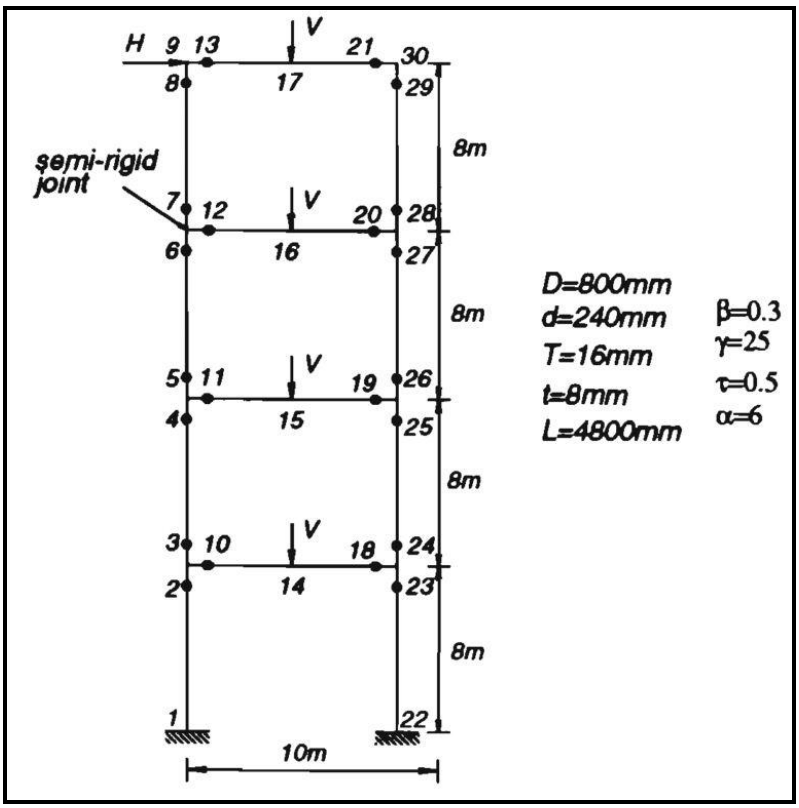

Figure 2.32: The frame analysed by Souissi (1990)

His results are:

Loading No. 1: H≠0, V = 0

1) 9% to 11% underestimation of displacements for the conventional analysis, and
2) Overestimation of bending moments up to 35% at joints 10 to 12 for the conventional analysis.

Loading No. 2: H = 0, V≠ 0

Overestimation of axial force up 37% for joint 10 and bending moment up to 23% at joints 10 to 12 for the conventional analysis.

Souissi (1990) concluded the need of a simple method to assess the flexibility of joints from analytical or numerical models.

2.8.5 **Recho Model** (Recho et al., 1990)

Recho et al. (1990) investigated the influence of flexibility on the fatigue design of tubular T-joints. The joint stiffness was determined by using the Finite Element method with static condensation technique. This method of stiffness calculation is the same as what Souissi (1990) carried out in his study. Three series of curves, based on the FE analyses, were established for the three load cases in the T-joints (IPB, OPB and axial loading).

Recho analysed two different structures, as shown in Figure 2.33, and calculated the fatigue life change when the joint flexibility was applied in the analysis.

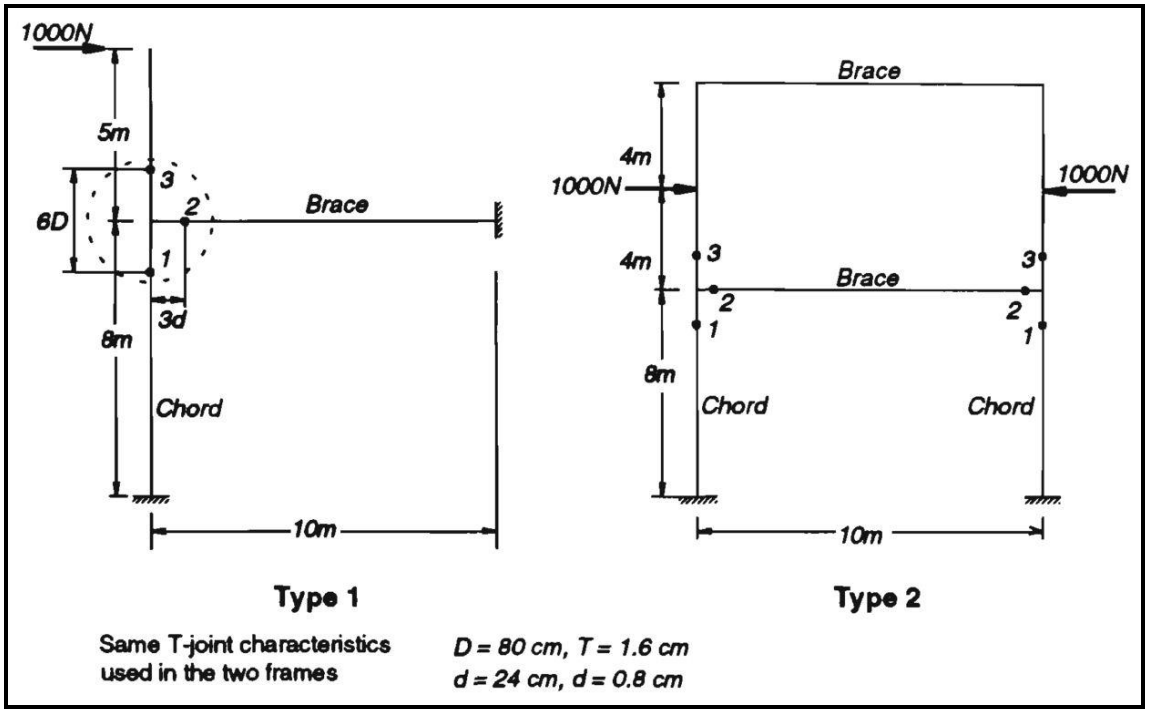

Figure 2.33: The structures analysed by Recho (Recho et al., 1990)

The results obtained for the forces at joint 2 in the two frames are given in Table 2.9

Table 2.9: Effect of joint flexibility on internal forces by Recho (1990)

Type No.	Rigid joint	Flexible joint	Difference %
Type 1	$F_{axial} = 1739N$	$F_{axial} = 1762N$	$F_{axial} = +1.3\%$
	$M_{IPB} = 37Nm$	$M_{IPB} = 45Nm$	$M_{IPB} = +21.6\%$
Type 2	$F_{axial} = 763N$	$F_{axial} = 724N$	$F_{axial} = -5.1\%$
	$M_{IPB} = 4.4Nm$	$M_{IPB} = 4.8Nm$	$M_{IPB} = +9.1\%$

Recho et al. (1990) then calculated the fatigue life of joint 2 using the French Standards (ARSEM, 1985) and compared the results of the rigid and semi-rigid analyses. The details of the fatigue calculation are not given by Recho, however, the influence of flexibility on the fatigue life of the two frames are reported. Table 2.10 shows this influence as the ratio of N_R (the number of cycles to failure when connection is

considered rigid) to N_F (the number of cycles to failure when connection is considered flexible).

Table 2.10: Fatigue life difference (N_R / N_F) when joint flexibility is considered (Recho et al., 1990)

Rupture	**Type 1**	**Type 2**
at the saddle point	1.04	0.85
at the crown point	1.80	1.30

The study does not include a realistic loading common to the offshore structures since the loading in the sea environment is a distributed load and depends on the wave or current characteristics, whereas Recho considered one or two point loads in his analysis examples. Furthermore, when comparing the fatigue life of rigid and flexible joints in Table 2.10, the location of fatigue rupture is not specified. The failure of a joint under fatigue is because of rupture at either the saddle or crown locations, and is not likely to be at both. Therefore, only two comparisons out of the four shown in Table 2.10, correspond to the fatigue life of the joints analysed by Recho.

2.8.6 Elnashai Model (Elnashai & Gho, 1992)

Despite the attention paid to the joint flexibility models so far, little attention has been paid to the issue of the joint flexibility effect on the responses of the structure and only a few researchers have studied the static responses of the structures. In the meantime, the issue that has not been given any attention is the investigation of the joint flexibility effects in dynamic analyses, and, especially, in the nonlinear range. Elnashai's study is one of the rare studies that have dealt with this issue. It should be noted that in this modelling, the flexibility coefficients of the joints are obtained from Fessler's (1986)

equation and the interaction between the axial and flexural (bending) deformations of the joint are neglected.

In Elnashai's model, a new formulation was used for column beam elements that can determine the response with high precision in large deformations. An interactive curve is used for the plastic hinge formation limit and the strain stiffening is neglected. In this method, a nonlinear model is used, which represents the behaviour of the structure in the linear and nonlinear range so that the structure's behaviour is different in tension and pressure. The gravitational force resulting from deck weight and added mass effect are taken into account and an imperfection of 1% is considered for all members.

Three analyses are conducted in this method:

a. Rigid joint
b. Flexible joint with linear elastic behaviour
c. Flexible joint with plastic behaviour

The third condition does not take place in this analysis because the failure factor is the buckling of secondary members rather than the flowing of the joint.

It can be observed that the maximum capacity only decreases 0.14% and the process of the plastic hinge formation is changed as shown in figure 2.34 to figure 2.36.

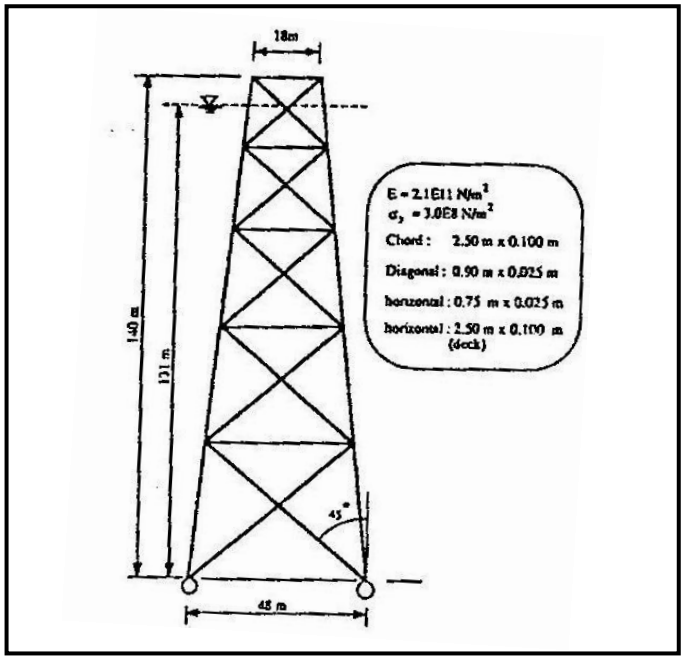

Figure 2.34: The platform studied by Elnashai (Elnashai & Gho, 1992)

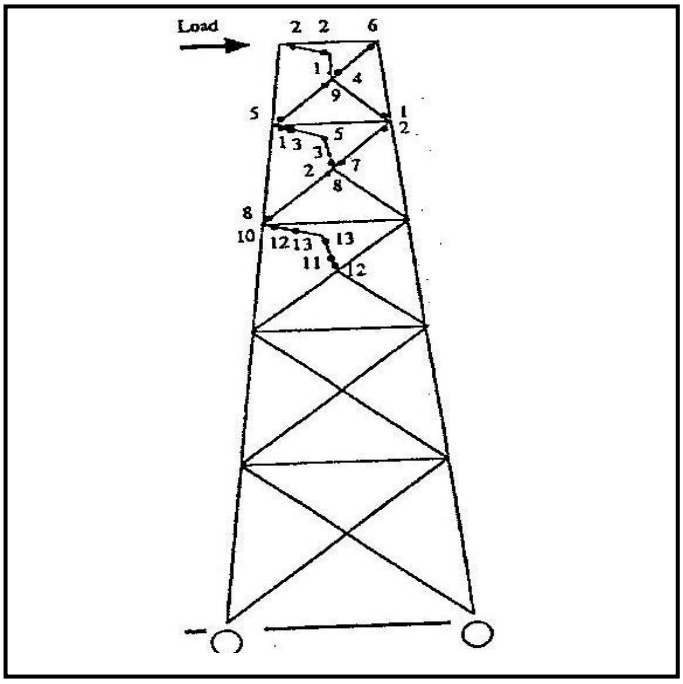

Figure 2.35: The process of plastic joints formation in a structure with flexible joints (Elnashai & Gho, 1992)

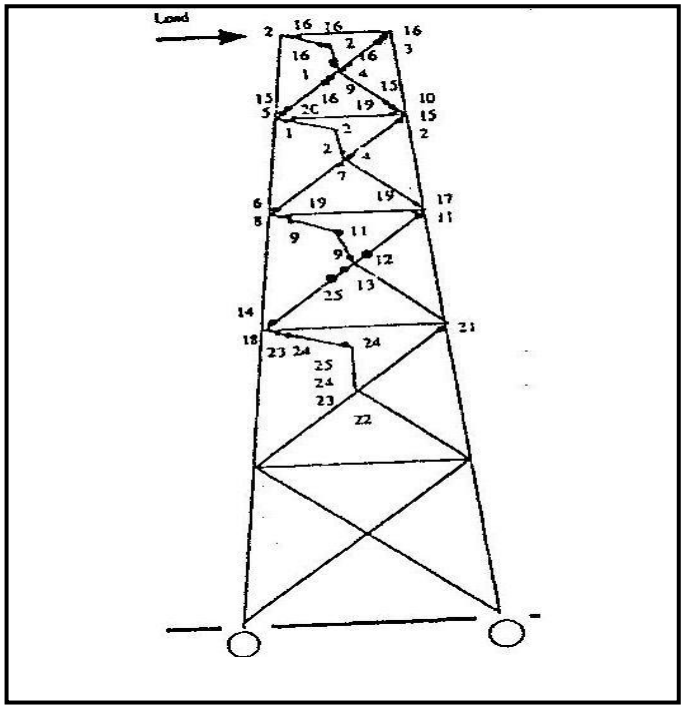

Figure 2.36: The process of plastic hinge formation in a structure with rigid joints

(Elnashai & Gho, 1992)

The dynamic properties are changed as follows:

- Change in structure periods; the periods of the first, second, third and fourth modes change 6.9%, 10.5%, 0.4% and 11%, respectively, and the changes in higher modes are higher than 12%.
- Changes in the mode mass contribution; in the first mode, the mode mass contribution in the flexible condition changes 0.41%; in the second mode, it increases 5.31%; and, in higher modes, it increases more than 10% compared to the rigid case.

The record applied to the structure is the artificial record extracted from the API spectrum.

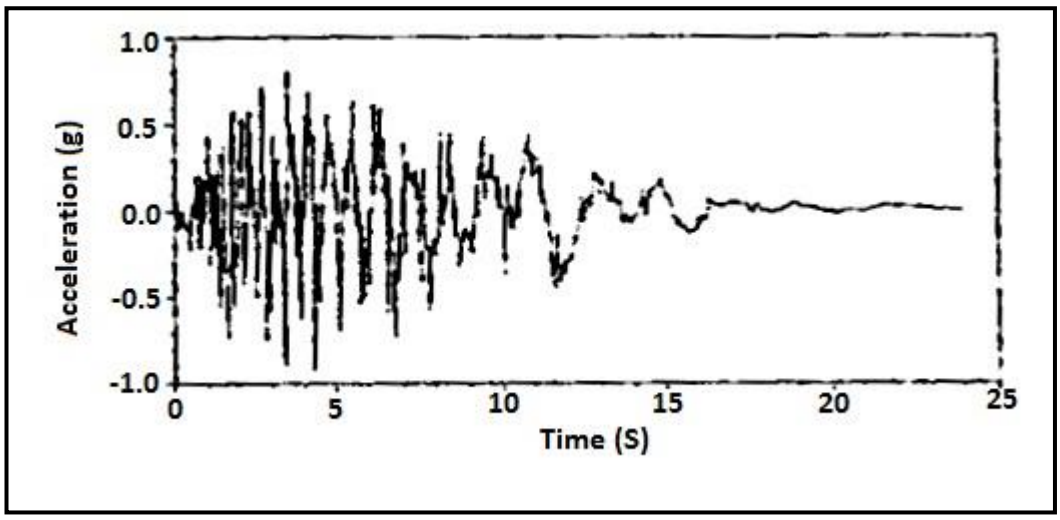

Figure 2.37: The extracted record (Elnashai & Gho, 1992)

The time history of response will change as follows:

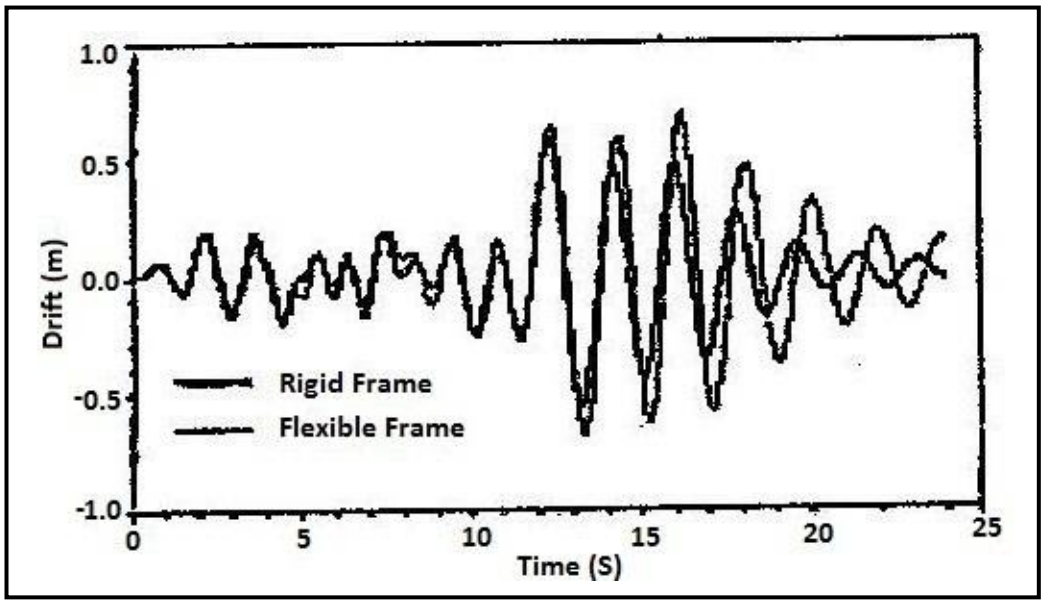

Figure 2.38: The time history of the Platform's response (Elnashai & Gho, 1992)

In addition, the plastic joints formation mechanism for the two platforms have been shown in figure 2.39 and 2.40.:

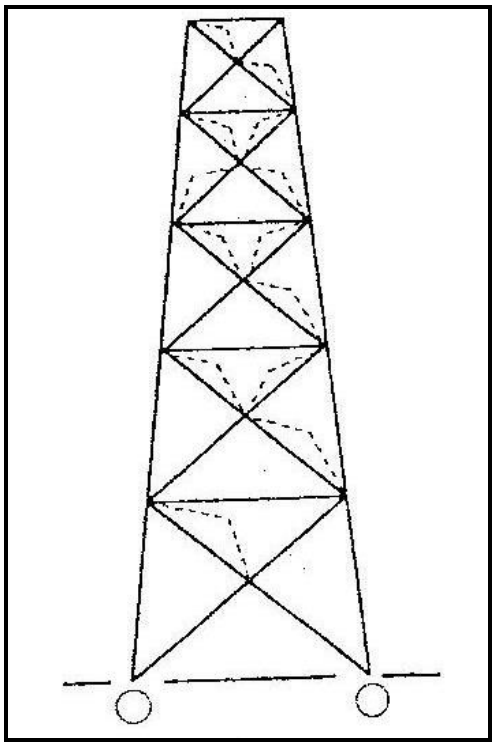

Figure 2.39: The plastic joints formation mechanism in the platform with rigid joints

(Elnashai, 1992)

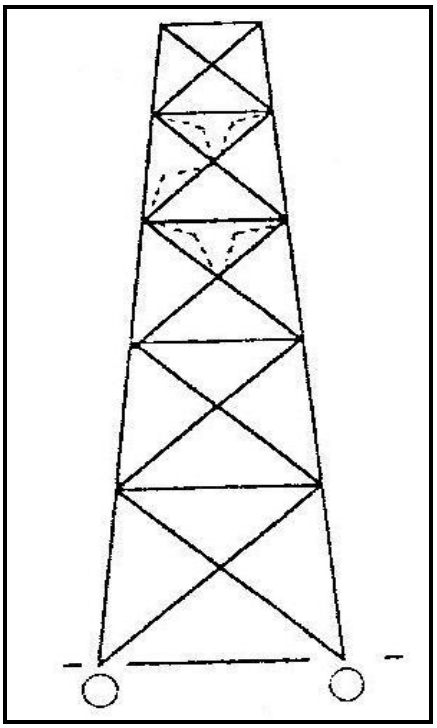

Figure 2.40: The plastic joints formation mechanism in the platform with flexible joints (Elnashai, 1992)

2.8.7 Mirtaheri Model

Mirtaheri et al. (2009) modelled a 2-dimensional offshore platform using the FE method. The general configuration and member sizes of the frame is shown in Figure 2.41. The platform was modelled in two states – rigid and flexible – and their dynamic and static behaviour were compared.

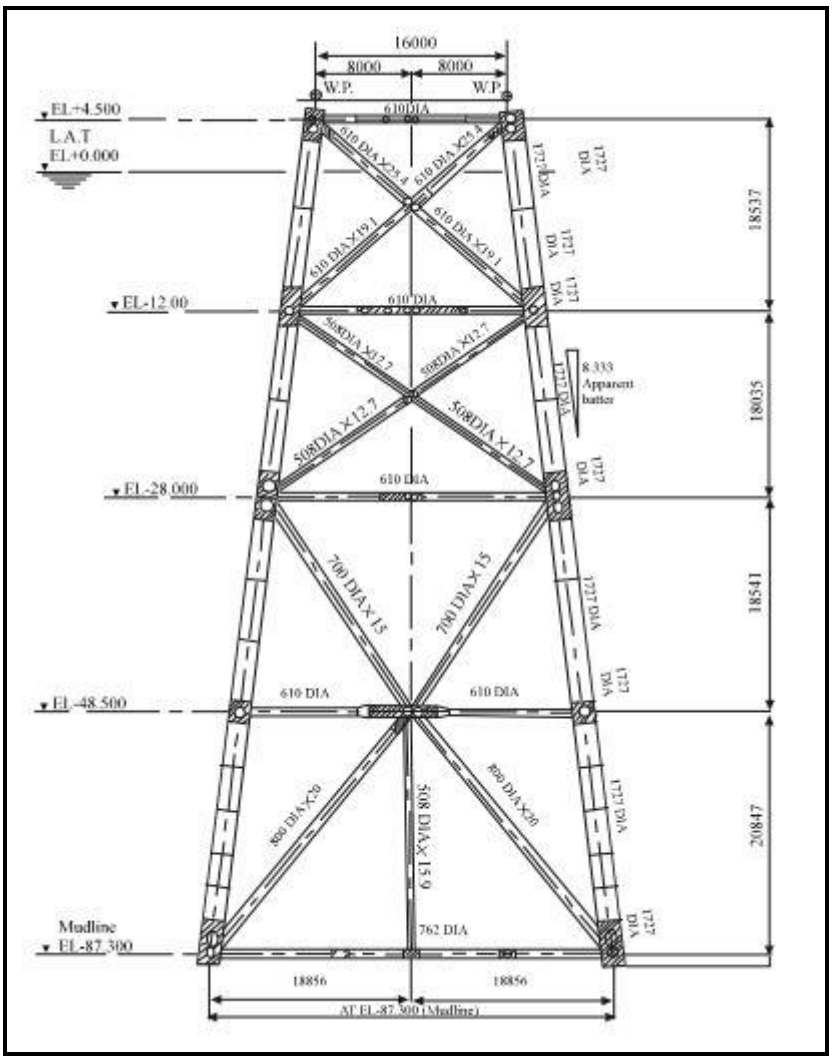

Figure 2.41: General configuration of the Mirtaheri frame (Mirtaheri et al., 2009)

The results of his research show that:

a) Considering the effects of connection flexibility has a significant effect on the platform response and we cannot relinquish the effects of flexibility in the analyses.

b) The period of the first mode of factor increases to 12.4% amount in the flexible model, and considerable changes are observed in the shape of the vibration modes and effective modal masses.

c) The diagrams of push-over analysis in the two models have significant differences with each other, and the maximum deck displacement is decreased by the flexible mode. The peak amount of the base shear reduced almost 20% in the flexible model (Figure 2.42).

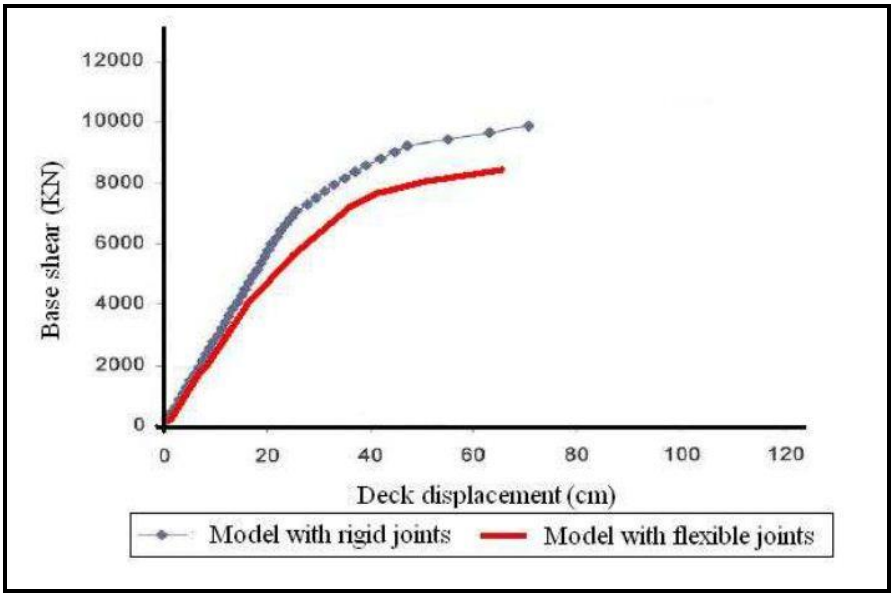

Figure 2.42: Result of Push-over analysis (Mirtaheri et al., 2009)

d) The result of his nonlinear time-history analysis using the Tabas earthquake is shown in Figure 2.43. It can be seen that the higher base shears induced in the model with rigid connections are quite apparent, as the structure is stiffer, and, as a consequence, the internal forces tend to be greater.

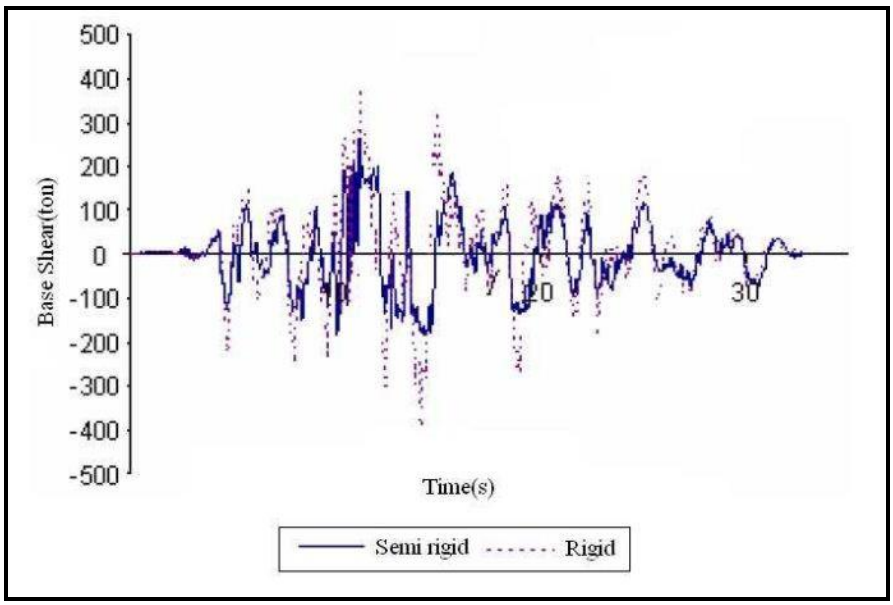

Figure 2.43: Results of nonlinear dynamic analysis on both models (Tabas record) (Mirtaheri et al., 2009)

e) Nonlinear dynamic analysis results (Figure 2.44) demonstrate that a platform with flexible connections has higher displacements and inter-storey drifts and lower base shear due to the lower stiffness and strength of the jacket structure.

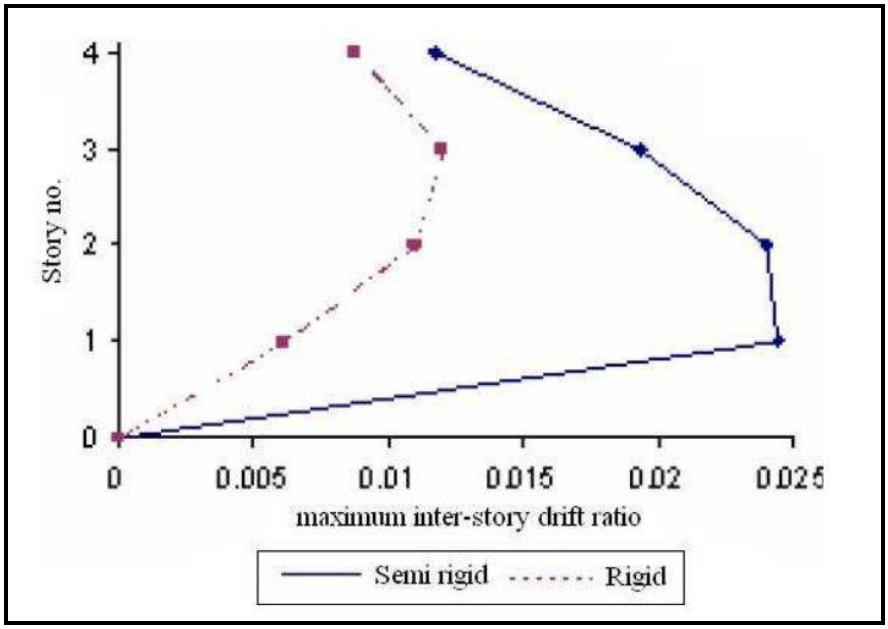

Figure 2.44: Maximum inter-storey drift ratio of two models subjected to Tabas EQ record (Mirtaheri et al., 2009)

CHAPTER III

DEVELOPMENT OF FINITE ELEMENT MODELS

3.1 Introduction

In this thesis, modelling the joints is done separately for the joints with Joint-can and without Joint-can, as well as in flexible and inflexible ways, using ANSYS software. The capabilities and the method of modelling in this software will be discussed in this chapter.

In the modelling and analysis, some assumptions are considered as follows:

1. The decks, piles and Joint-can are modelled as a simple model. The effect of the interaction of the structures, piles and soil are considered as an equivalent pile in which its length is eight times its diameter (SP6-1-300, 2002).
2. The platform studied is modelled as grouted with a defined element of interaction between the pile and the leg.
3. The effects of added mass are considered as a concentrated mass at the nodes.

Using some simple assumptions like those mentioned above can reduce the analysis time. On the other hand, since this study basically aims to compare the platforms, using such assumptions does not cause any problems in the results obtained.

In this study, the bilinear isotropic hardening criterion has been used for determining the behaviour of steel plates and profiles.

3.2 Finite Element Method

The thin shells finite element in tubular joint analysis and the theory of the finite element in cylinder shells are divided into different sections to investigate the behaviour

and performance of joints. All finite element computer software programs use the stiffness method in which the force and displacement strain of elements are formulated as the indefinite joint (node) deflection displacement, with the assumption that the continuity behaviour is taken into account, such as stable strain, stable curvature and linear changes of strain and curvature. We can create convergence in the elements by considering:

a) The force and displacement of an element depend on the displacement of its nodes.

b) The compatibility condition in elements that hold the force and deflection of adjacent elements should only exchange on common nodes.

c) No work or energy should exchange on their common boundary.

A common definition of the intersection line in coordinate systems from the main and secondary members is necessary. Without using these programs, modelling becomes so difficult that the cost of analysing finite elements may be more than the cost of the empirical method of measuring strain in stress analysis in an accurate model of joints (Comartin et al., 1996).

3.2.1 3-D Isoperimetric Finite Element

The isoperimetric elements of a polynomial model deflection are assumed along the element boundaries in an actual element that can be a curve, and the properties of element stiffness are obtained by numerical integration. This step-by-step interpolation function is used again to obtain the stresses from the deflection equation, thus the name isoperimetric is used. In order to model the range of shell thickness, and, more importantly, the geometry of welding in the section, it is necessary to use solid elements. This prevents the contradictory results sometimes obtained for stresses in semi(half)-plan of section in applying thin

shell analysis. The shell theory analysis and finite element analysis for thin and homogeneous thick shells provide a comprehensive plan for stresses in the main member. However, in terms of welding, which is the innermost area for critical points stress, modelling the thick shell seems more realistic. So, it can be summarised that using thin shelled elements in the connecting area in a joint leads to some errors in the calculation of stress. Despite many computational calculations, the best case is the use of 3-D elements in the whole connecting area, especially the welded part (Comartin et al., 1996).

3.2.2 The Inelastic Analysis of Finite Element

The finite element inelastic analysis can overcome some problems related to the use of big, permissible local stresses resulting from the elastic analysis and can be used as the design basis. The procedure of the finite element method is explained step-by-step, as follows:

1. It describes the internal deflection (displacement) of the elements, assuming a deformation pattern that is relatively continuous and has a compatibility on element boundaries, and their magnitude is presented for any degree of freedom through the generalisation of coordinates.

2. The node deflection (displacement) of inner strains is specified, regarding the similar general coordinates and deflection models and vice versa.

3. Evaluating the inner stresses from inner strains, is provided by the properties of the materials, which may have isotropic, orthotropic, elasto-plastic or other specific properties.

4. In the general coordinates method, the virtual interior work is summed in terms of the inner stresses and strains and the exterior work is

calculated in terms of the node forces and their displacement. In order to obtain the stiffness of elements, the two equations are solved simultaneously.

5. Transfer to a stiffness matrix of desirable nodes for an element. This method is repeated for the whole structure with the aim of building a total stiffness matrix for all elements. As for the linear structures, this method is performed using an inverse matrix or numerical calculation methods. Two other basic methods are used for non-linear structure frames, i.e. incremental and repetitive loadings to analyse FE inelastically (for inelastic FE analysis).

Wherever only the non-linear method is used in terms of the yielding point of the material, it is possible to describe the stress-strain relationship successively during the analysis of inner elements virtual work and stiffness.

Although the criteria have been created in the last 20 years and there are many useful computer software programs available, the means for designing the inelastic analysis of limited elements faces the problems indicated in the method in elastic analysis.

3.3 Elements Used in modelling

In the ANSYS software, 11th edition, there are about 175 types of element. In the modelling of this thesis, three types of element – SHELL 43, PIPE 20 and MASS21 element – have been used.

3.3.1 PIPE 20 Element

PIPE 20 is a uniaxial element with the ability to tolerate tension, pressure, bending and torsion and can consider behaviour in the nonlinear range. This element has six degrees

of freedom at each node (three transitional degrees of freedom and three rotational degrees of freedom).

As shown in Figure 3.1, the output of this element can be obtained on the first (i) and end node (j) in eight points with 45 degree angles from each other on the cross-section.

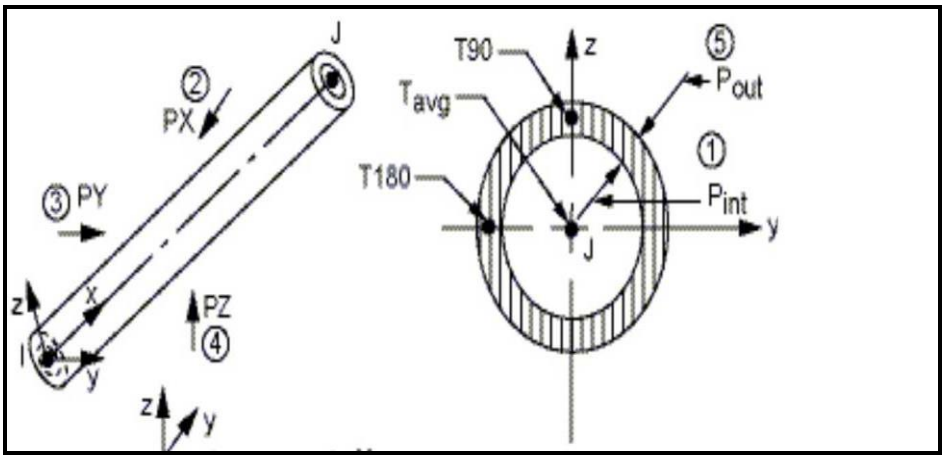

Figure 3.1: PIPE 20 element (SW ANSYS Academic Teaching, 2011)

3.3.2 SHELL 43 Element

The SHELL 43 (Figure 3.2) is an element with four nodes and six degrees of freedom per node. This element is known as the plastic shell element and it is suitable for nonlinear studies and flat plates or plates with curvature. This element, which is a thin shell element, can be used in plastic, creep, stress, hardening, and large deformations-issues. This element can also be used as 3- or 4-groups.

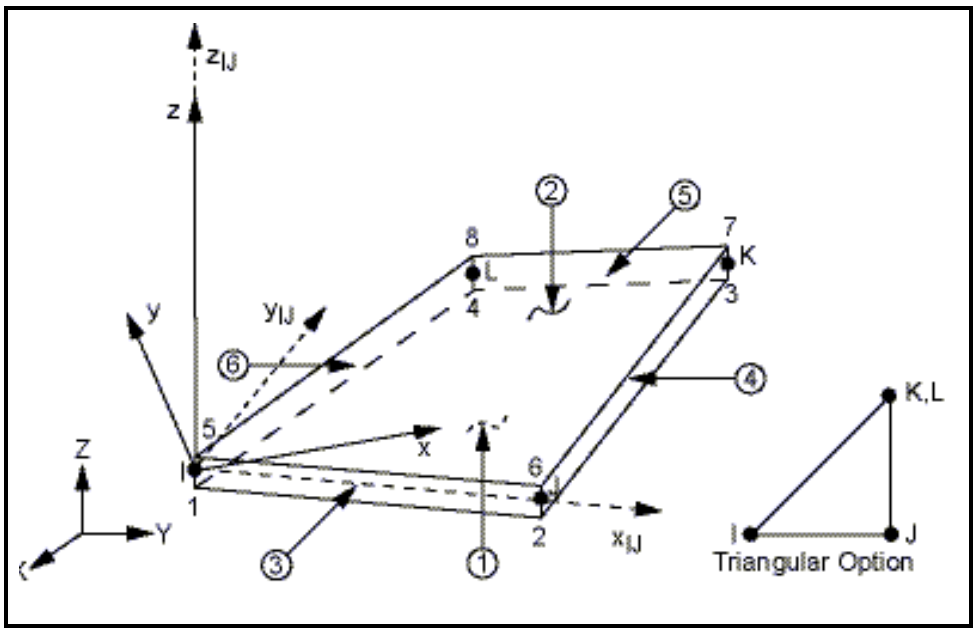

Figure 3.2: SHELL 43 element (SW ANSYS Academic Teaching, 2011)

3.3.3 MASS21 Element

MASS21 (Figure 3.3) has been used to put the concentrated mass on the platform. This element, which has six transitional degrees of freedom and six rotational degrees of freedom around the coordinate axes, is defined by a separate node. The component of concentrated mass and rotational inertia is applied to this element and the important property of this element is that it includes different types of non-linear material and non-linear geometry.

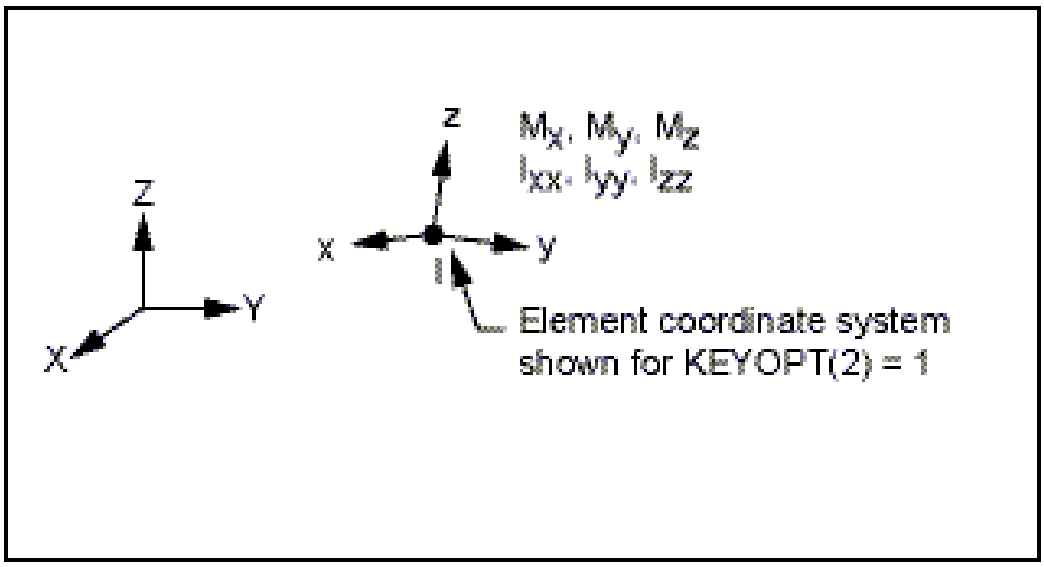

Figure 3.3: MASS21 element (SW ANSYS Academic Teaching, 2011)

3.4 Material Behaviour Model

The model considered for the further phases of research is the bilinear kinematic hardening behavioural model. This model is a behavioural model of bilinear stress-strain, based on the hardening principle, which uses the Von-Misses criterion as the yield criterion. In this model, as shown in Figure 3.4, stress increases linearly up to δ_Y with the gradient of E, and then the slope will be converted to E2 and the curve of stress – strain continues linearly with the new slope. While unloading it returns with the initial slope of E and this trend continues to a maximum of $2\delta_Y$ after which the curve would continue on a linear reverse gradient of E2. This behavioural model is used to express the behaviour of materials, such as steel.

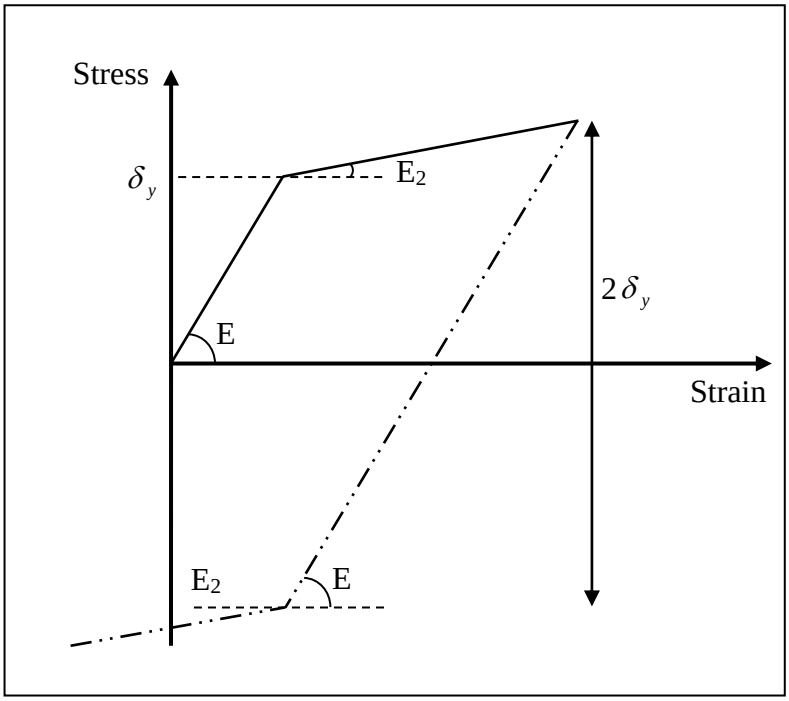

Figure 3.4: Stress-strain diagram of materials in ANSYS modelling

3.4.1 Von-Mises Criterion

The maximum strain energy hypothesis in shear deformation is called the Huber-Hencky-Von-Mises. It was proposed by M.T. Huber from Poland in 1904 and was then extended by R. Von-Mises from Germany and H. Hencky. The difference between this hypothesis and the energy change hypothesis is its assumption that the part of the deformation energy that causes change in the volume of materials creates no flow and causes no damage and failure, and only creates the part of the complexity and angular energy that affects the material failure directly.

$$Ud = \frac{1}{12G}\left[\left[\sigma_1 - \sigma_2\right]^2 + \left(\sigma_2 - \sigma_3\right)^2 + \left(\sigma_3 - \sigma_1\right)^2\right] = \frac{{\sigma_y}^2}{2G}$$

$$\Rightarrow \quad \left(\sigma_1 - \sigma_2\right)^2 + \left(\sigma_2 - \sigma_3\right)^2 + \left(\sigma_3 - \sigma_1\right)^2 = 2{\sigma_y}^2 \qquad (3.\ 1)$$

$$\left(\frac{\sigma_1}{\sigma_y}\right)^2 - \left(\frac{\sigma_1}{\sigma_y}.\frac{\sigma_2}{\sigma_y}\right) + \left(\frac{\sigma_2}{\sigma_y}\right)^2 = 1 \qquad (3.\ 2)$$

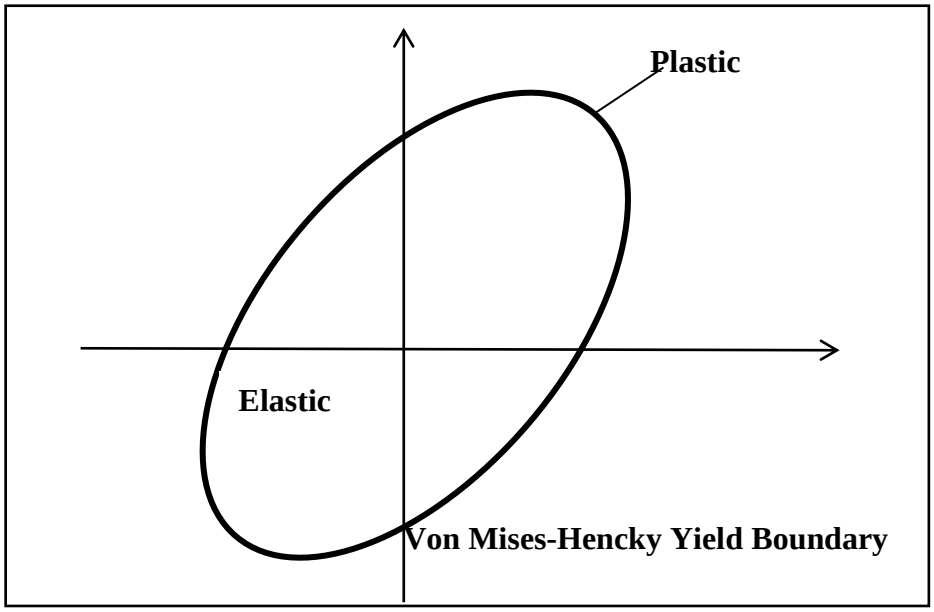

Figure 3.5: The Von-Mises yield criterion

The relationship mentioned above is the equation of an ellipse, which is illustrated in Figure 3.5. Any point within the ellipse indicates the elastic behaviour of materials and the points on the ellipse indicate the flowing of materials.

3.4.2 Steel Profile

The steel used in modelling has the following characteristics: (API, 2000)

- Specifications: API-5L-B (Table 3.1)
- Yield Stress: 36 kg/mm^2
- Elastic Module: 20000 kg/mm^2
- Poisson's Ratio: 0.3
- Strain hardening Ratio: 0.0034

Table 3.1: Structural Steel Pipe (API, 2007)

Group	Class	Specification & Grade	Yield Strength ksi	Yield Strength MPa	Tensile Strength ksi	Tensile Strength MPa
I	C	API 5L Grade B*	35	240	60 min.	415 min.
		ASTM A53 Grade B	35	240	60 min.	415 min.
		ASTM A135 Grade B	35	240	60 min.	415 min.
		ASTM A139 Grade B	35	240	60 min.	415 min.
		ASTM A500 Grade A (round)	33	230	45 min.	310 min.
		(shaped)	39	270	45 min.	310 min.
		ASTM A501	36	250	58 min.	400 min.
I	B	ASTM A106 Grade B (normalized)	35	240	60 min.	415 min.
		ASTM A524 Grade I (through $^3/_8$ in. w.t.)	35	240	60 min.	415 min.
		Grade II (over $^3/_8$ in. w.t.)	30	205	55–80	380–550
I	A	ASTM A333 Grade 6	35	240	60 min.	415 min.
		ASTM A334 Grade 6	35	240	60 min.	415 min.
II	C	API 5L Grade X42 2% max. cold expansion	42	290	60 min.	415 min.
		API 5L Grade X52 2% max. cold expansion	52	360	66 min.	455 min.
		ASTM A500 Grade B (round)	42	290	58 min.	400 min.
		(shaped)	46	320	58 min.	400 min.
		ASTM A618	50	345	70 min.	485 min.
II	B	API 5L Grade X52 with SR5 or SR6	52	360	66 min.	455 min.
II	A	See Section 8.2.2				

*Seamless or with longitudinal seam welds.

3.4.3 Grout Profile

The grout used in the model has the following characteristics:

- Elastic Module: $12 * 10^9\ kg/mm^2$
- Poisson's Ratio: 0.25
- Bond Strength: $15 * 10^6$ Pascal

3.5 Modelling the joints in the ANSYS software

3.5.1 The Length of Connecting Area

The PIPE 20 element was used to model members of the jacket, and the connecting area was modelled using the SHELL 43 element. The length of the connecting area of the element, which should be modelled with SHELL, depends on several factors. The length should be long enough so that the connection conditions of the SHELL element to the PIPE element have no effect on the flexible behaviour of the joint.

The connecting length is taken as the minimum length of the Joint-can and five times the diameter of the member (SP6-1-300, 2002).

3.5.2 Connecting SHELL and PIPE Elements

Another important issue is how to connect the shell element to the pipe element. This connection should be such that no rupture is created along the member. In fact, the degrees of freedom of point i from the linear element ij should be close to the degrees of freedom of the nodes located on the shell in such a way that the structural behaviour at this point is continuous.

In the ANSYS software there is an instruction to bind the degrees of freedom to each other, according to a clear equation (instruction Cp); however, to identify the relationship between different degrees of freedom is complicated. Another method adopted in this thesis is using linear elements with a relatively high hardness; each point on the shell is connected to the node i (or the end node j) so that the linear elements transfer the shell behaviour to the node of the linear element.

These linear elements create a relatively high stiffness in the vertical plate on the member axis. If the length of the modelled area by the shell element, the distance between this stiff plate and the connecting area, which is filled with filling material between the pile and leg, is not enough, this stiffness can influence the flexible behaviour of the joint.

3.5.3 Connecting the Pile to the Leg

Another issue is modelling the piles as grouted inside the leg. Connecting the members of the leg and pile in grouted structures is done using a type of grout filling material, which has been described above. Therefore, members of the pile on the horizontal levels of the jacket are connected to the leg in such a way that only the displacement in the

plate perpendicular to the axis of the member of pile and the leg elements bind together, and the pile is allowed to move in the Z direction (element axis).

There are different methods to model this connection. The Cp command mentioned above can be used. It should be noted that each of the commands in the ANSYS software can be defined on the coordinate system.

In some modelled platforms, secondary members are attached to the main member by an offset, and secondary members in some joints also overlap. These joints have been precisely modelled.

3.5.4 Buoyancy effects

The submerged pipe element in the software (pipe 59) does not model the nonlinear behaviour. On the other hand, since the PIPE 20 element is not submerged, it does not consider the hydraulic effects of being submerged. In order to take such effects into account, the following can be done:

- A macro is written in the ANSYS software, which takes into consideration the geometry of the tubular cross-section (diameter and thickness).
- The effect of structure floatation is taken into account by obtaining a new value for ρ : (ρ =density, r = radius, t = thickness)

$$\rho = \rho - \frac{r^2}{2rt - t^2} \qquad (3.3)$$

3.6 Determining the Appropriate Dimensions for Meshing

To prepare a suitable model of a tubular connection using the finite element method, the finite element network must have the features, as given in Table 3.2 below, according to the design manual.

Table 3.2: Platform weight based on the design manual (SP6-1-300, 2002)

No	Load Definition	Weight (kN)
1	Plate Elements	≈ 0
2	Member Elements	----------
3	Member Element Normal Added Mass	10380.260
4	Flooded-Member Element Entrapped Fluid	4789.925
5	Load Cases Converted to Weights	62141.826

Several points need to be considered for optimum meshing, which include:

a. Since there are severe stress gradients on the junction of the main member and the secondary members, so elements with finer dimensions should be used in these areas.
b. Near the end of the secondary and main members, the stress is distributed almost uniformly so elements with larger dimensions can be used.
c. For the balance (equilibrium) equations to be numerically in the best condition, finite element form ratios, i.e. the ratios of length to width, should not be too large or too small; the quadrilateral elements should therefore be almost square in shape and triangular elements should be equilateral. Thus, the length to width ratio of the elements is very important. The appropriate dimensions to reach a maximum acceptable stress distribution is the ratio of 3 to 4, and for maximum displacements it is 10, but to reach above mentioned ratio, it is better to use smaller ratios.

In nonlinear analyses, the analysis time depends on the number of elements and it increases with the increase in the number of these elements. Therefore, the joint is

divided into several areas so that we will have a central area including a part of the main and secondary member. There is an external area including the main member with larger rectangular members, which uses an intermediary area to connect the central section to the external section with rectangular and triangular elements. It should be noted here that there should not be much difference between the dimensions of the elements of the external and central areas. If the sizes of the elements in the external areas are much larger than the sizes of the elements in the central area, unlike the common assumption that we can obtain the desirable answer with less elements, this big difference in dimensions will create too many elements in the intermediary area. There must be a suitable ratio between the dimensions of the elements in these two areas so that this ratio is approximately more than 2 to 2.5. Considering this ratio will reduce the number of elements in the joint, moreover, the triangular elements in the central section of the joint will also be reduced.

The parametric finite element model of the tubular joints has been created using the APDL software programming capability. APDL is an acronym for ANSYS Parametric Design Language, which is a powerful scripting language that allows the user to parameterize the model and automate common tasks. By using APDL, it is easier to:

- Input model dimensions and material properties in terms of parameters rather than numbers.
- Retrieve information from the ANSYS database, such as node location or maximum stress.
- Perform mathematical calculations among parameters, including vector and matrix operations.
- Define abbreviations for frequently used commands or macros.

- Create a macro to execute a sequence of tasks, with if-then-else branching, do-loop, and user prompts.

Due to the creation of high plastic strain in the interface of the connection of two tubes, the meshing of this section has been made finer than for the other parts. SHELL43 elements with four nodes (each node with six degrees of freedom) and the function type 1, which are suitable for analysing the issues related to the final displacement and elasto-plastic, have been used for modelling the connection components. Figure 3.6 depicts a schematic view of the transitional and torsional springs.

In this instance, the main connecting pipe diameter is 1727 mm with a thickness of 32 mm, and the secondary pipe diameter and thickness are 610 mm and 19.1 mm, respectively, which are characteristic of a sample platform connection. At a distance of 2500 mm from the junction of the axes, the load is applied as push-over. Since the members of the connection in the platform model also include axial force, a vertical stress in different forms of tensile and pressure is imported along the axis of the secondary member. The brace is gradually loaded until the failure strength of the joint is reached. Due to the axial compressive force and bending moment applied to the brace, plastification of the chord surface occurred in the vicinity of the joint, and the joint consequently failed.

3.7 Modelling the Connection

First, the effects of platform stiffness were applied by the equivalent springs. The equivalent stiffness of the joint is obtained using the SAP software and binding the nodes and applying forces and moments that create similar displacement and rotation of the members.

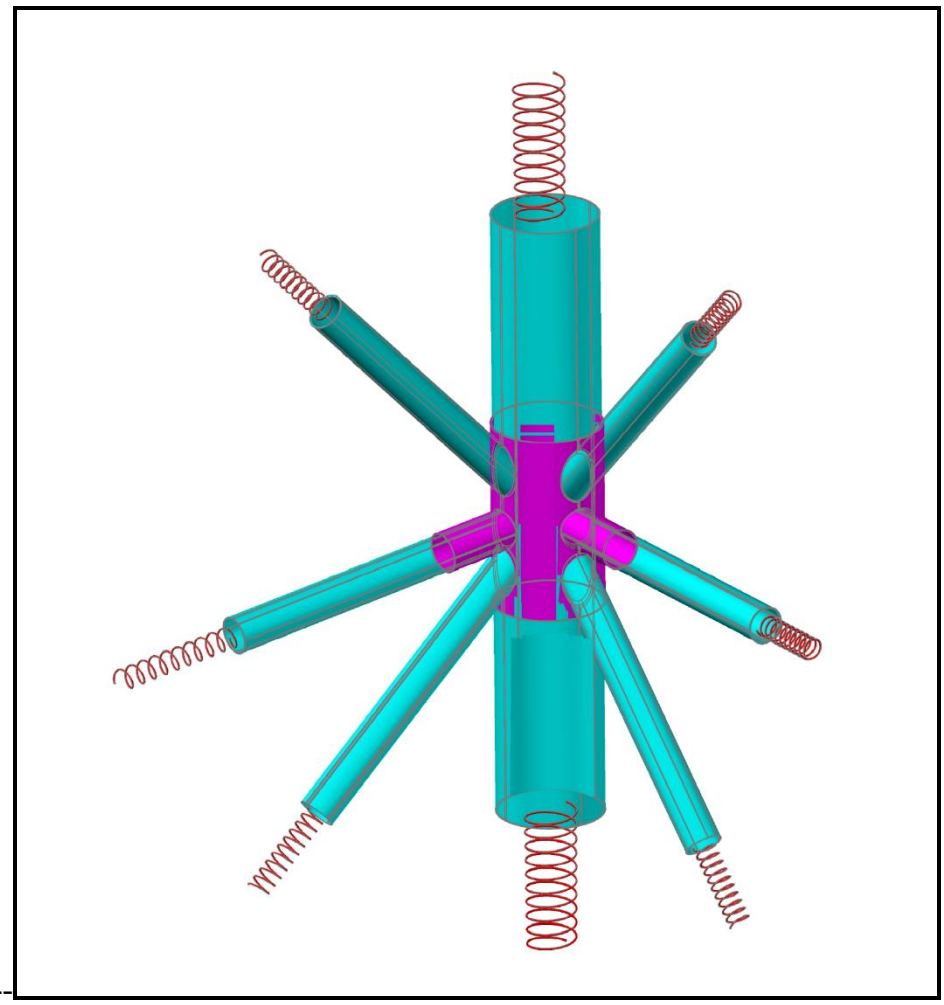

Figure 3.6: Schematic view of the transitional and torsional springs

An example of the modelled joints using the ANSYS software is shown in Figures 3.7 to 3.16. These connections have been modelled with the Joint-can and without the Joint-can. In the next section, the connections will be analysed and the $M-\theta$ diagrams for each joint will be obtained and the results in both cases will be compared to determine the effect of the Joint-can on the connection.

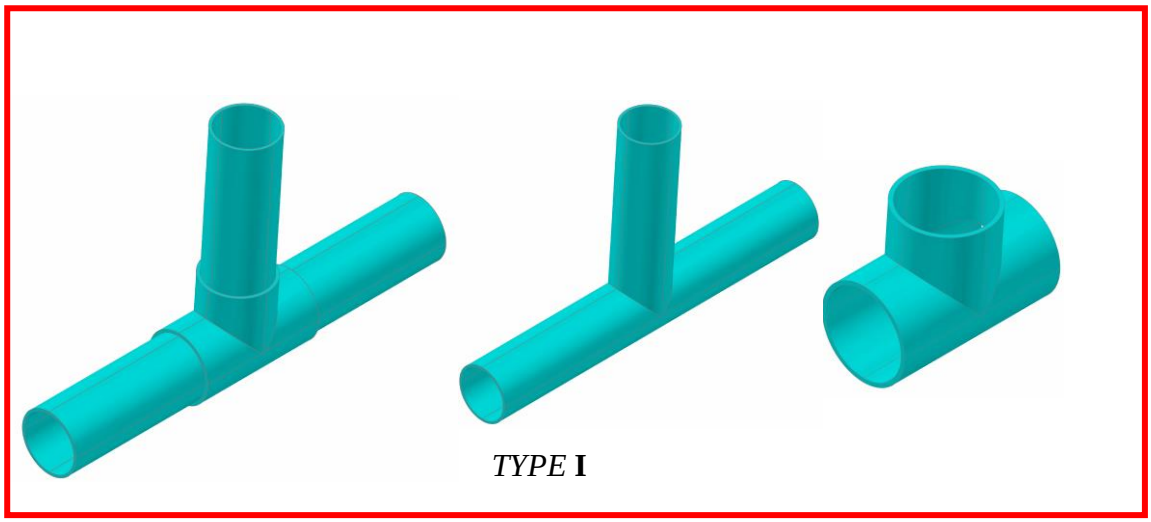

Figure 3.7: View of tubular joints (TYPE I) with Joint-can and without Joint-can

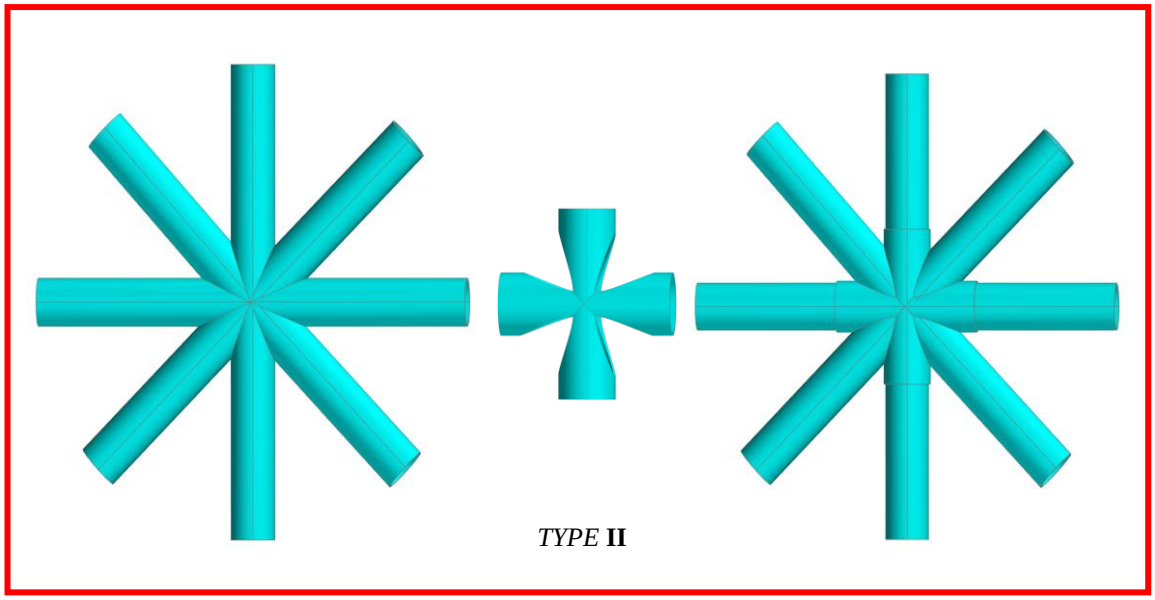

Figure 3.8: View of X tubular joints (TYPE II) with Joint-can and without Joint-can

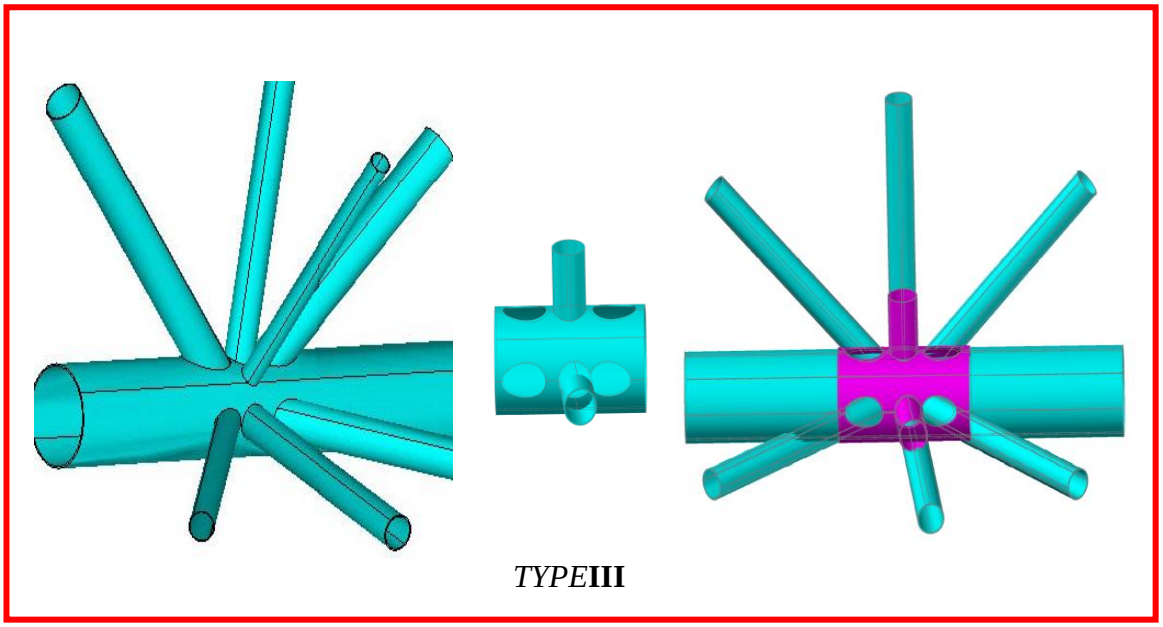

Figure 3.9: Tubular joints (TYPE III) with and without Join-can

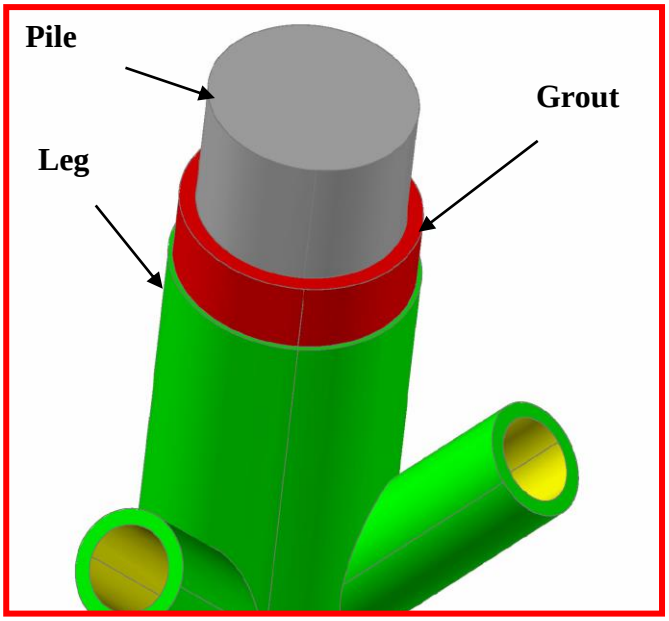

Figure 3.10: Grout modelled using a type interaction element

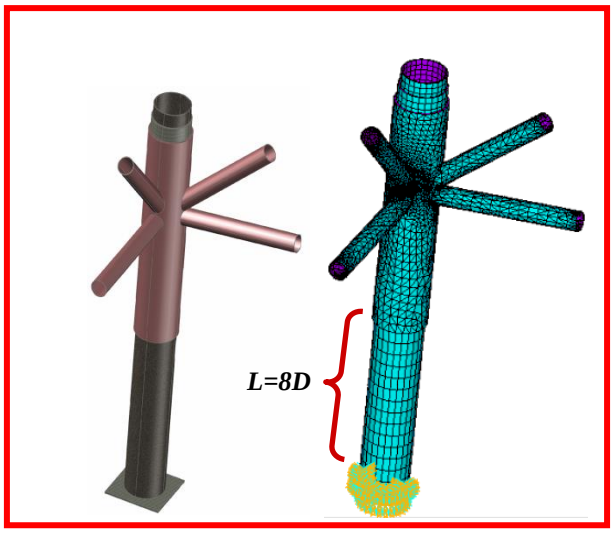

Figure 3.11: Sample modelling of a pile and its equivalent length

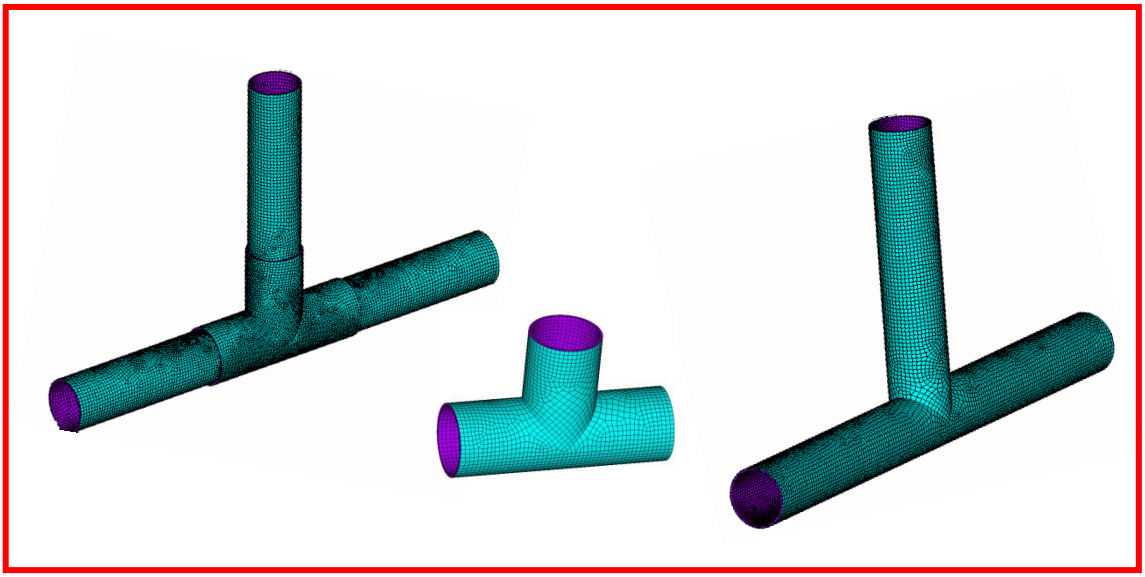

Figure 3.12: Finite element model and the model of T-joint meshing

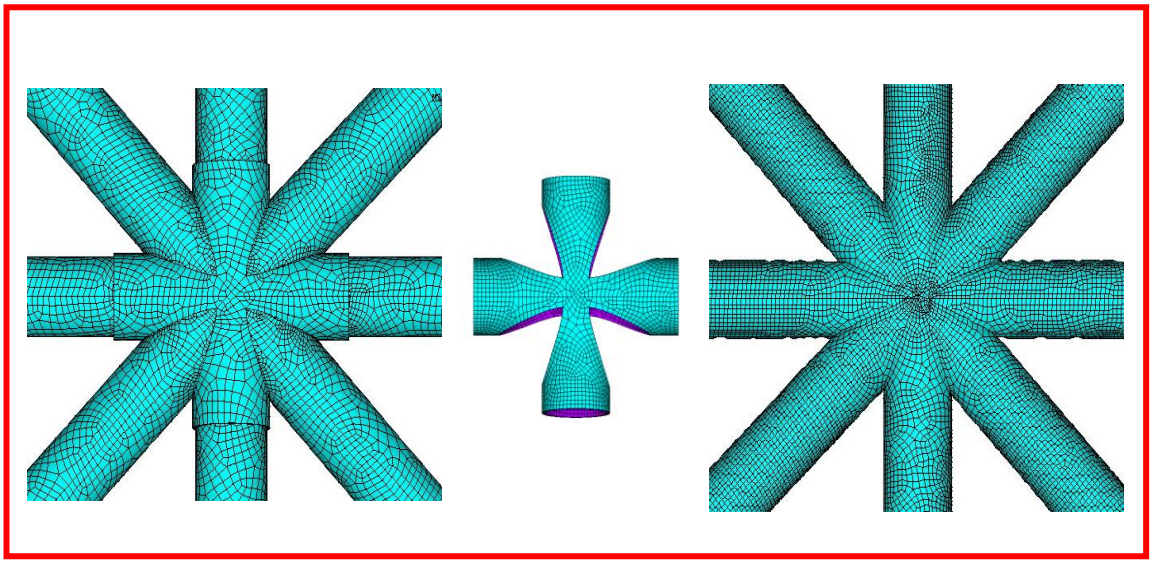

Figure 3.13: Finite element model and model of X-joint meshing

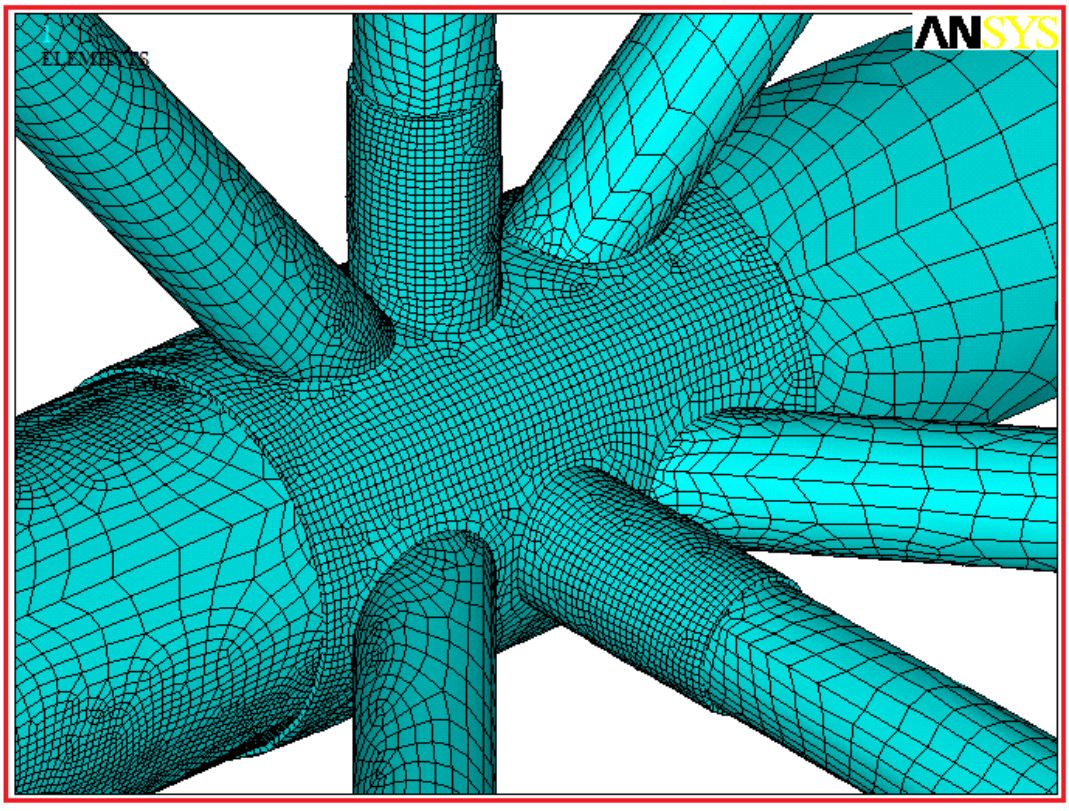

Figure 3.14: Finite element model and model of Joint-can meshing

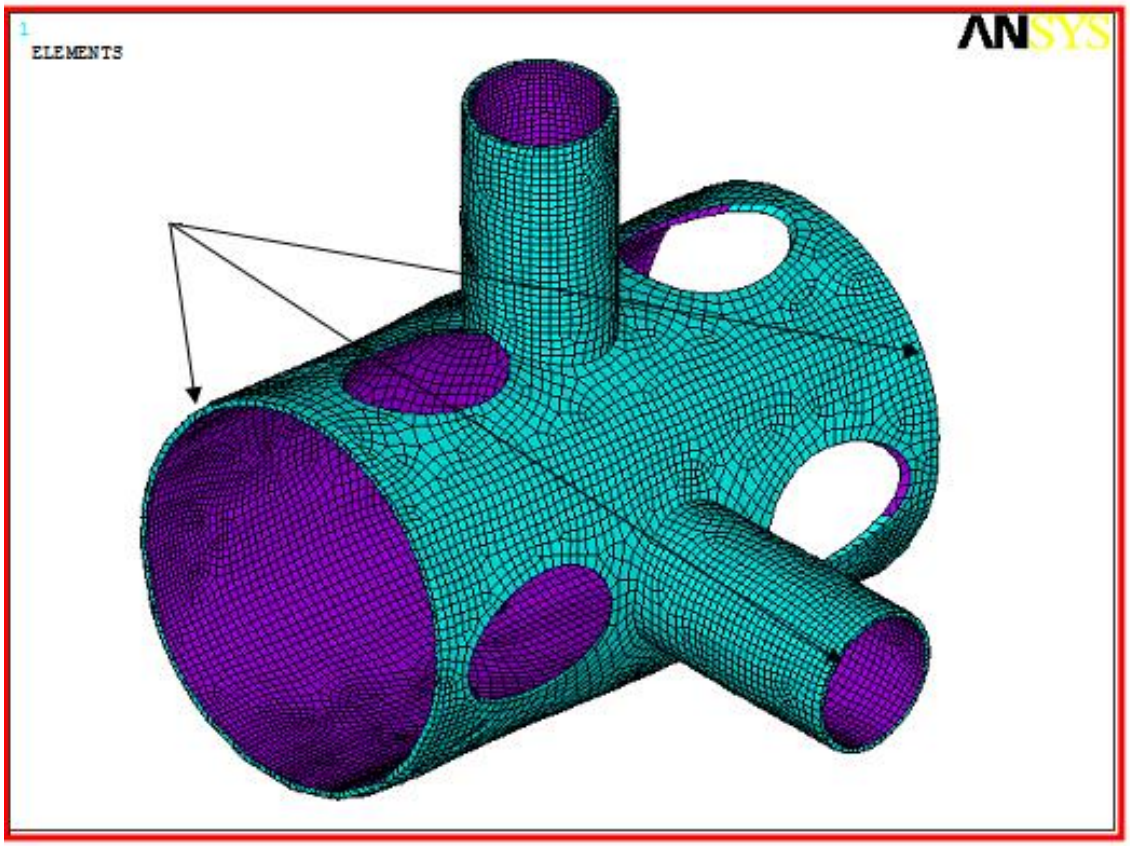

Figure 3.15: A sample of Joint-can glued to the connection

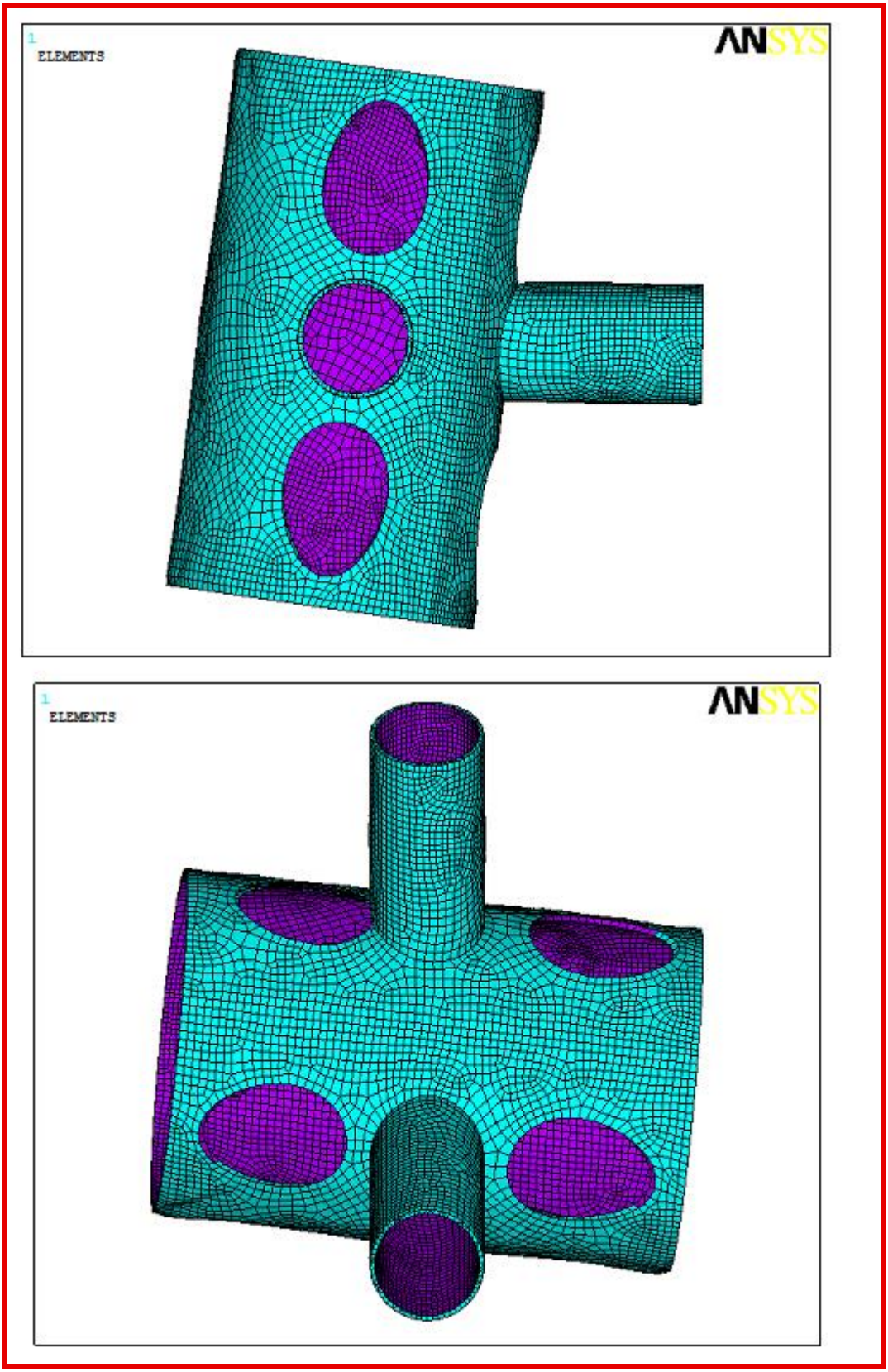

Figure 3.16: View of Joint-can in Bracing place

3.8 Modelling the Platform

The platform modelled in the current study is a South Pars Oil and Gas Field (SPD7), as shown in Figures 3.17 to 3.19. This platform can be modelled using the macro according to the available calculation manual file and the results can be obtained, as shown in Figures 3.17 to 3.19.

3.8.1 Specifications of the Platform

The platform with overall height of 80.50 m, consists of four bases, two of which have a slight slope of 12.27% on two plates and two other bases, one of which is on a vertical (upright) plate, and the other one has a slope of 6.99 %, respectively.

The jacket section is located between -60 m and +4.5 m levels to the LAT. The deck section has been built in four levels between the +5.30m and +20.5m levels. The platform is designed on the extreme load condition, which is the dead load plus extreme environmental load plus maximum live load.

Several points on the modelling condition are worth mentioning here. All the joints on SPD71 are flexible and the joints on SPD72 are rigid. The main purpose of this study is to compare the platform with rigid and flexible joints, and also obtain $M-\theta$ diagrams for different types of joint in flexible mode, without the Joint-can and with the Joint-can, and obtain results for various analyses. In this section, the deck, pile and Joint-can are modelled and all their effects on the entire structure are considered.

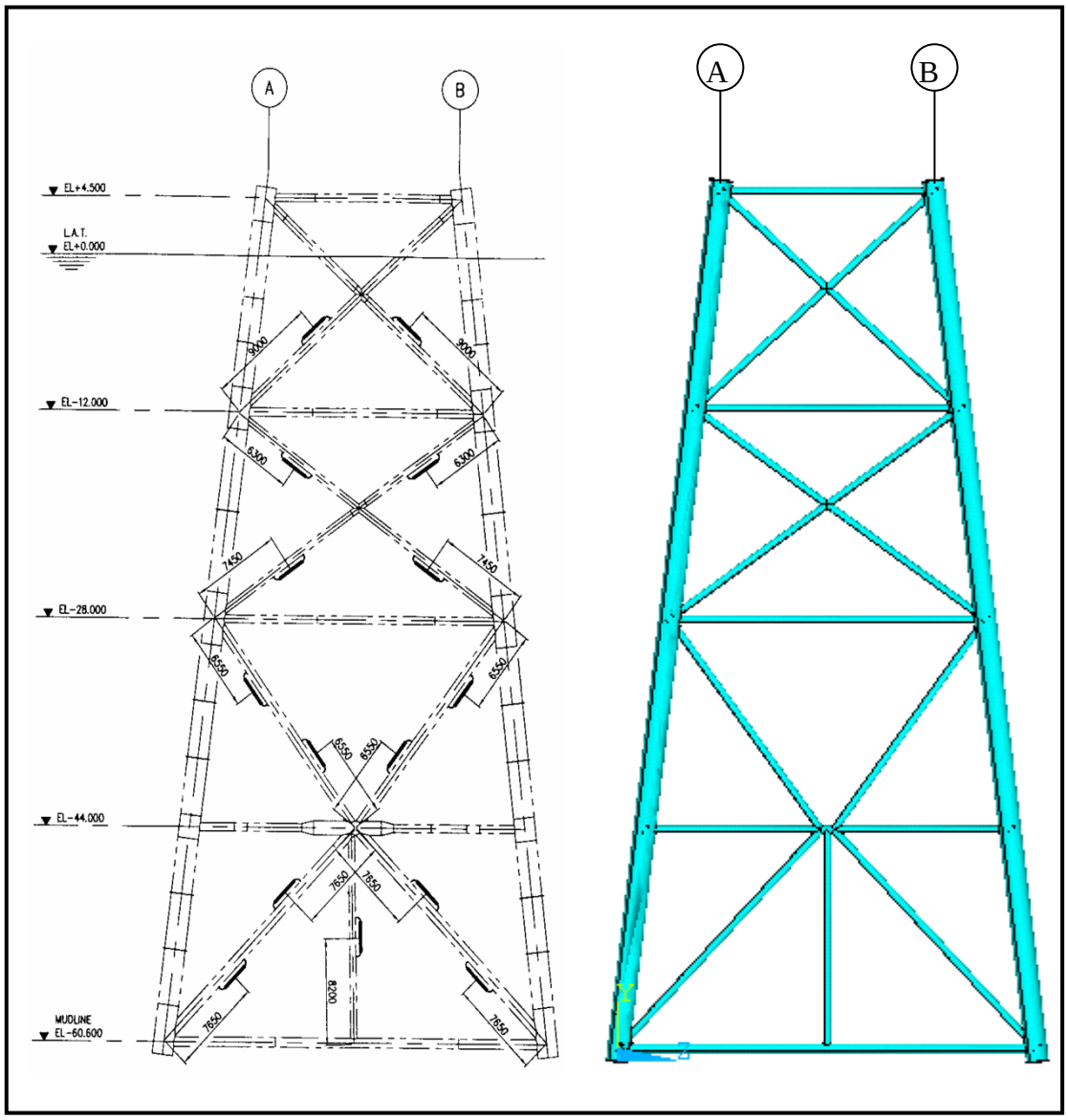

Figure 3.17: West view of platform SPD7

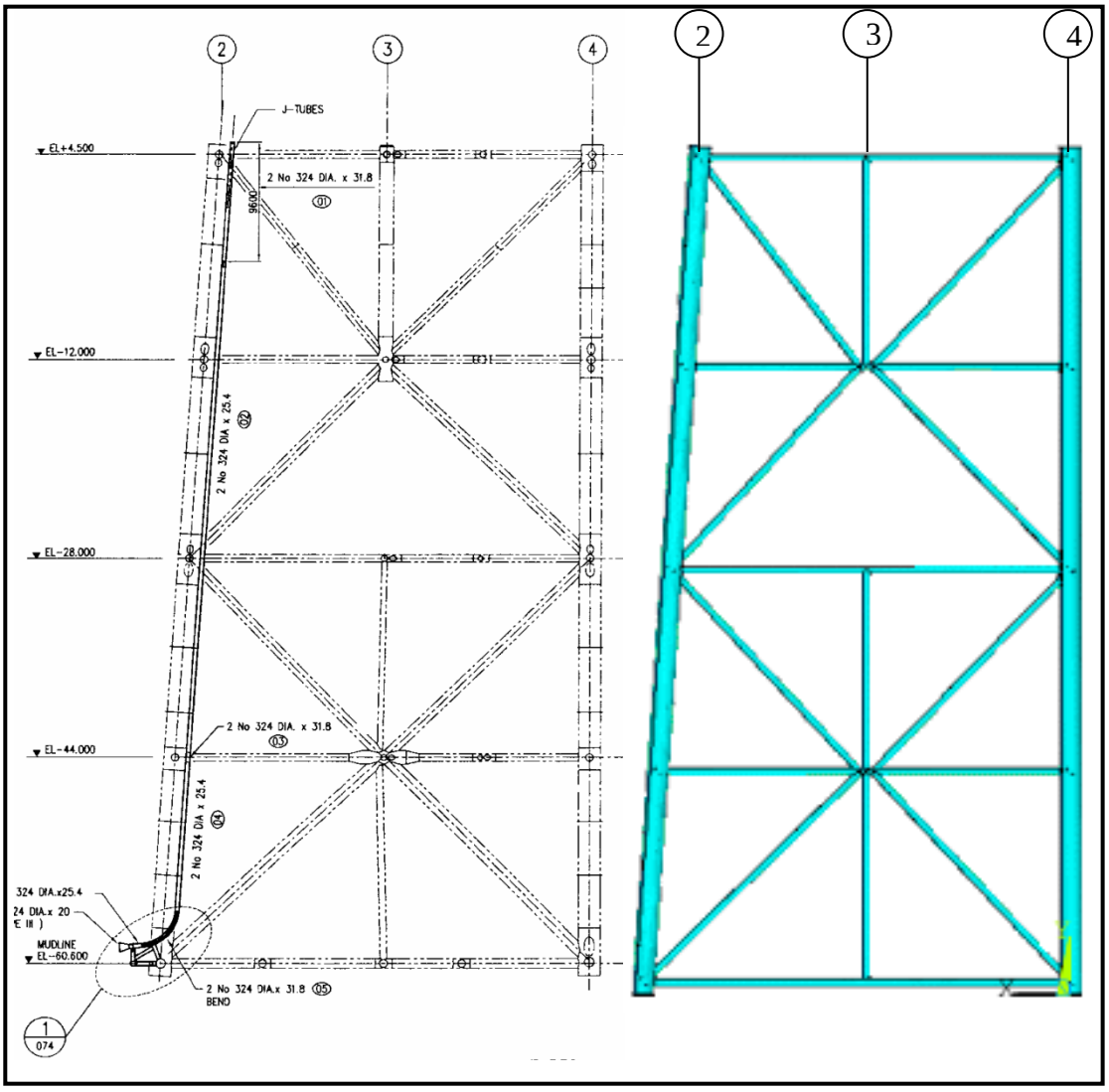

Figure 3.18: North view of platform SPD7

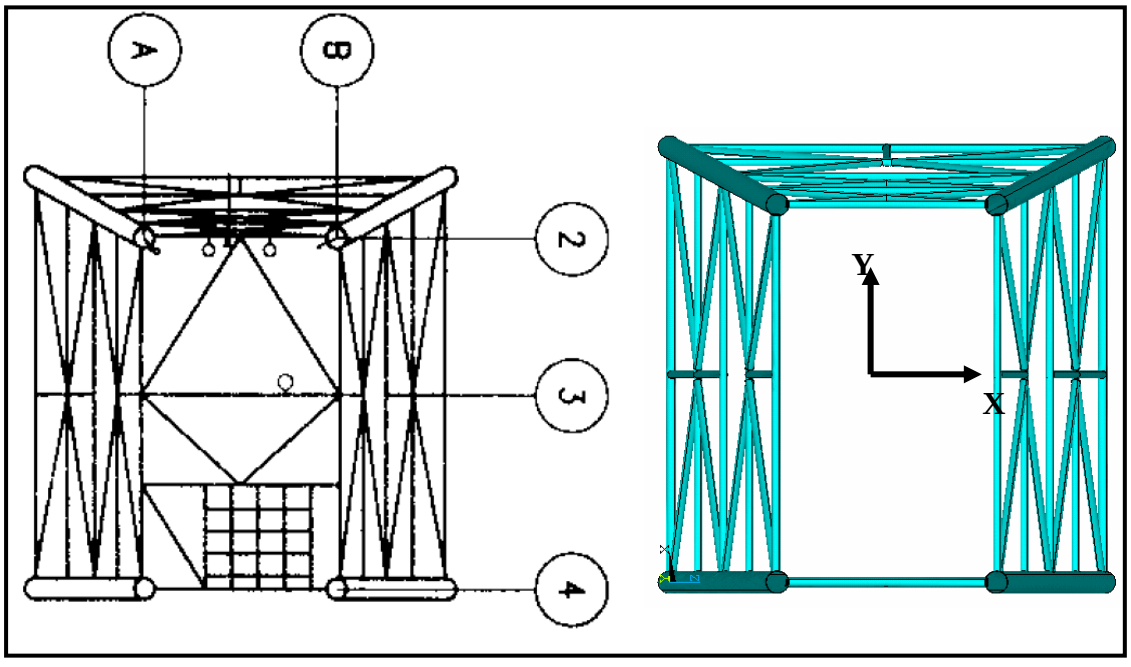

Figure 3.19: Top view of platform SPD7

The element PIPE 20 has been used in the rigid model. Each member is divided into sub-elements along its length (maximum 20 and minimum 8). The cross-section is divided into sub-areas; the number of sub-areas for tubular members is 12 sub-areas. The members (tubes) are connected to each other in a rigid manner. In most platform analysis and design software, this type of connection is used. In the flexible model, the SHELL 43 element with special mesh scheme is used. In Figure 3.20, the platform modelled with PIPE and SHELL elements is shown. There are 1,600 elements in the rigid model and 128,000 elements in the flexible model. Some of them are shown in Figures 3.21 to 3.25.

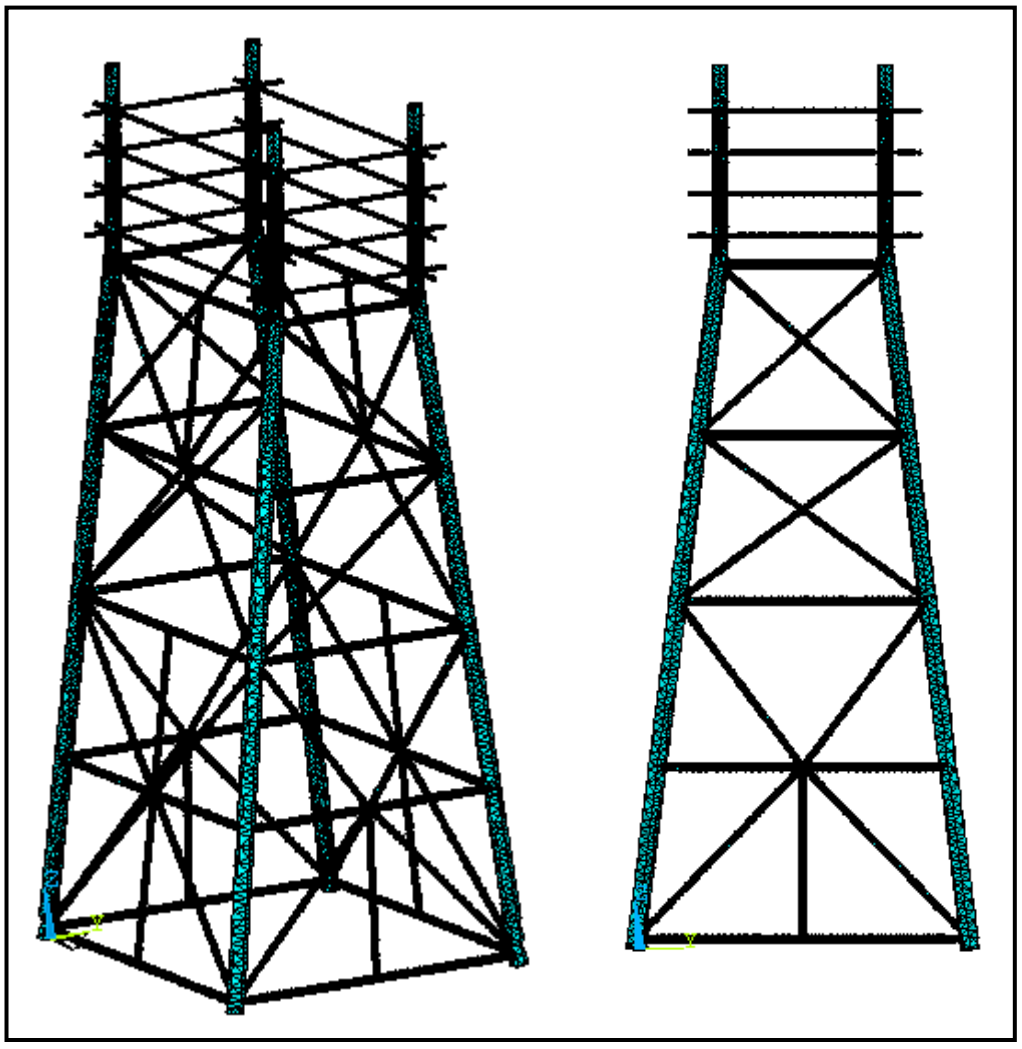

Figure 3.20: General view of the platform with PIPE & SHELL elements

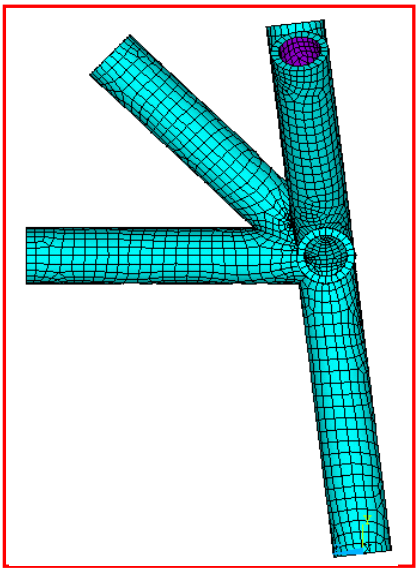

Figure 3.22 : View of secondary members' connection to the leg

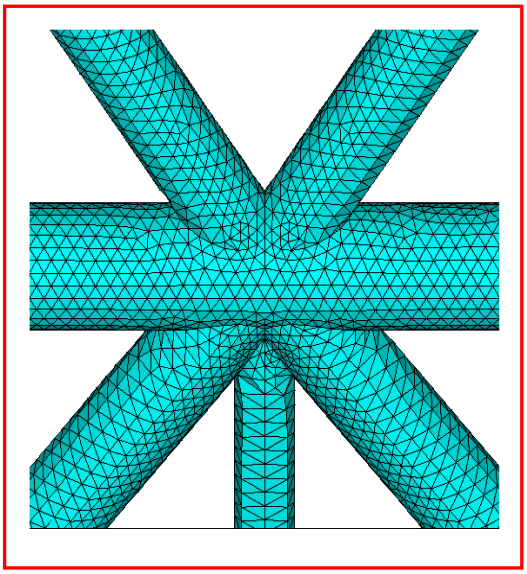

Figure 3.21 : View of intermediate joint (connection) of the platform

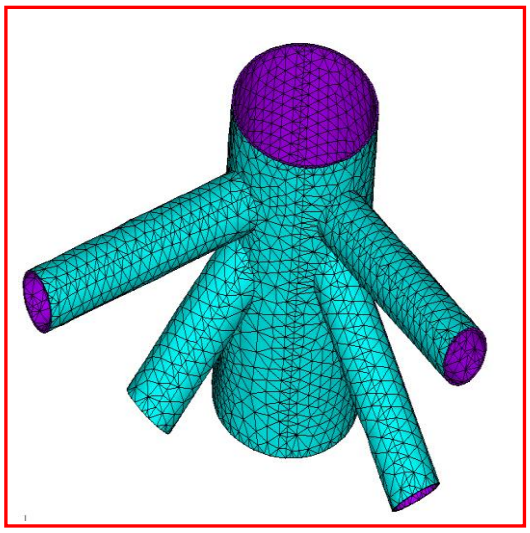

Figure 3.24 : View of horizontal and diagonal members' connection to the leg

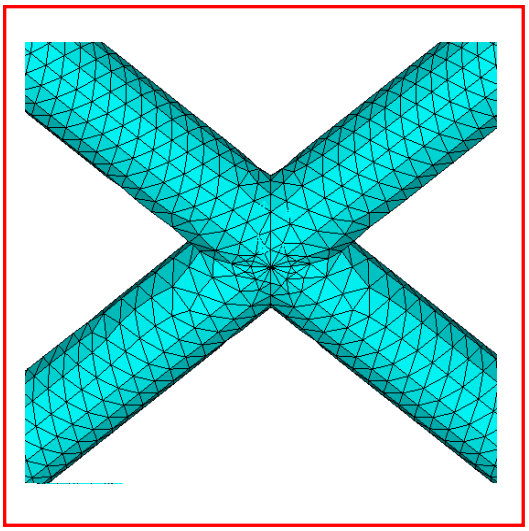

Figure 3.23 : View of the cross connection

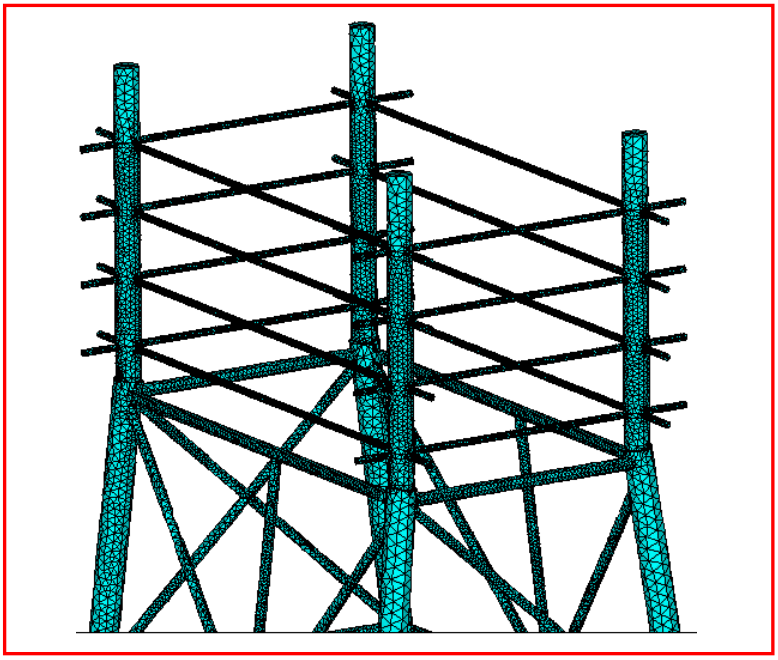

Figure 3.25: Connection of the deck to the leg

This platform has been modelled as a three-dimensional model. In the flexible model, the pile, deck and Joint-can are modelled. The following sections deal with the analyses and obtaining the results of the analyses in the two cases – with Joint-can and without Joint-can – and also obtaining the results for the joints in flexible and non-flexible platforms.

Since the platform is modelled three-dimensionally, all the masses in the design manual are applied to the platform.

3.8.2 Determining the Convergence Criteria of Nonlinear Analysis

The ANSYS software provides four criteria including force, moment, displacement and rotation in order to apply the convergence criteria and control of convergence of the results. Therefore, we can specify the convergence criteria in each one of the cases, i.e. force, moment, displacement and rotation, or it is possible to choose a combination of the above-mentioned items as the convergence criteria. In addition, for each of the

above-mentioned cases, we can define different tolerable convergence limits. The force convergence criterion should be introduced to the program as one of the convergence criteria.

3.8.3 Strategies of Convergent Results in Nonlinear Analysis

Facing non-convergence of the model, we can apply the following method, which is helpful in achieving convergence of the results in the nonlinear analyses.

1 - Automatic Time Step Selection

This feature can be used to determine the number of subdivision steps of the loading step. The program is allowed to determine the number of loading sub-steps according to the number of iterations and its lack of convergence. For this purpose, the maximum number of sub-steps of a loading step should be introduced to the program. It works in such a way that if the initial results in the introduced loading sub-steps do not converge, the program, according to the maximum number of sub-steps defined, continues to reduce the sub-step into smaller sub-steps until the results converge.

2 – Halving the Load Sub-Steps

If the repetitive analytical operations in a sub-step do not lead to convergence, using this feature, that sub-step is divided into two halves automatically and an analysis is repeated to converge the results. If the results still do not converge, the halved load sub-steps are halved again automatically. This action continues until the sub-steps are equal to the minimum time defined by the user.

3.9 Code Considerations in Offshore Platform Analyses

The most important and popular code for the analysis and design of offshore fixed platforms is the API-RP-2A Code, which was proposed by the American Institute of

Petroleum. The first edition of the code, which was published in 1969, proposed the UBC code for the seismic designing of such structures. In this code, two levels of earthquake have been defined for designing offshore fixed platforms:

- *Resistance level earthquake*:

  The probability of its occurrence during the life of a structure (equal to a 100 or 200 year period) is about 20% to 50%. In this case, the efficiency of all the elements and joints of the platform must be inspected and assured, assuming the perfectly elastic behaviour of the structure.

- *Plasticity level earthquake*:

  The probability of its occurrence during the life of a structure is about 10% to 20% (equal to a 1000 to 2000 year period). In this case, it should be shown that the platform has sufficient capacity to absorb the energy caused by powerful earthquakes (in addition to resistance against structural damage but without the total failure of the structure).

A brief description of the design principle that is currently used in the above-mentioned code is as follows:

a. The choice of analysis method

   The analysis of offshore platforms' response to the forces resulting from earthquakes should be carried out using well-known methods like spectral analysis or history analysis. However, other methods can also be used depending on the designer's opinion.

b. Earthquake risk estimation

   In areas with a high risk of earthquake, the intensity and other properties of the earthquake should be obtained as the basis of the design (resistance or plasticity level), which is done through a separate specialised study.

c. Seismic zoning

In areas with a lower risk of earthquake, the environmental loadings, such as waves and winds, are more detrimental than earthquake loadings in the overall design of the platform. In areas in which the horizontal acceleration of earthquake resistance level is less than 0.05 g (since environmental loadings other than earthquakes will definitely govern the designing results), there is no need for any kind of specific analysis and design against earthquake forces. For areas where the horizontal acceleration of earthquake resistance level ranges from 0.05 to 0.10 g, we can carry out the seismic analysis and design of the platform using the properties of a plasticity level earthquake based on the proposed method in the resistibility level earthquake (i.e. linear elasticity analysis).

d. Designing for resistance level earthquake

In this case, the load-carrying efficiency of all the elements and joints (connections) of a structure should be provided through an elasticity analysis, using methods like spectral analysis or history analysis, without imposing any structural damage to the platform.

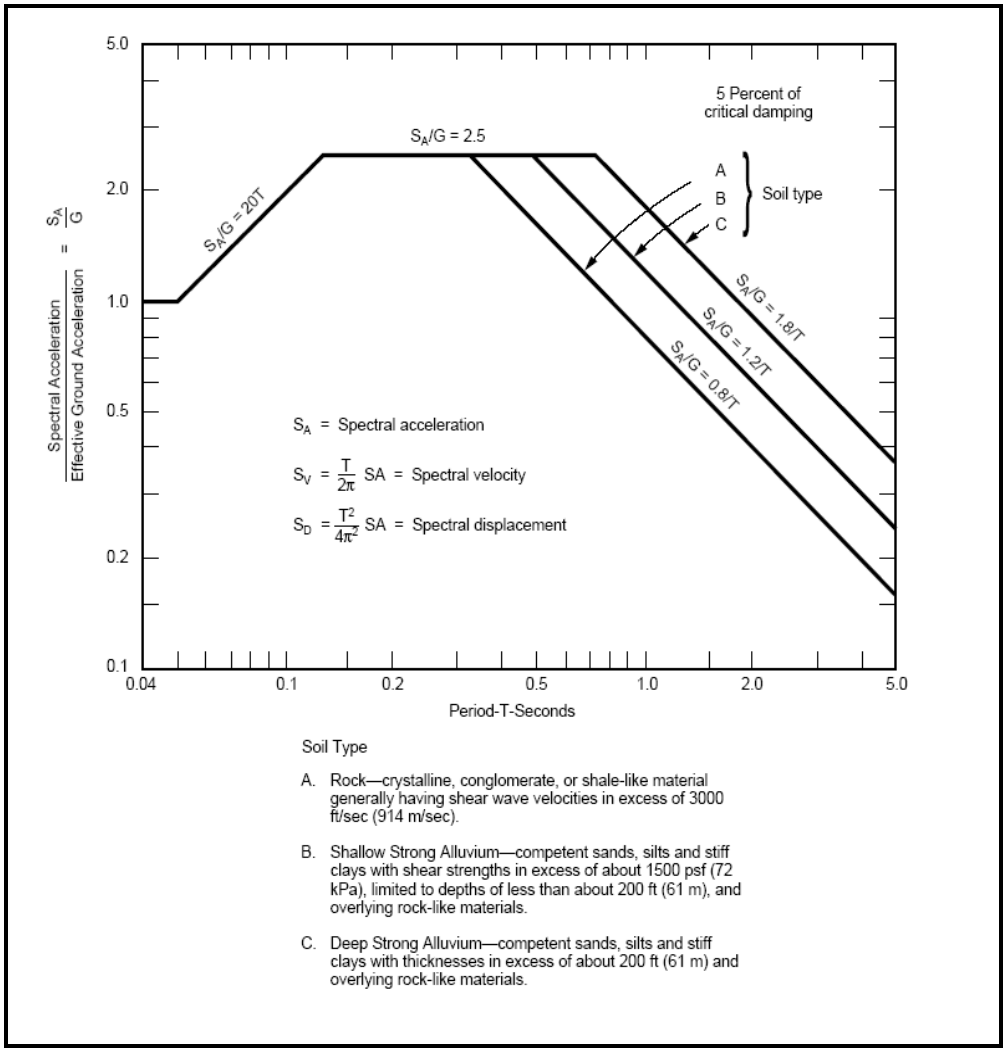

Figure 3.26: The spectrum proposed by API for designing offshore platforms which are resistant against earthquakes (API, 2000)

The spectrum proposed by the API is shown in Figure 3.26. In using this spectrum, the maximum value of spectral acceleration read on this curve should be multiplied by the value of the ratio of maximum earthquake acceleration to gravity acceleration. In this response spectrum, four different areas have been presented for the spectral acceleration values, based on the varying values of the main period of structure vibration. This spectrum has been devised for earthquakes with a return period of 200 years and a damping percentage (ξ) of 5% (API, 2000).

e. Designing for plasticity level earthquakes

The aim of providing special regulations for controlling the plasticity of platforms in areas with a high risk of earthquakes is to ensure that there is a sufficient energy absorption capacity in such structures without the total failure and collapse of the structure in the case of a powerful earthquake.

The properties of a plasticity level earthquake should be determined by special seismic studies and earthquake risk analysis in a certain area. In this case, using a nonlinear elasto-plastic analysis, we should be able to show that the total energy created by an earthquake can easily be absorbed by the elements (members) and connections of a structure without it suffering any total failure or even progressive failures (damages) in the structure. In investigating the load carrying condition of a platform against the lateral forces caused by a plasticity level earthquake, it should be shown that a structural system, despite having some degrees of uncertainty, is capable of redistributing and creating sufficient plastic deformations before the occurrence of total failure and the collapse of the whole system.

3.10 General Description of the Analyses Performed in this Study

The analyses performed on the models include non-linear static, modal analysis and dynamic non-linear analyses, which are described in the following sections.

3.10.1 Nonlinear Static Analysis

In nonlinear analysis, dividing the load into incremental parts is important. The incremental loads can be applied to several steps or sub steps of a loading. After the completion of each phase of the analysis process, the program rewrites the stiffness matrix for entry to the next phase. If the solution is done purely incrementally, it can cause accumulation errors (Figure 3.27).

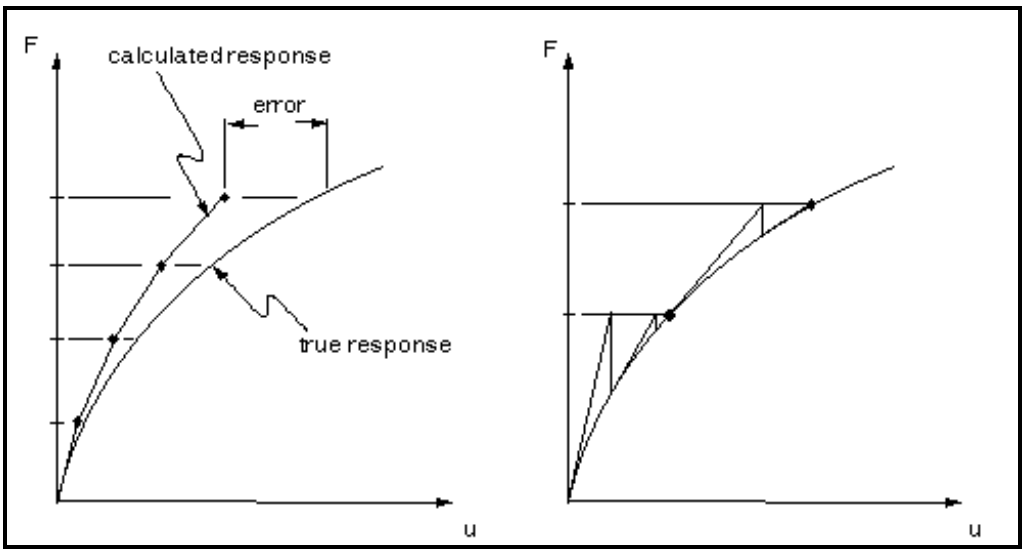

Figure 3.27: The direct solution in comparison with Newton-Raphson method (SW ANSYS Academic Teaching, 2011)

The ANSYS software will fix these errors using the Newton-Raphson method. Before each analysis step, in the Newton-Raphson method, the amount of non-balanced load resulting from the difference between internal and external forces is calculated. The program makes a linear solution and controls the error value with the permissible limit. If the convergence criterion is not adopted, the unbalanced value is recalculated and the stiffness matrix can be rewritten and a new solution is created. This will continue until the problem becomes convergent.

Loading is done in different forms in the nonlinear analysis, for example, Figure 3.28 shows the loading history that includes three steps. In the first step, we have incremental loading, in the second step a fixed load, and, in the third step, the load is removed. Also dividing the loading steps into different forms is based on the desired model. In Figure 3.29, the first step includes five sub-steps, each of which is performed with a repetition. The second step includes a load step with several repetitions.

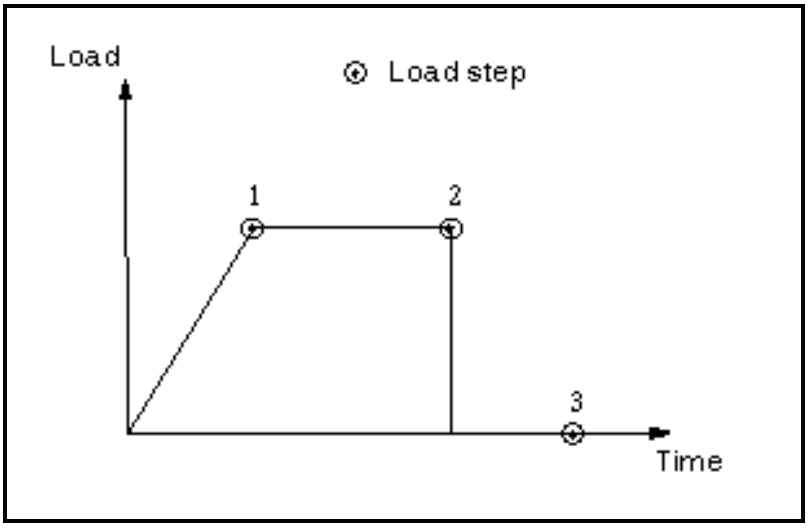

Figure 3.28: Steps of a loading (SW ANSYS Academic Teaching, 2011)

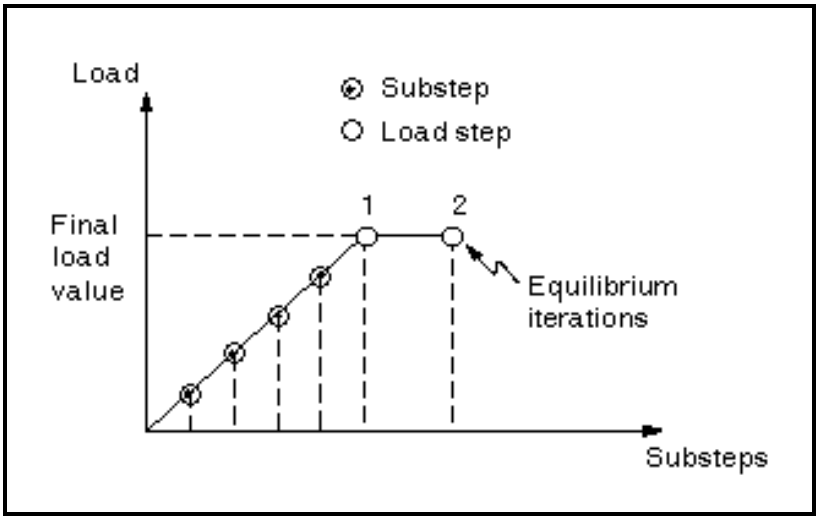

Figure 3.29: Dividing load steps into different parts (SW ANSYS Academic Teaching, 2011)

The nonlinear static analysis procedure is:

1. Loading is applied to the structure as step-by-step.
2. The coordinates of nodes are updated in each step.

3. Structural stiffness at each stage is determined based on the new geometry of the structure.
4. Each element is controlled to check whether or not the stress has exceeded the plastic stress limit. In the event of this, loading will be scaled in such a way that the amount of load is exactly the amount needed for the section to be plastic.
5. As the element load reaches the flow level, a plastic hinge (joint) is formed. This joint will be removed in the case of unloading and the element entering the elastic range.
6. In the case of diagnosis of instability in the overall system, unloading will be performed.

3.10.2 Modal Analysis

In the stage of the structural design of industrial components which are subject to fluctuations due to the loads and vibration stimuli, performing modal analysis is necessary because the component should be designed so that it is away from the severe frequency range as much as possible because the fluctuations in the severe frequency range increase the oscillatory domain, and, hence, the high risk of the disintegration of the component.

Modal analysis is used to determine the value of the natural frequencies and the shape of its mode in that frequency. The natural frequency value of each structure depends on its shape, material and its supports.

The ANSYS software provides the user with a variety of numerical methods to extract and calculate the modes and characteristic values, which are:

• Block Lanczos Method

• Subspace Method

• Reduced Method

• Powerdynamics Method

The Block Lanczos Method is a very efficient algorithm to perform a modal analysis for large models. It is a fast and robust algorithm and used for most applications as the default solver.

The Subspace Method was popular in earlier years since very little computer resources were necessary to perform a modal analysis. However, compared with the Block Lanczos Method, the Subspace Method is fast for small models but the solution time increases as soon as larger models are considered.

The Reduced Method is also an old eigensolver, which works with reduced matrices in order to minimize the number of dynamic degrees of freedom. Master degrees of freedom have to be chosen that represent the dynamic response of the system as accurately as possible. Neither the Subspace Method nor the Reduced Method is popular today.

The Powerdynamics Method is a special algorithm based on the Subspace Method. During the Subspace Algorithm linear systems of equations have to be solved. For this purpose, ANSYS provides several equation solvers. Typical solvers for problems in structural mechanics are the Sparse Solver, the Frontal Solver and the Pre-conditioned Conjugate Gradient Solver (PCG-Solver). Each of these equation solvers has its special characteristics. In this stage, we focus especially on the Frontal Solver and the PCG-Solver since both can be used within the Subspace Method. By default, the Subspace Method, as mentioned above, uses the Frontal Solver to obtain the first natural frequencies of a structure. This solver works efficiently for small models of up to 50,000 active degrees of freedom. However, if models consist mainly of solid elements with more than 50,000 active degrees of freedom, the Subspace Method combined with

the PCG-Solver should be the preferred solution method. In ANSYS the combination of the Subspace Method together with the PCG-Solver is called the Powerdynamics Method. For large models of up to 10,000,000 degrees of freedom, this method significantly reduces the solution time. Another characteristic of the Powerdynamics Method is the lumped mass matrix formulation. In a lumped mass approach, the mass matrix is diagonal since the mass is considered concentrated at the nodes. Note that the Subspace Method is the only eigensolver in ANSYS where the user has the option to specify the equation solver.

In considering the above information, the Block Lanczos method is used in the present study since it is suitable for large deformations and symmetrical shapes.

To perform the modal analysis in the ANSYS software the following main steps were carried out:

1. Input the geometry
2. Define the material
3. Generate the mesh
4. Apply loads by applying constraints to the model
5. Obtain the solution by choosing the Modal type of analysis and Block Lanczos option
6. Review the results by listing the natural frequencies and animate the eight mode shapes

3.10.3 The Transient Dynamic Analysis

One of the important decisions in a structural analysis is assuming the linear or nonlinear relationship existing between the forces. Linear analysis has been used for the

static or dynamic loads in structural design. The nonlinear analysis method has been used extensively because performance-based tips require presentation of nonlinear response (behaviour). There are two sources of nonlinear response (behaviour). First, the nonlinear relationship between the force and displacement, which is true in all cases. Second, the type of nonlinear response caused by entering large displacements in equilibrium and compatibility equations.

Table 3.3 : Trends of structural analysis for designing purposes (API, 2000)

Category	Analysis Procedure	Force–Deformation Relationship	Displacements	Earthquake Load	Analysis Method
Equilibrium	Plastic Analysis Procedure	Rigid-plastic	Small	Equivalent lateral load	Equilibrium analysis
Linear	Linear Static Procedure	Linear	Small	Equivalent lateral load	Linear static analysis
	Linear Dynamic Procedure I	Linear	Small	Response spectrum	Response spectrum analysis
	Linear Dynamic Procedure II	Linear	Small	Ground motion history	Linear response history analysis
Nonlinear	Nonlinear Static Procedure	Nonlinear	Small or large	Equivalent lateral load	Nonlinear static analysis
	Nonlinear Dynamic Procedure	Nonlinear	Small or large	Ground motion history	Nonlinear response history analysis

Generally, a seismic analysis involves gravity loads and the presentation of ground motion in a structure location. The vibrating motion of the ground including the mass of the structure for creating acceleration, and the history of the created response can be calculated using the dynamic analysis methods. In most designing trends, it is usual to perform a dynamic analysis with a response spectrum representing the expected ground motion in the specified point (API, 2000).

For the seismic analysis, the transient dynamic analysis used in this study. By using this analysis (which is sometimes called the Time History analysis), we can calculate the dynamic response of a structure under the influence of time-related loadings. It is

possible to calculate displacements, stress, strain and forces changing with time in a structure via this analysis.

This analysis is usually more difficult than a static analysis. It requires more hardware resources for its calculations and consumes more time to solve any problem.

There are three methods to perform matrix calculations in the transient dynamic analysis:

1. Full Method
2. Reduced Method
3. Mode Superposition Method

The Full Method does not reduce the dimension of the considered problem since original matrices are used to compute the solution. As a consequence, it is simple to use, all kinds of nonlinearities may be specified, automatic time stepping is available, all kinds of loads may be specified, masses are not assumed to be concentrated at the nodes, and, finally, all the results are computed in a single calculation. The main disadvantage of the Full Method is the fact that the required solution time will increase with the size of the model considered.

The Reduced Method originates from earlier years. Because of the reduced system matrices, which are used to solve the transient problem, this method has an advantage when compared with the Full Method with respect to the required solution time. However, the user has to specify the master degrees of freedom, which represent the dynamic behaviour as good as possible. The only nonlinearity that can be specified is node-to-node contact via a gap condition. However, automatic time stepping is not possible. Consequently, this method is not very popular any more since its disadvantages do not really compensate the advantage of lower costs in solution time.

The Modal Superposition Method usually reduces the dimension of the original problem as well since the transient analysis is finally performed in the modal subspace, which has the dimension of the number of mode shapes used for the superposition. The main advantage is again the reduction of solution time. It turns out that this method is actually the most efficient one compared with the other two. The accuracy just depends on the number of mode shapes used for the modal superposition. Even if a few mode shapes are taken the requested solution time might still be less when compared with the Full and the Reduced Method. Contact can be applied using the gap condition we mentioned in the discussion of the Reduced Method. The time step has to be chosen as constant, which means that automatic time stepping is not available for this method. It should also be noted that a modal analysis has to be performed before the transient problem can be solved with the modal superposition technique. Hence, the solution process basically consists of two analyses, the modal analysis and the transient analysis in the modal subspace. Since for most problems in structural dynamics the natural frequencies of a structure are of interest, this is not really a disadvantage. Summing up, using the modal superposition technique for a transient analysis reduces not only the solution time, but the user also obtains information about the natural frequencies and the undamped mode shapes, respectively.

In comparing the above solution options, the Modal Superposition Method is the most powerful method considering the required solution time. However, it cannot handle nonlinearities. The Full Method requires more time to finish the analysis but can handle nonlinearities. The method used in the current study was the full method of calculation.

In this study, the modelled structure was subjected to the acceleration from Tabas earthquakes. Acceleration mappings were taken from data from the PEER Strong Motion Database website.

By using the Macro software programming capability, the models were analysed dynamically. Thus, the first acceleration of gravity was applied on the structure, followed by applying the acceleration to all nodes of the structure in each time step. Each time step is also divided into five parts or sub-steps.

The main steps given below were followed to perform the dynamic time history analysis in this study:

1. Define analysis type and set performance
2. Input geometry
3. Define element type, real constants and material model properties
4. Generate mesh
5. Apply loads by applying the Tabas acceleration to the model
6. Obtain solution
7. Review results

CHAPTER IV

RESULTS AND DISCUSSION

4.1 Introduction

As noted before, the results of the analyses based on the assumption of rigid joints, differ considerably with the actual behaviour of structures, and these differences can be observed in several cases.

In this section, a platform and its joints are modelled in two rigid and flexible joint cases using three-dimensional modelling. The selected platform (platform SPD7, Phase 8) belongs to the South Pars oil field. The platform, which is a fixed type platform with four bases, is a wellhead platform of the Resalat platform set. The jacket of the platform consists of five main levels and its bracing system is of the X type. In addition, its joints are equipped with a Joint-can system.

4.2 Joint Analysis

First, before obtaining the dynamic characteristics of the platform, we need to have an estimation of the flexibility rate of the joints to make it clear whether there is a need to consider the flexibility of the platform joints as considerable or negligible. This can be observed through the comparison of the $M-\theta$ curves for the connections with the Joint-can and without the Joint-can.

Figure 4.1 shows the stress distribution of the von-mises type, which resulted from the static analysis for connection types I, II and III. As can be observed, the maximum combined stress is around the intersection area and by moving away from the intersection the stress is seen as reducing.

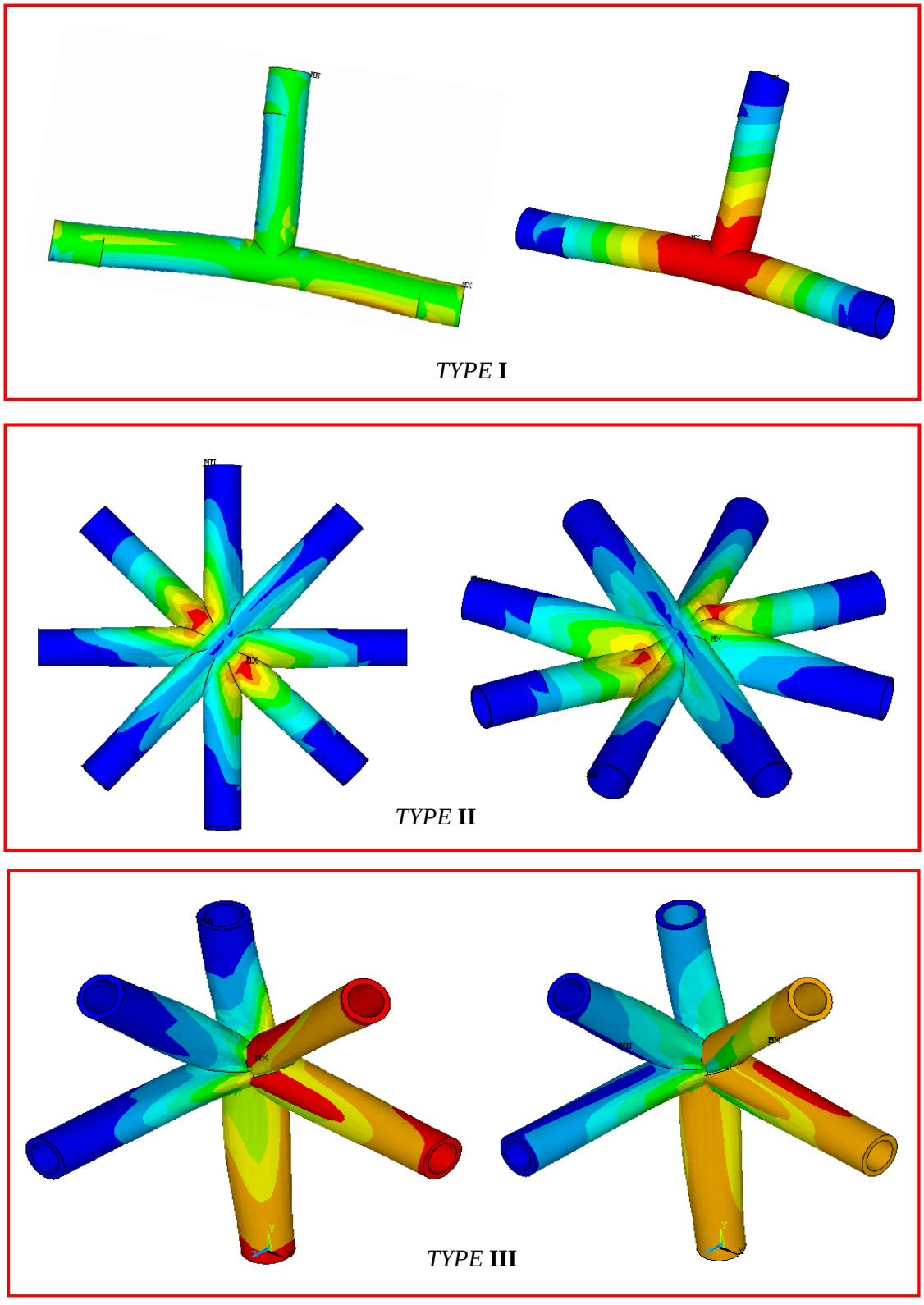

Figure 4.1: Stress distribution of von-mises for different types of joint

Figures 4.2 to 4.10 illustrate the Moment-rotation relationships for the three mentioned types in three axes. Comparing the $M-\theta$ diagrams for each joint in the x, y and z directions for the with Joint-can and without Joint-can cases, it can be concluded that the flexibility of the joints in the with Joint-can case decreased considerably compared to the without Joint-can case.

It should be noted that the plasticity parameter was used for the quantitative expression of the flexibility rate because the flexibility rate cannot be calculated in terms of quantity.

Therefore, comparing the $M-\theta$ diagrams and calculating the amount of plasticity for each joint in the with Joint-can and without Joint-can cases, we can observe that the plasticity reduces about 10% and the energy dissipation reduces about 5%.

As a result, these diagrams can be used as equivalent springs in joint locations in the future, reducing the total amount of computing in all platforms.

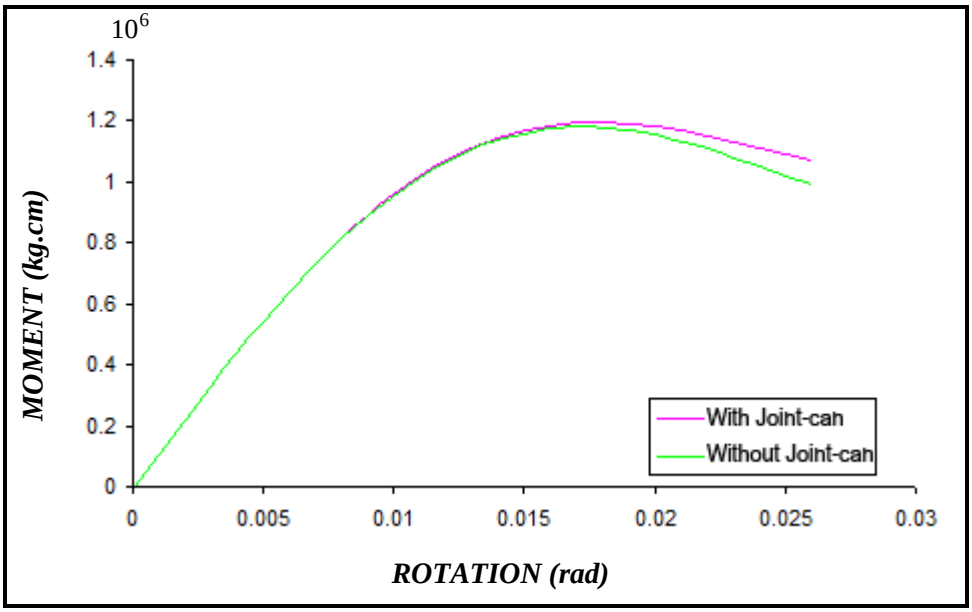

Figure 4.2: Moment-rotation diagram of joint TYPE I around X-axis

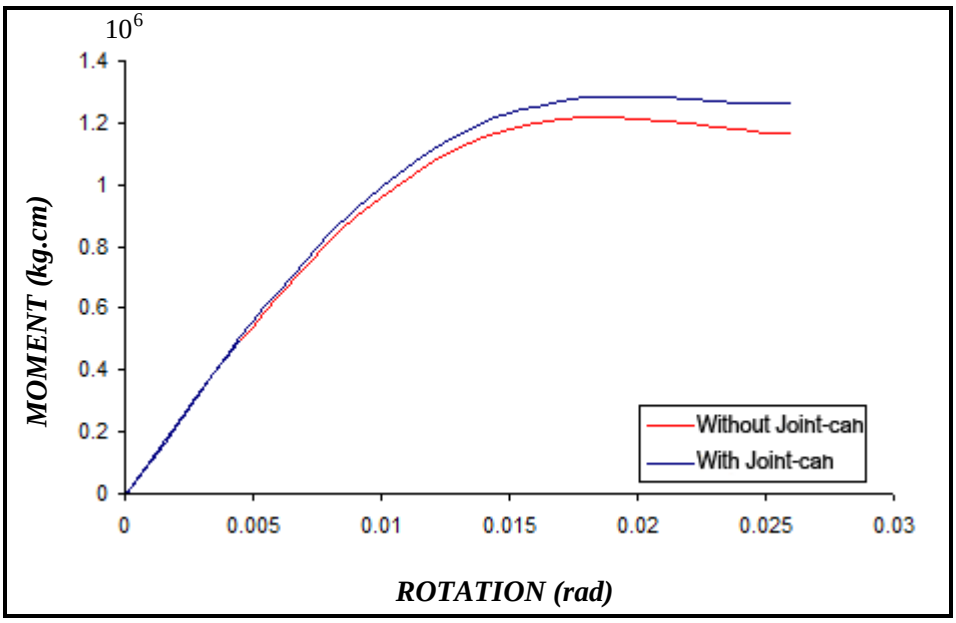

Figure 4.3: Moment-rotation diagram of joint TYPE I around Y-axis

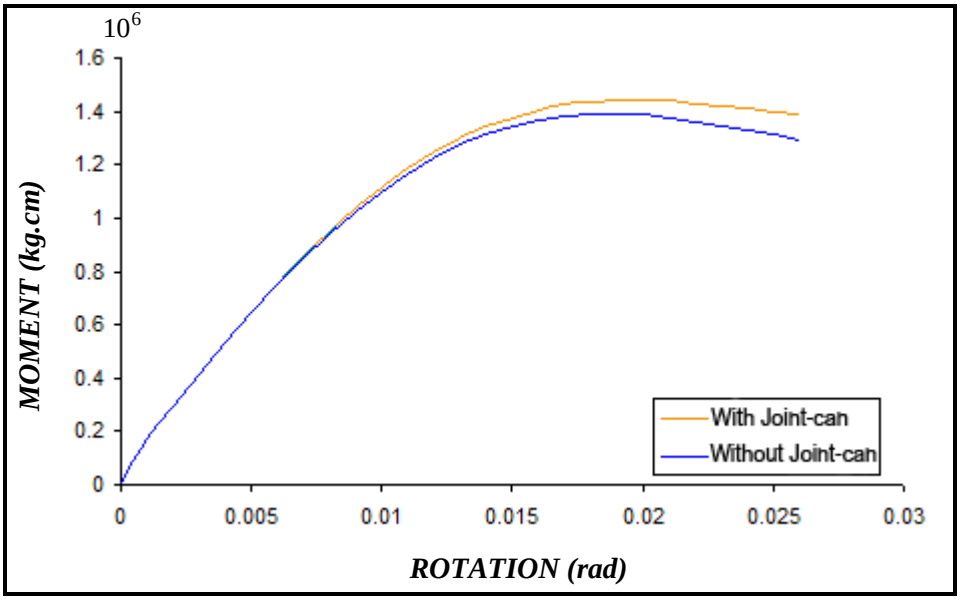

Figure 4.4: Moment-rotation diagram of joint TYPE I around Z-axis

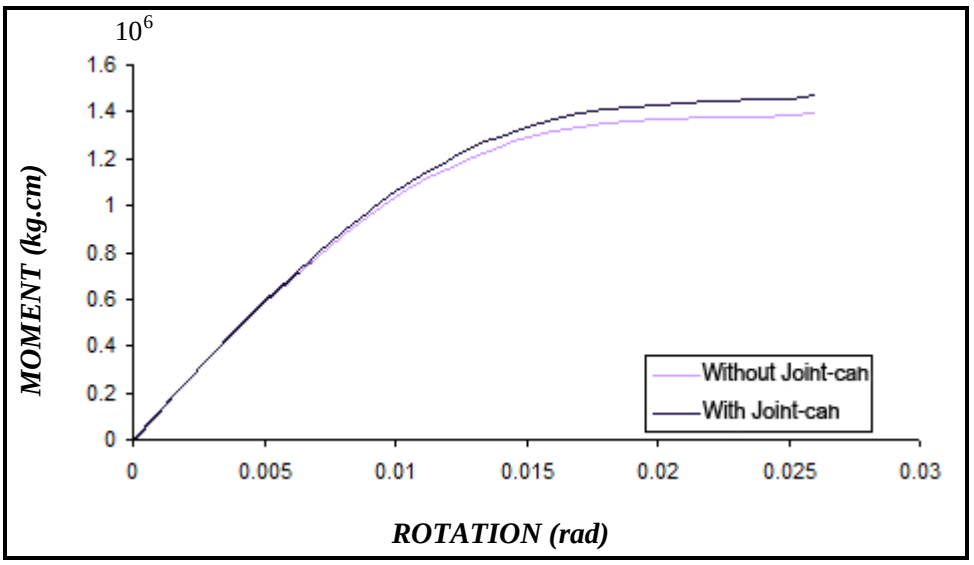

Figure 4.5: Moment-rotation diagram of joint TYPE II around X-axis

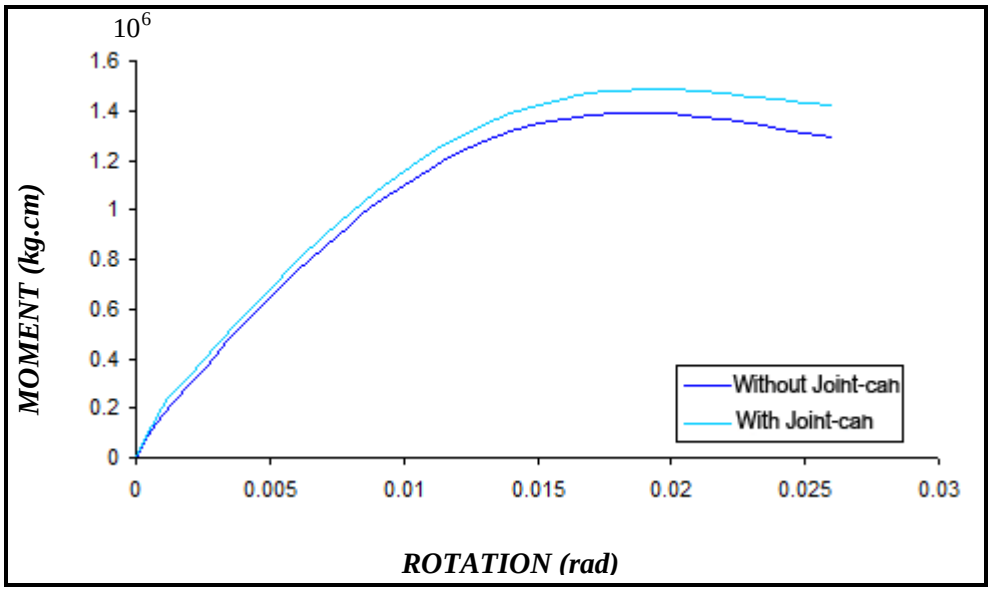

Figure 4.6: Moment-rotation diagram of joint TYPE II around Y-axis

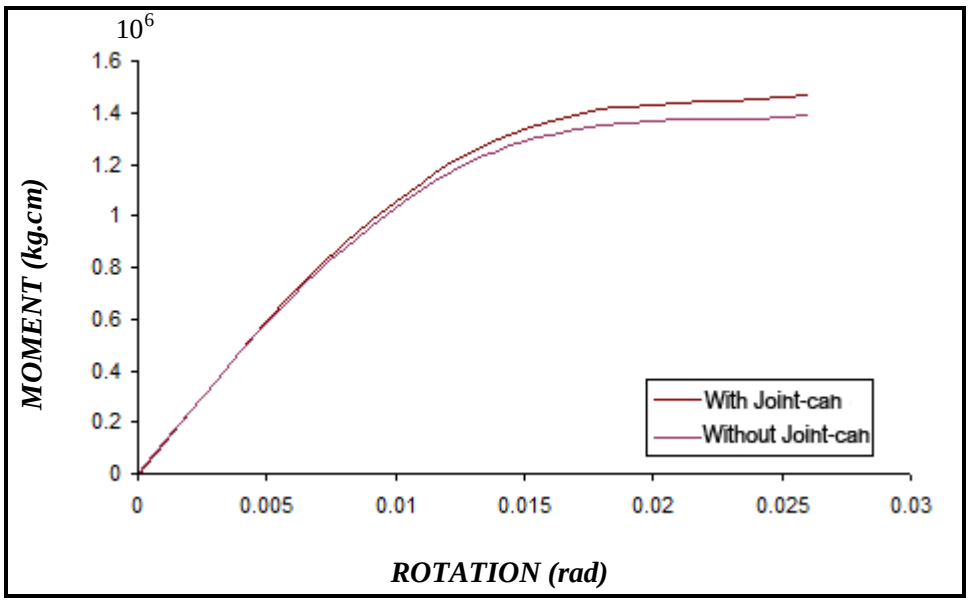

Figure 4.7: Moment-rotation diagram of joint TYPE II around Z-axis

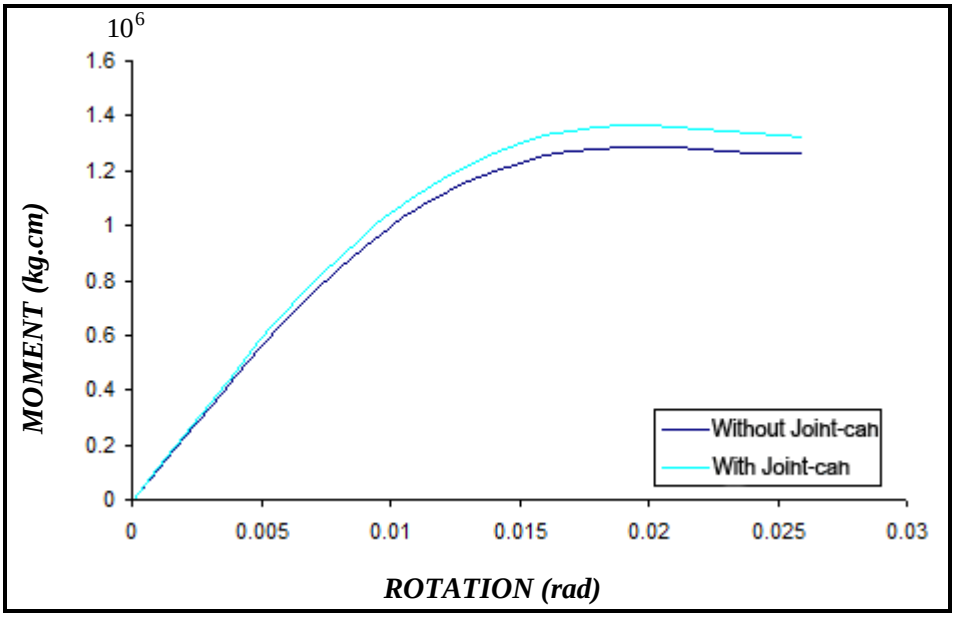

Figure 4.8: Moment-rotation diagram of joint TYPE III around X-axis

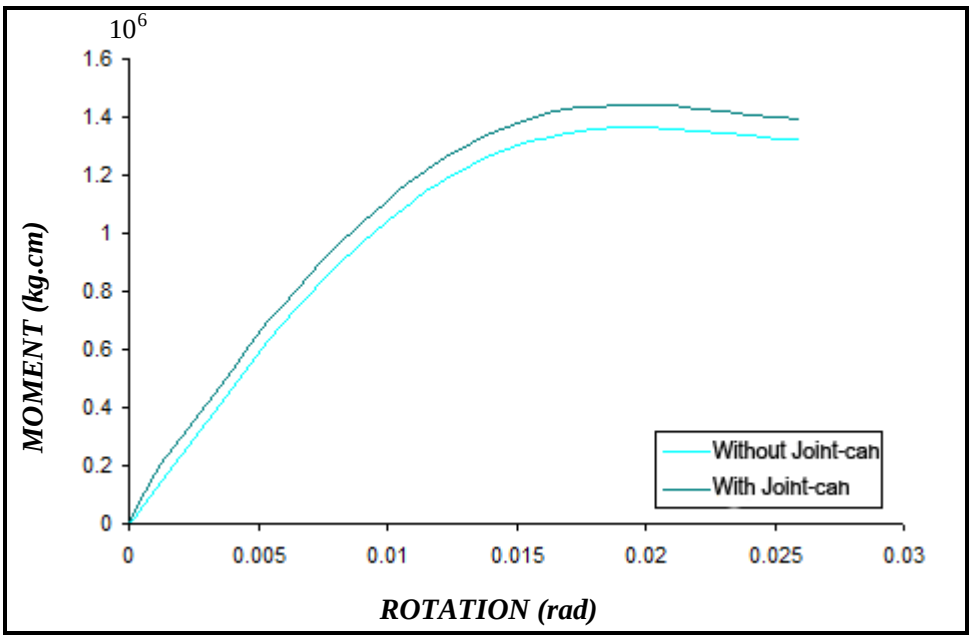

Figure 4.9: Moment-rotation diagram of joint TYPE III around Y-axis

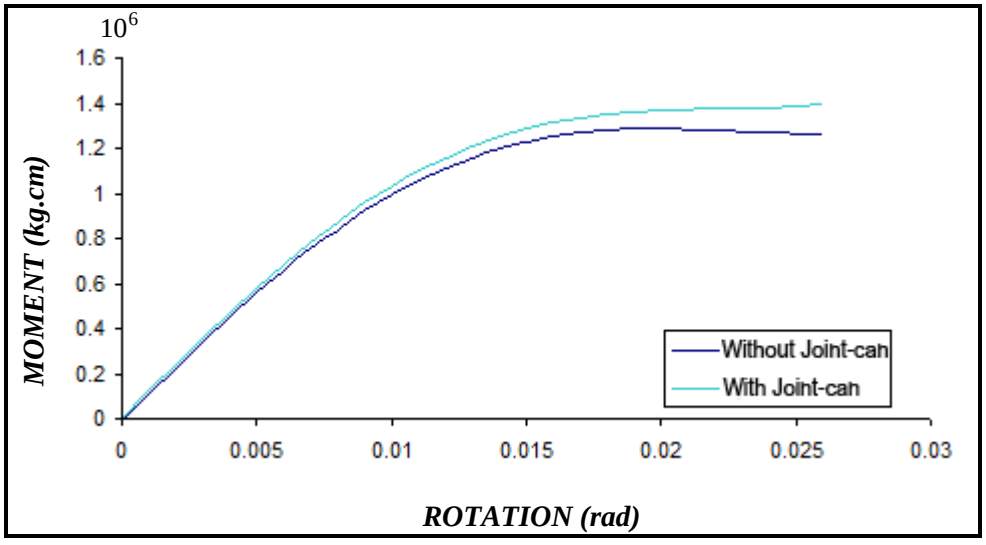

Figure 4.10: Moment-rotation diagram of joint TYPE III around Z-axis

Closer examination on above graphs in Figure 4.2 to 4.10 demonstrates the respectable impact of initial axial loads in struts on flexural capacity of the joints. As the initial load moves from pressure towards strain, the capacity of the joint is expanded and the other

way around. This demonstrates the impact of stress-stiffening in struts on the behaviour and capacity of connections, which, essentially, expresses that the tensile axial load strengthens the strut and also its joint.

This is specifically pertinent to local buckling reduction due to tensile forces whilst, compressive stress causes local buckling of plates to be experienced more quickly. Additionally, it is obvious that connections are not perfectly rigid even with the Joint-can and they still show flexibility when loaded laterally. This flexibility assists the energy dissipation of the platform structure and it should be accounted for when exact deformability of the platform structure is needed.

4.3 Spectral Analysis

In this method, the dynamic analysis is performed assuming the linear elastic behaviour of the structure and using the maximum reflection of all oscillatory modes in the structure, which have a significant effect on the total reflection of the structure. The maximum rate in any mode is obtained according to its frequency time from the spectrum. The overall structure reflection is estimated from the statistical combination of the maximum reflections of each mode.

The number of modes should be such that the sum of the effective modal masses in line with the spectrum effect is at least 90% of the total modal mass of the structure. The maximum dynamic reflection of the structure in each mode should be determined using known statistical methods, such as the square root sum of squares method (SRSS) or the compound perfect square method (CQC).

The design spectrum used in this study is the plan (design) spectrum of API code, RP 2A-WSD version (API, 2000).

Figure 4.11 shows the spectrum proposed by API for designing offshore platforms which are resistant against earthquakes so the value for G has been considered to be 1 and the soil type has been considered to be C.

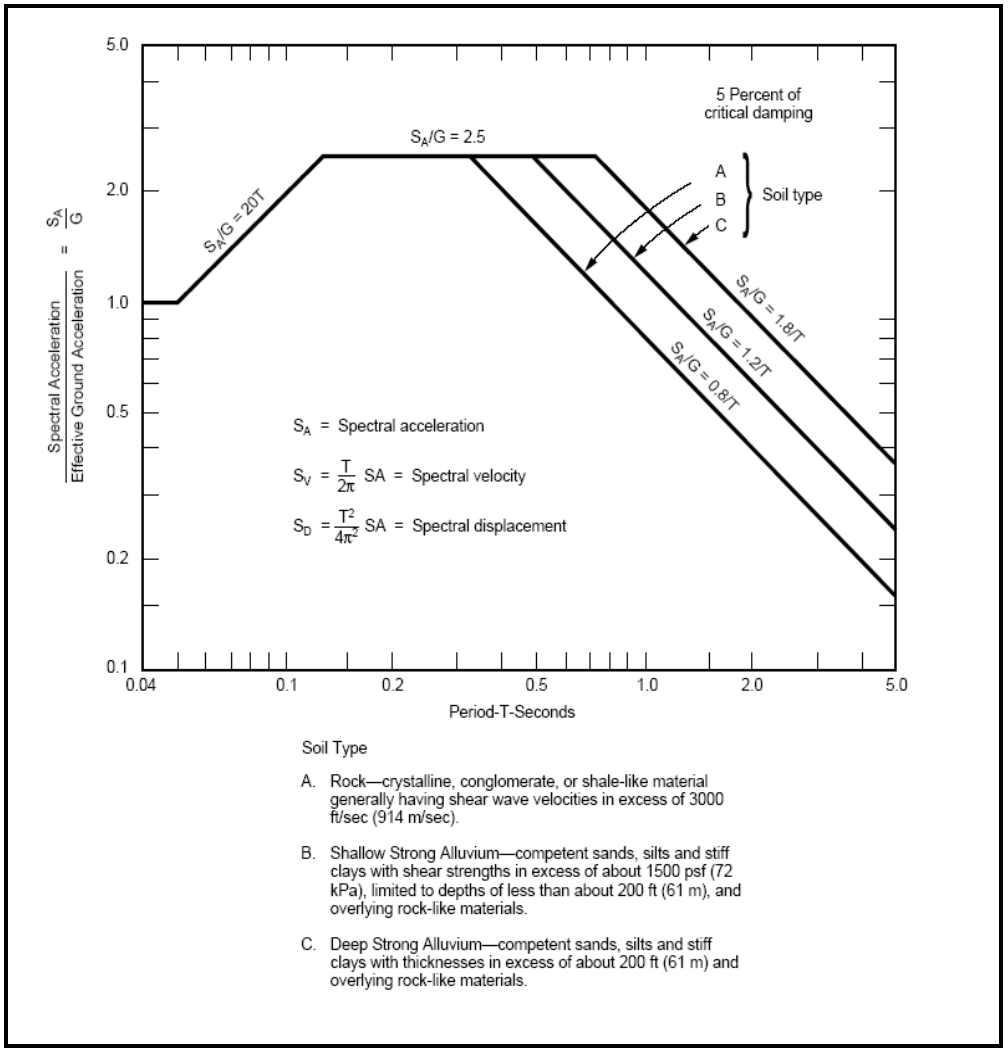

Figure 4.11: Response Spectra-Spectra Normalized to 1.0 Gravity

Since the platform does not have a symmetric geometry in the X and Y directions, the loading is done in both directions on this platform. The modal contribution above 90 per cent for the X (or Y) directions is achieved through at least 10 modes.

Tables 4.1 and 4.2 present the percentage of base shear in the X and Y directions, respectively. The load pattern obtained for performing push-over analysis has been calculated from the spectral analysis results. This model is equivalent to the deformation

of the structure after conducting the spectral analysis with the participation of 10 modes, on a structure with rigid joints.

Table 4.1: Platform SPD7

Loading pattern for X-direction	
Height	Percentage of Base shear
0.000	0
8.940	1.3
17.880	5.1
26.820	13.4
35.760	27.8
44.700	48
53.640	71.2
62.580	92
71.520	98
80.500	100

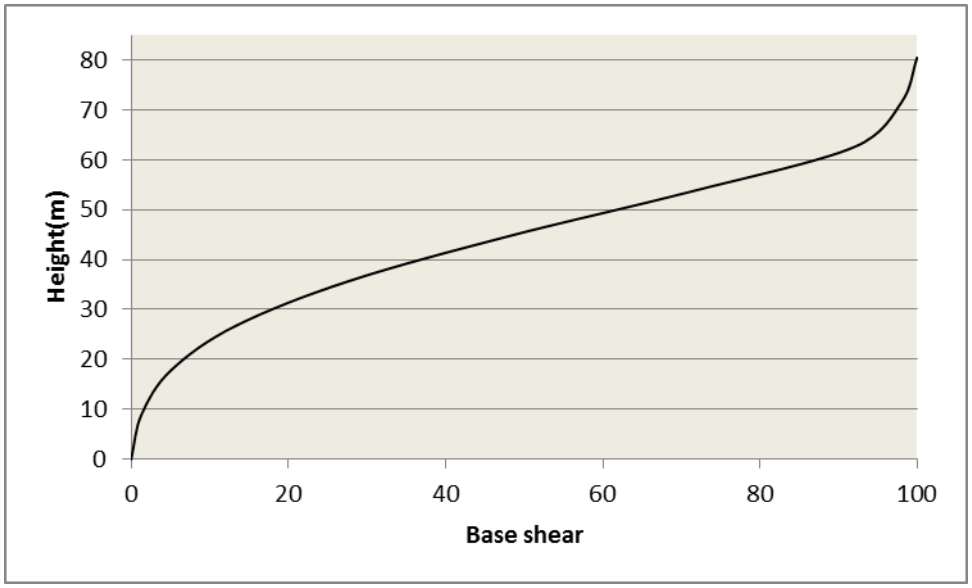

Figure 4.12: Loading pattern on platform SPD7 for X-direction

Table 4. 2: Platform SPD7

Loading pattern for Y-direction	
Height	Percentage of Base shear
0.000	0
8.940	1.1
17.880	4.6
26.820	12.4
35.760	28.6
44.700	45.4
53.640	75.8
62.580	89
71.520	95.4
80.500	100

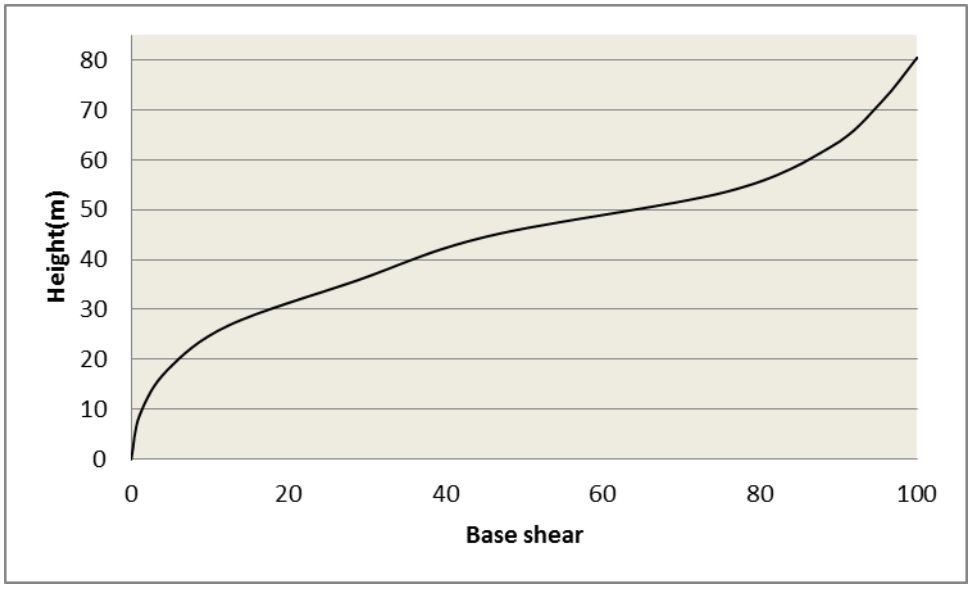

Figure 4.13: Loading pattern on platform SPD7 for Y-direction

4.4 Nonlinear Static Analysis (Push-Over)

In this analysis, a loading model (pattern) is considered on the nodes of the platform, and then this model is increased steadily until the point when the platform is not able to tolerate its gravity loads (or in many cases to reach the extent of displacement whereby the numerical analysis of the platform structure becomes unstable).

The loading pattern obtained from spectral analysis, as shown in Figures 4.12 and 4.13, is exerted on the structure in the X and Y directions, respectively. Since this platform has a non-symmetric geometry in the directions of X and Y, the loading on the platform is done in both directions.

4.4.1 Loading in the Direction of X

Figure 4.14 shows the diagram for the push-over analysis of the SPD7 platform, obtained from the nonlinear static analysis performed using the ANSYS11 software.

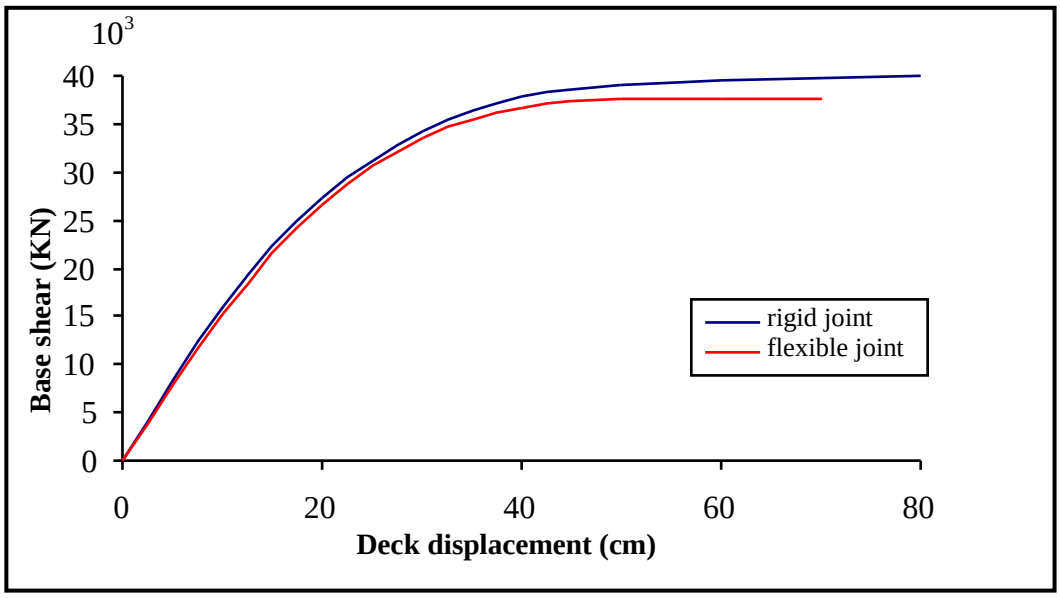

Figure 4.14 : Deck displacement in X-direction for rigid and flexible SPD7 platform

It can be seen that there is little difference between the graphs obtained for the model with rigid joints and the one with flexible joints; however, this difference increases with increasing load and enters the nonlinear range.

Failure in the model with rigid joints starts with the buckling of the bracings between the second-third and third-fourth levels, and with increasing levels of load, the bracings start buckling at the other levels one by one. Finally, the structure collapses with these bracing failures.

In the model with flexible joints, failure starts with the buckling of the bracings at the second-third and third-fourth levels. With increasing load, the other braces and the joints attached to them start flowing, and, ultimately, what causes the structure to collapse is the buckling of relative braces and the failure of the joints connected to them. The responses of the two different models differ slightly because of the lower level of joint flexibility in the platform due to using Joint-cans.

4.4.2 Loading in the Direction Y

Figure 4.15 depicts the diagram for the push-over analysis for the platform SPD7, obtained from the nonlinear static analysis performed using the ANSYS11 software.

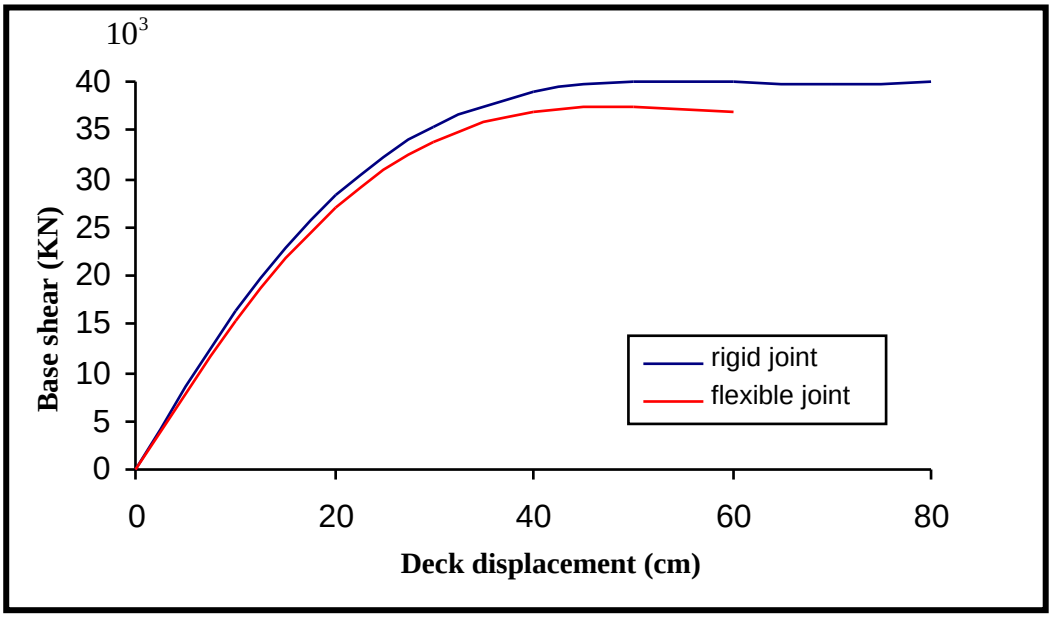

Figure 4.15: Deck displacement in Y-direction for the SPD7 platform with rigid and flexible joints

It can be seen that there is little difference between the graphs obtained for the model with rigid joints and the one with flexible joints; however, this difference increases with increasing load and enters the nonlinear range.

Failure in the model with rigid joints starts with the buckling of the bracings between the second-third and third-fourth levels, and with increasing levels of load, the bracings start buckling at other levels one by one. Finally, the structure collapses with these bracing failures.

In the model with flexible joints, failure starts with the buckling of the bracings at the second-third and third-fourth levels. With increasing load, the other braces and the joints attached to them start flowing, and, ultimately, what causes the structure to collapse is the buckling of relative braces and the failure of the joints connected to them.

The responses of the two different models differ slightly because of the lower level of joint flexibility in the platform due to the use of Joint-cans.

4.5 Modal Analysis of SPD7 Platform

Three-dimensional modelling of the SPD7 platform has been done with six degrees of freedom. The schematic structure and the mass rate imposed on the model are shown in Figures 4.16 and 4.17.

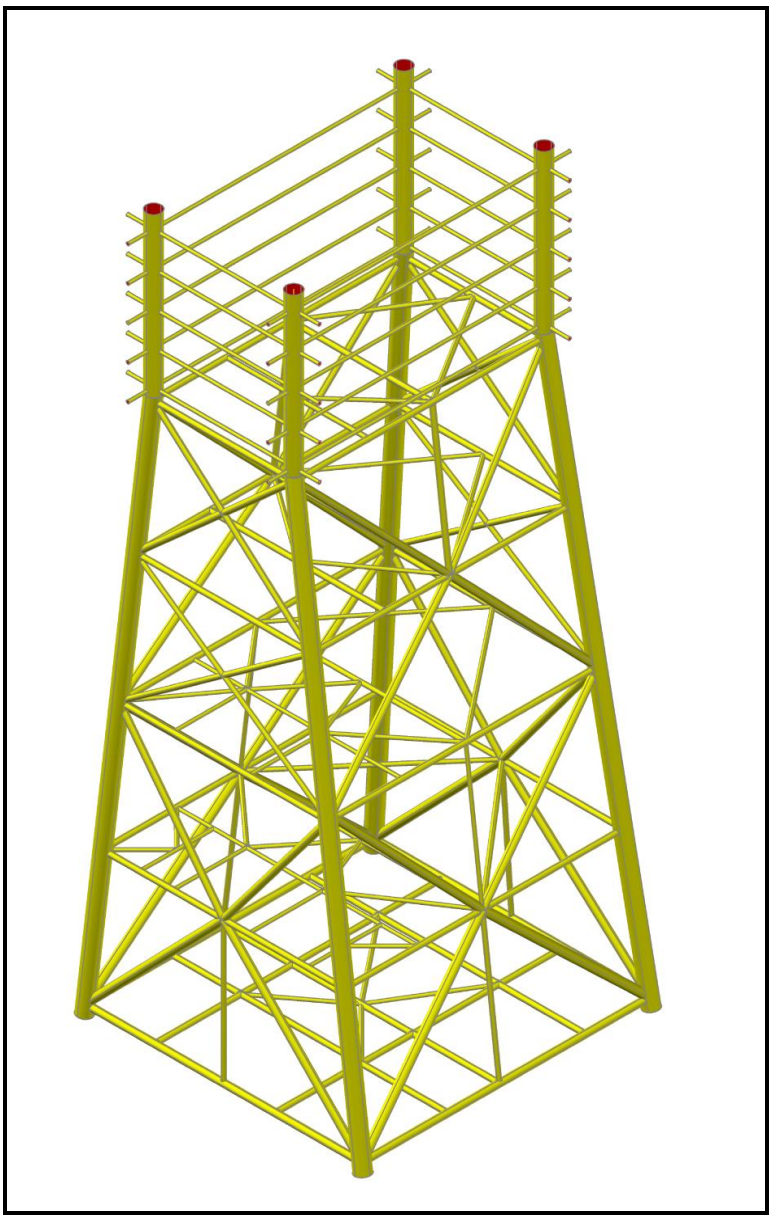

Figure 4.16: Three-dimensional view of the sample platform SPD7

As shown in Tables 4.3 and 4.4 the structure has undergone modal analysis; the modal response of the structure in the flexible joint case is different from its modal response in the structure with rigid joints. In addition, the vibration modes and modal mass participation rate had significant changes.

Figure 4.16 shows the actual view and three-dimensional model of the structure model. The horizontal diagonal braces are not modelled in this study to simplify the model and reduce the calculate process and its time.

As shown in Table 4.5, the period of vibration modes in the flexible joint model differs significantly from the model with rigid joints; the difference reaches its maximum rate of about 10 per cent.

The period of structure modes increases with modelling the flexibility of a joint. Regarding the fact that by modelling the joints with the SHELL element and meshing these elements the structure stiffness decreases, the increase in the period of the structure mode is justified.

Referring to Tables 4.6 to Table 4.11, in structures with rigid joints the first vibration mode is the rotation (torsion) mode around the Z-axis, consisting of about 78 per cent of modal mass participation, and its maximum mass participation in other directions reaches 6 per cent. However, in structures with flexible joints, the first mode consists of only 48 per cent of modal mass participation in rotation (torsion) around axis Z. In the directions of X and Y it has about 35 per cent mass participation, and in rotation around X and Y it consists of approximately 15 per cent mass participation.

The second and third vibration modes in structures with rigid connections were the dominant movement mode in the X and Y directions with more than 86 per cent of modal mass participation. However, in structures with flexible joints the second mode only contributed 42 per cent in movement in the Y-direction, and in displacements in the X-direction and rotation around the Z- and X-axis, it has about 21 per cent participation. The third mode in structures with flexible joints remains the dominant displacement mode in the X-direction, with the only difference being that its modal contribution rate decreases by 19 per cent, reducing to about 67 per cent.

The fourth vibration mode in both models is the vibration mode around the X-axis, but the modal mass participation of the two models has about a 10 per cent difference, and, as can be observed, the higher the number of modes, the lower the difference.

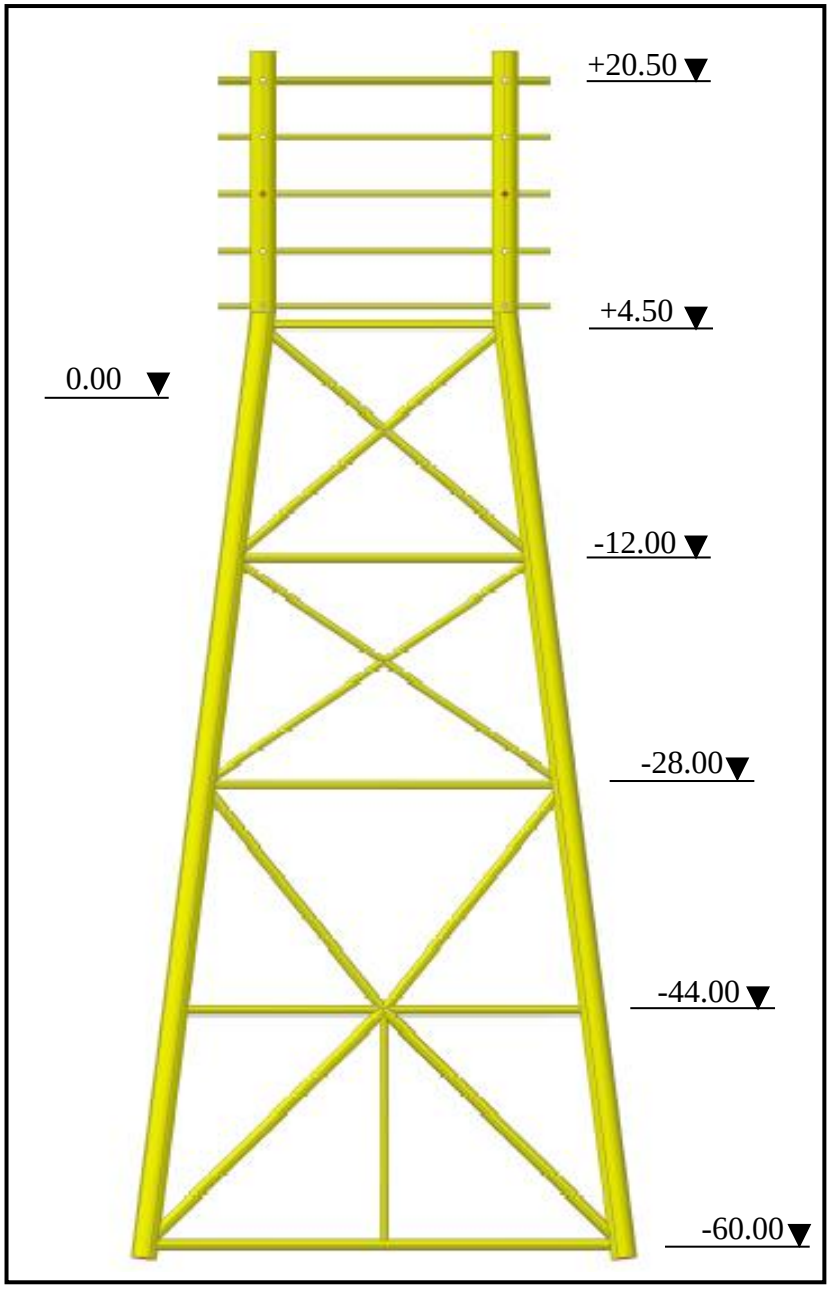

Figure 4. 17 : Two-dimensional view of the modelled platform SPD7

Table 4.3: Modelled Platform SPD7 with flexible connections

Mode no.	Frequency	Period
1	0.432	2.271
2	0.477	2.055
3	0.501	1.956
4	2.211	0.444
5	2.312	0.424
6	2.556	0.383
7	2.610	0.375
8	2.697	0.363
9	2.750	0.356
10	2.849	0.345
11	2.986	0.329
12	3.142	0.312
13	3.205	0.306
14	3.384	0.290
15	3.396	0.289
16	3.411	0.287
17	3.651	0.268
18	3.964	0.248
19	4.305	0.228
20	4.393	0.217

Table 4.4: Modelled Platform SPD7 with rigid connections

Mode no.	Frequency	Period
1	0.478	2.050
2	0.508	1.929
3	0.543	1.807
4	2.120	0.462
5	2.380	0.412
6	2.555	0.383
7	2.565	0.382
8	2.624	0.373
9	2.787	0.351
10	2.923	0.336
11	3.013	0.326
12	3.286	0.298
13	3.411	0.287
14	3.420	0.286
15	3.436	0.285
16	3.632	0.270
17	3.807	0.257
18	4.169	0.235
19	4.235	0.232
20	4.379	0.224

Table 4.5: Comparison of vibration period of the two models

Mode no.	Model with flexibility	Model without flexibility	Percentage of discrepancy
1	2.271	2.050	9.721
2	2.055	1.929	6.166
3	1.956	1.807	7.642
4	0.444	0.462	4.241
5	0.424	0.412	2.804
6	0.383	0.383	0.000
7	0.375	0.382	1.847
8	0.363	0.373	2.725
9	0.356	0.351	1.389
10	0.345	0.336	2.586
11	0.329	0.326	0.904
12	0.312	0.298	4.444
13	0.306	0.287	6.149
14	0.290	0.286	1.365
15	0.289	0.285	1.370
16	0.287	0.270	5.862
17	0.268	0.257	4.059
18	0.248	0.235	5.200
19	0.228	0.232	1.739
20	0.217	0.224	3.196

Table 4.6: Modal mass contribution in the direction of X

Contribution %			Cumulative contribution %	
Mode no.	Model with flexibility	Model without flexibility	Model with flexibility	Model without flexibility
1	0.3468	5.733	0.34	5.85
2	18.6354	0.0098	18.9754	5.8598
3	67.9218	79.0958	86.8972	84.9556
4	0.2958	0.0196	87.193	84.9752
5	6.5892	6.1936	93.7822	91.1688
6	0	0	93.7822	91.1688
7	0.153	0.0098	93.9352	91.1786
8	0	0	93.9352	91.1786
9	5.4366	4.067	99.3718	95.2456
10	0	0	99.3718	95.2456
11	0	0.0392	99.3718	95.2848
12	0	2.0188	99.3718	97.3036
13	0	0	99.3718	97.3036
14	0	0.0294	99.3718	97.333
15	0.6282	0.5684	100	97.9014
16	0	0.1176	100	98.019
17	0	3.981	100	100
18	0	0	100	100
19	0	0	100	100
20	0	0	100	100

Table 4.7: Modal mass contribution in the direction of Y

Contribution %			Cumulative contribution %	
Mode no.	Model with flexibility	Model without flexibility	Model with flexibility	Model without flexibility
1	34.1582	1.0504	34.1582	1.0504
2	42.1574	86.9408	76.3156	87.9912
3	8.9991	0.0303	85.3147	88.0215
4	4.4238	5.9085	89.7385	93.93
5	1.0504	0.0202	90.7889	93.9502
6	0.0707	0.2626	90.8596	94.2128
7	5.1005	1.9089	95.9601	96.1217
8	0	0.5353	95.9601	96.657
9	0.2222	0	96.1823	96.657
10	4.3531	0.2424	100.5354	96.8994
11	0.2222	3.6461	100.7576	100.5455
12	0.1717	0.0303	99.3718	100.5758
13	0.0101	0	99.3718	100.5758
14	0	0.0101	99.3718	100.5859
15	0	0	100	100.5859
16	0	0.1212	100	100.7071
17	0	0	100	100
18	0	0	100	100
19	0	0	100	100
20	0	0	100	100

Table 4.8: Modal mass contribution in the direction of Z

Contribution %			Cumulative contribution %	
Mode no.	Model with flexibility	Model without flexibility	Model with flexibility	Model without flexibility
1	0.0102	0	0.0102	0
2	0	0	0.0102	0
3	0	0	0.0102	0
4	0.0612	0.3468	0.0714	0.3468
5	1.2342	0.2754	1.3056	0.6222
6	0	0	1.3056	0.6222
7	0.1734	0.0306	1.479	0.6528
8	0.918	0	2.397	0.6528
9	0.3468	0.0714	2.7438	0.7242
10	0	0.1734	2.7438	0.8976
11	0.6834	4.7328	3.4272	5.6304
12	2.1216	2.856	99.3718	8.4864
13	0.3774	0.612	99.3718	9.0984
14	65.688	3.519	99.3718	12.6174
15	3.3762	2.6418	100	15.2592
16	0.102	86.4042	100.102	101.6634
17	0.3876	0.8466	100.4896	100
18	0	0	100	100
19	0	0	100	100
20	0	0	100	100

Table 4.9: Modal mass contribution in rotation around X-axis

Contribution %			Cumulative contribution %	
Mode no.	Model with flexibility	Model without flexibility	Model with flexibility	Model without flexibility
1	16.728	0.357	16.728	0.357
2	20.196	41.0652	36.924	41.4222
3	4.2942	0.0102	41.2182	41.4324
4	40.137	48.5418	81.3552	89.9742
5	3.6006	0.1938	84.9558	90.168
6	0.255	0.6426	85.2108	90.8106
7	11.7504	3.2538	96.9612	94.0644
8	0	1.581	96.9612	95.6454
9	0.102	0.0102	97.0632	95.6556
10	2.2746	0.0306	99.3378	95.6862
11	0.102	1.2138	99.4398	96.9
12	0.255	0	99.3718	96.9
13	0.0102	0	99.3718	96.9
14	0.0204	0.0102	99.3718	96.9102
15	0.8772	0	100	96.9102
16	0	0.0918	100	97.002
17	0	0	100	100
18	0	0	100	100
19	0	0	100	100
20	0	0	100	100

Table 4.10: Modal mass contribution in rotation around Y-axis

Contribution %			Cumulative contribution %	
Mode no.	Model with flexibility	Model without flexibility	Model with flexibility	Model without flexibility
1	0.1428	3.111	0.1428	3.111
2	9.4554	0.0102	9.5982	3.1212
3	32.9358	40.3308	42.534	43.452
4	2.2032	0.2244	44.7372	43.6764
5	44.6964	47.9298	89.4336	91.6062
6	0.0102	0.0102	89.4438	91.6164
7	0.5916	0.0612	90.0354	91.6776
8	0	0	90.0354	91.6776
9	11.4342	9.894	101.4696	101.5716
10	0.0102	0.0306	101.4798	101.6022
11	0	0.0102	101.4798	101.6124
12	0.4692	0.1326	99.3718	101.745
13	0.0306	0.0102	99.3718	101.7552
14	0	0.0612	99.3718	101.8164
15	0	0.0306	100	101.847
16	0	0.0102	100	101.8572
17	0	0.0306	100	100
18	0	0	100	100
19	0	0	100	100
20	0	0	100	100

Table 4.11: Modal mass contribution in rotation around Z-axis

Contribution %			Cumulative contribution %	
Mode no.	Model with flexibility	Model without flexibility	Model with flexibility	Model without flexibility
1	47.8074	77.5812	47.8074	77.5812
2	21.8688	1.6626	69.6762	79.2438
3	6.0588	3.5598	75.735	82.8036
4	0.0612	0	75.7962	82.8036
5	0.0204	0	75.8166	82.8036
6	0	0.0102	75.8166	82.8138
7	0.0306	0.0102	75.8472	82.824
8	0	0.0102	75.8472	82.8342
9	0.0816	0	75.9288	82.8342
10	1.2138	21.0222	77.1426	103.8564
11	24.633	1.1526	101.7756	105.009
12	0.1836	0	99.3718	105.009
13	0	0	99.3718	105.009
14	0.0306	0	99.3718	105.009
15	0	0	100	105.009
16	0	0	100	105.009
17	0	0	100	100
18	0	0	100	100
19	0	0	100	100
20	0	0	100	100

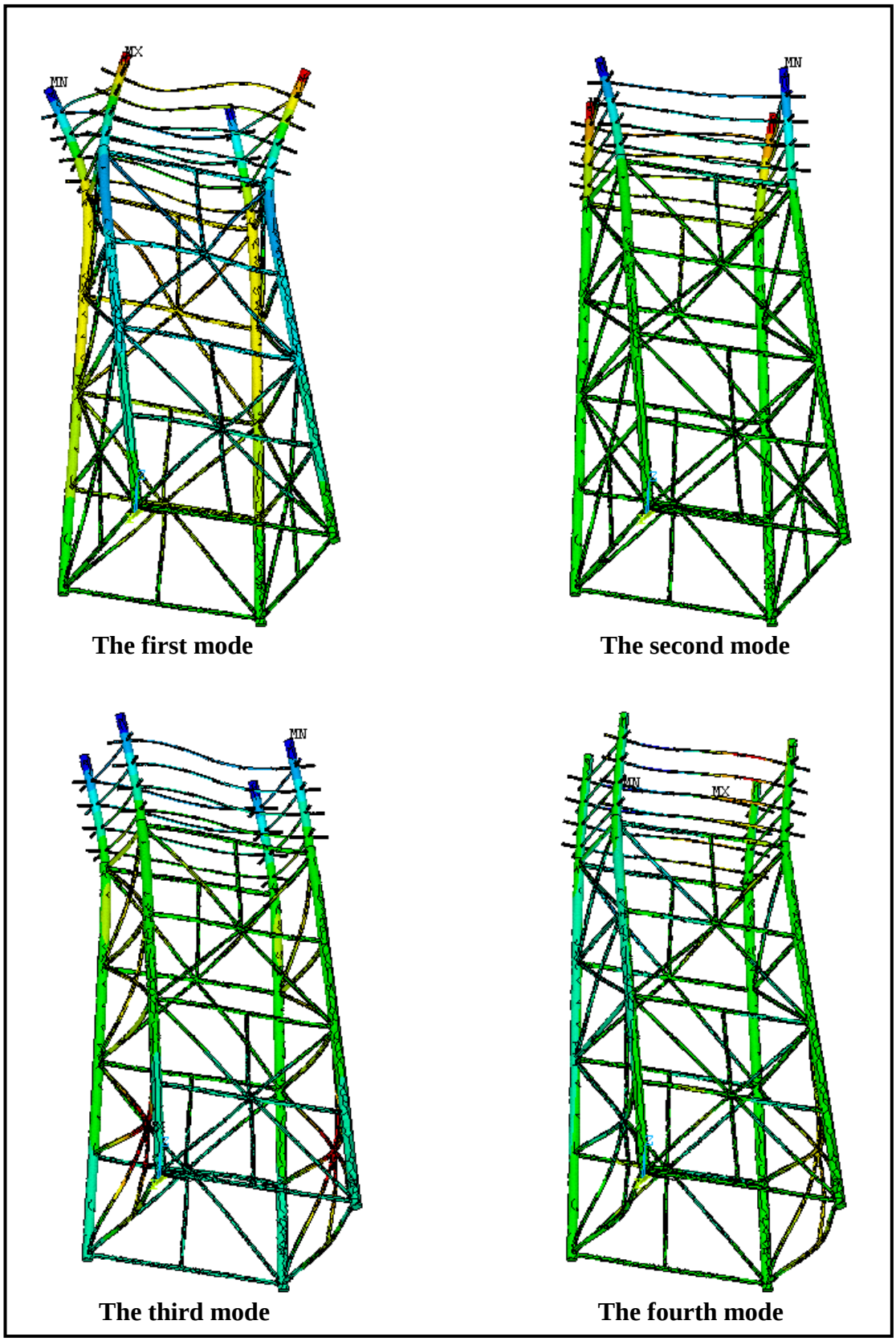

Figure 4.18 : Displacement modes of the flexible platform

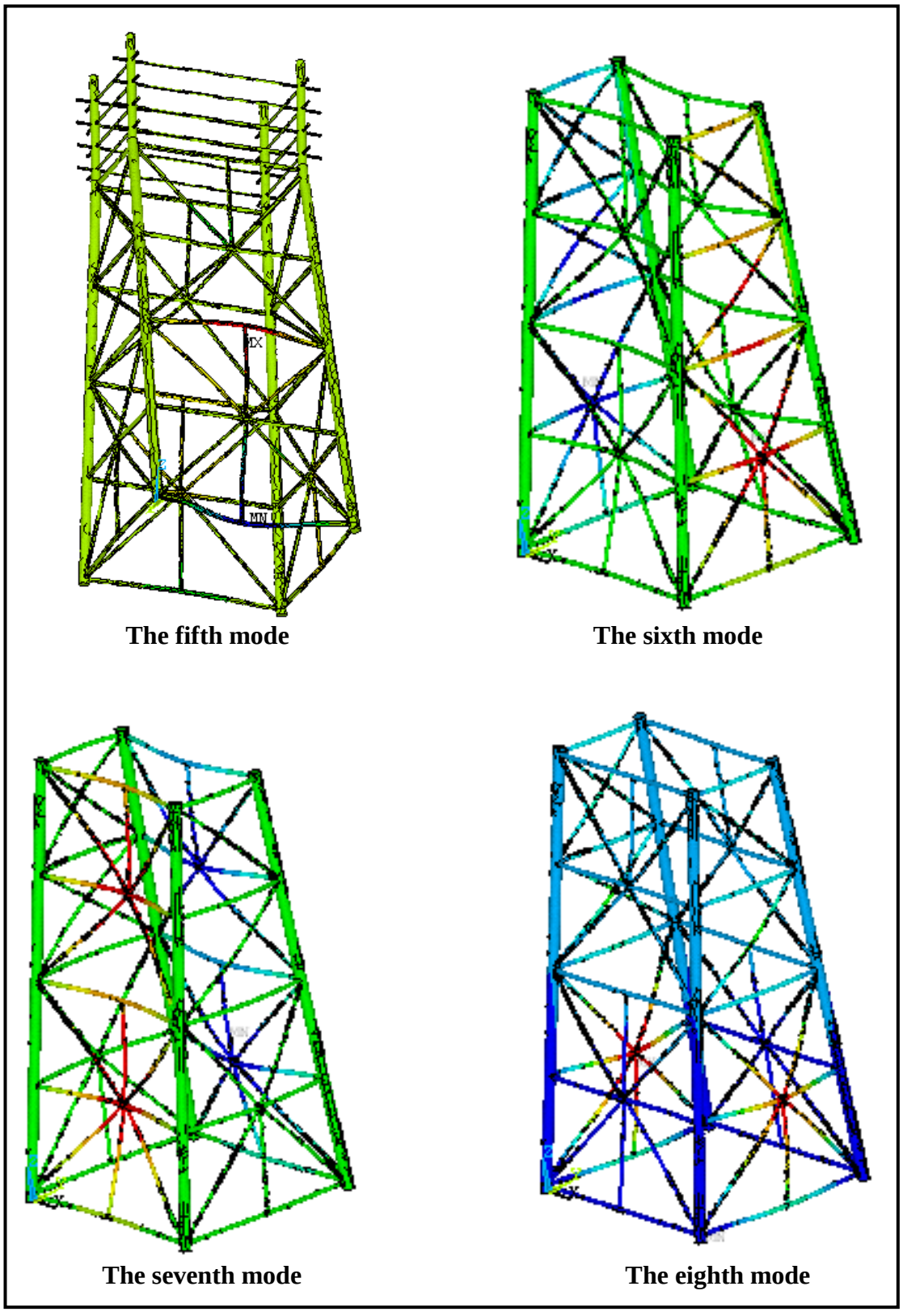

Figure 4.19: Displacement modes of the flexible platform

Table 4.5 presented the vibration period of the two models with and without flexibility. By comparing this Table with the Mirtaheri (2009) modal analysis results which is given in Table 4.12, it can be seen that there are remarkable differences in the vibration

period amount. Hence, this clearly shows that the result of modal analysis in the 3-D model was more accurate and reliable as compared to the 2-D model.

Table 4.12 : Natural periods of vibration of two platforms (Mirtaheri et al., 2009)

Mode No.	Model with flexible connections	Model with rigid connections	Percentage of discrepancy
1	2.313	2.026	12.4
2	2.065	1.916	7.215
3	1.943	1.818	6.427
4	0.635	0.608	4.318
5	0.435	0.424	2.521
6	0.371	0.368	0.761
7	0.672	0.663	1.378
8	0.341	0.333	2.214
9	0.379	0.375	1.037
10	0.317	0.310	2.115

4.6 Transient Dynamic analysis

Using the Macro software programming capability, the models were analysed dynamically. Thus, the first acceleration of gravity was applied on the structure, followed by applying the acceleration to all nodes of the structure in each time step. Each time step is also divided into five parts or sub-steps.

- **Selecting the Acceleration Recorder**

The modelled structure was subjected to the acceleration from the Tabas earthquake. Acceleration mappings were taken from data from the PEER Strong Motion Database website. Figure 4.20 shows the Tabas earthquake record.

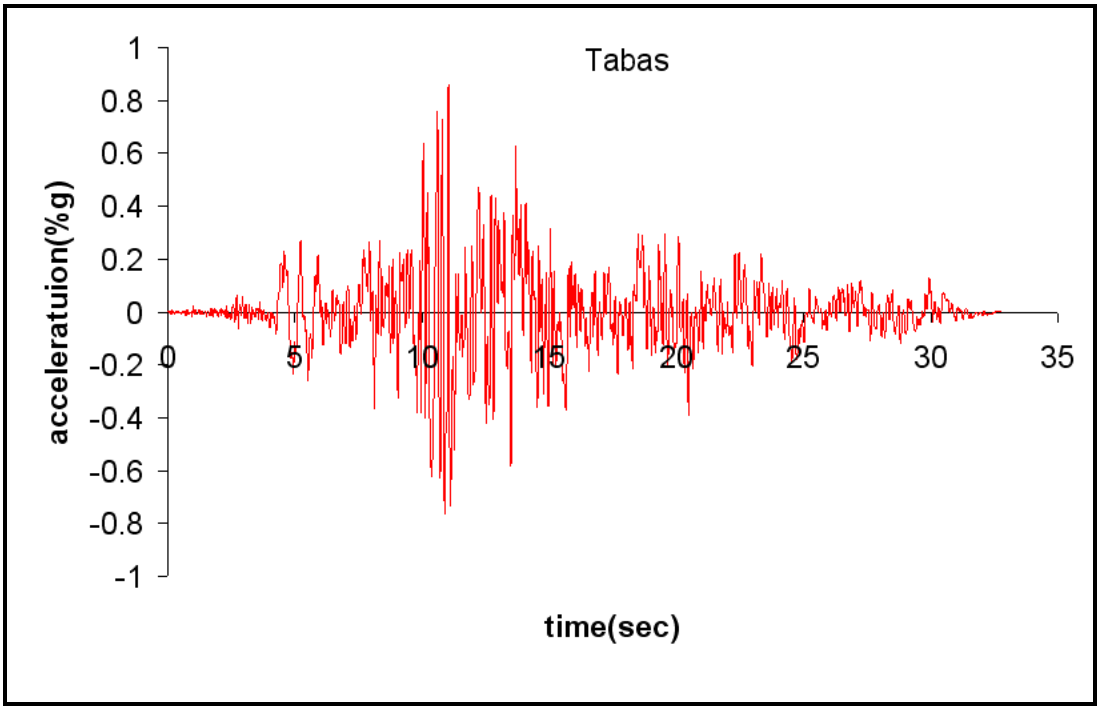

Figure 4.20: Record of Tabas earthquake in Iran – 1978

The values for base shear and the relative peak drift of the levels are shown in Figures 4.21 to 4.23.

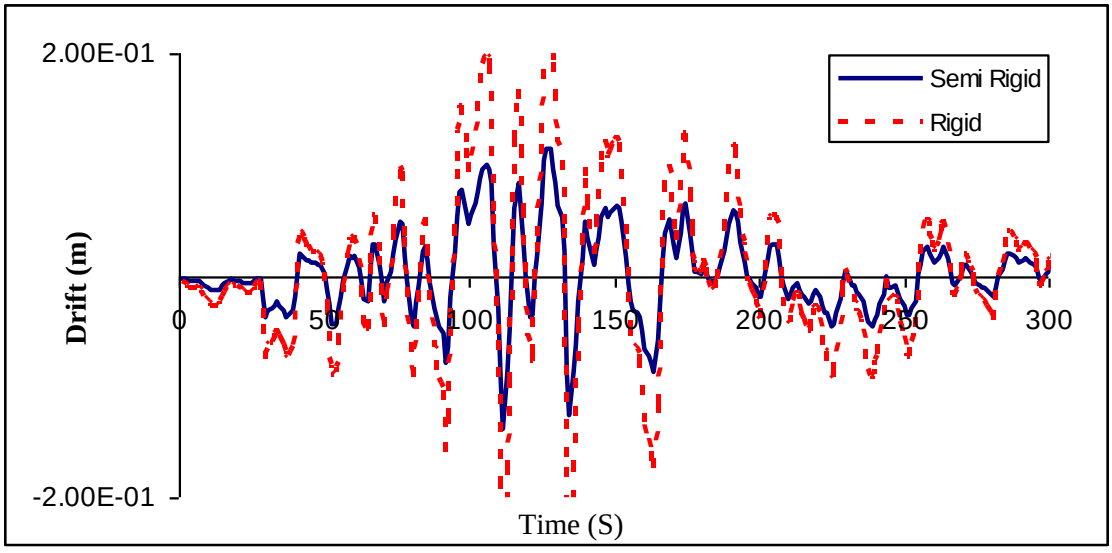

Figure 4.21: The response of two models under the Tabas earthquake

Nonlinear transient analysis was performed on two models, with and without flexibility joints, subjected to the Tabas earthquake record, and the response of them was observed accordingly. Figure 4.21 shows the comparison of the results in which the flexible

model has lower base shears but the rigid model behaves as a stiffer structure with bigger internal forces.

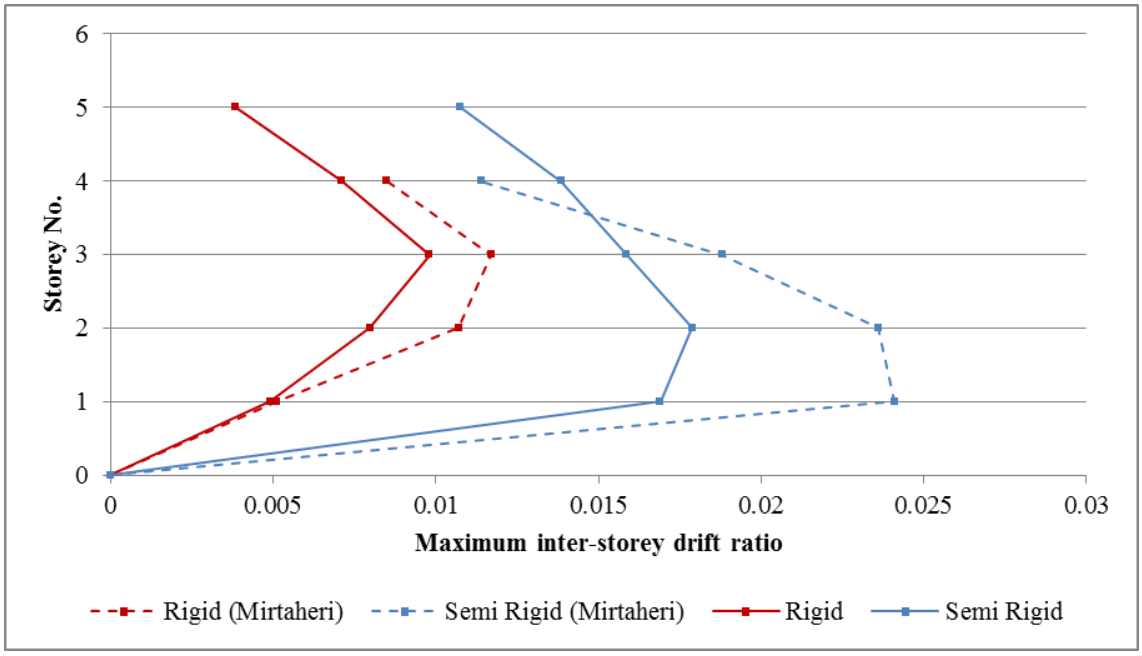

Figure 4.22: Maximum inter-storey drift ratio in the X-direction

Figure 4.22 shows the comparison of the relative lateral displacement of rigid and semi-rigid structures in the direction of X when subjected to the Tabas earthquake. As can be seen in this Figure, the second storey of the flexible model has the highest drift among the other storeys. However, in the rigid model, the highest drift belongs to the third storey.

In comparison with Mirtaheri et al. (2009) result, it can be seen that the drift ratio is lower than Mirtaheri result which lead to better structural response to the earthquake. it is obvious that the maximum inter-storey drift for the rigid model occurred in third storey which is same in both results; however, for semi rigid model there is a difference in the two studies result which shows maximum inter-storey drift happened in second storey and first story for this study and Mirtaheri study respectively.

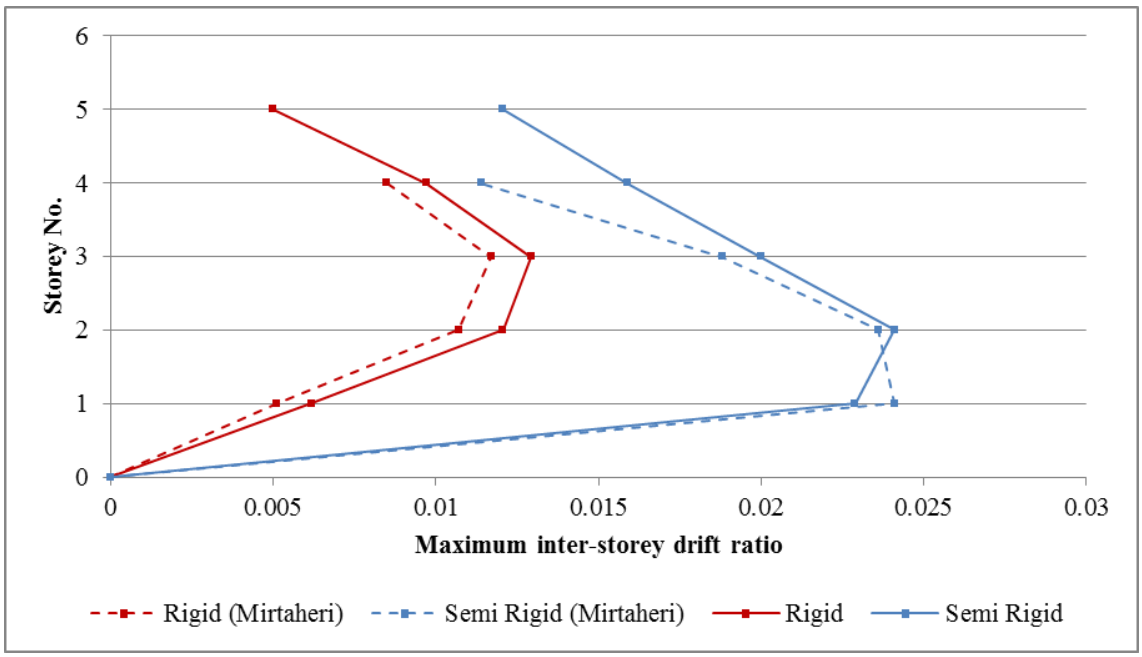

Figure 4.23: Maximum inter-storey drift ratio in Y-direction

Figure 4.23 shows the comparison of the relative lateral displacement of two rigid and semi-rigid structures in the Y-direction under the acceleration mapping of the Tabas earthquake. Comparison of these results with Mirtaheri's results leads to the similar structural response; however the maximum drift in semi rigid model is occurred in second storey and first storey for this study and Mirtaheri's study respectively. The highest drift in the flexible model belongs to the second storey, similar to the X-direction.

Moreover, the joints' flexibility has a remarkable effect on the structural response to the earthquake, which is highlighted in these Figures.

The results obtained demonstrate that in the flexible model (semi-rigid), the base shear value is reduced by about 30% compared to the rigid (without flexibility) model. Also, the comparison of the relative drift values of the lower levels shows that the flexible structure with the Joint-can, despite the lower base shear force, experienced more lateral

displacement, which is different in the direction of X and Y, so that the displacement in the direction of X is less.

Mirtaheri et al. (2009) also concluded that the platform with flexible connections in nonlinear dynamic analysis shows higher displacements, inter-storey drifts, and lower base shear, which supports the above results.

CHAPTER V

CONCLUSION AND RECOMMENDATIONS

5.1 Introduction

In the computer analysis of structures with tubular members, such as sea platforms, the connections between members are considered to be rigid based on common traditional methods.

In fact, a joint is considered to be a dimensionless point where the members are connected to each other in a rigid manner and is not modelled as a structural member. This means there is an absence of any axial or rotational deformation on the end points of secondary members against the axis of the main member. Whereas, in reality, some deformations occur locally in the circular cross-section of the main member under the loads from the secondary member.

This shows that the tubular joints have considerable flexibility in the elasto-plastic range. Hence, analysis results based on the rigid-joint assumption are different from the actual behaviour of the structure in terms of structural deformations, the distribution of internal forces, the buckling forces of the members and also the natural frequency of vibration in the structures, especially in three-dimensional structures. Therefore, taking into account the effects of flexibility in the overall analysis of the structure is very important.

Several studies and tests have been conducted on tubular joints so far. Most models have been proposed for joints with a simple geometry and in linear range, and they are not responsive to the flexible behaviour of multi-plate joints or joints with multiple bracing members.

Despite the numerous methods proposed to consider flexibility in the structural models of the joints, all these methods yield an estimate of the level of joint flexibility and cannot be applied in all conditions. In this case, a complete modelling of the connecting area using shell elements with a continuous nonlinear behaviour is the most appropriate method that not only responds to modelling different types of joints, but can also model the nonlinear behaviour of the joint.

In this thesis, an SPD7 platform from the South Pars Oil Field (Phase 8) in the Persian Gulf has been modelled in three dimensions. Modelling of the platform was carried out in both rigid and flexible using finite element methods. The modelling was performed using the ANSYS software and the connecting area was modelled using the shell element. The structure joints were modelled in two cases, i.e. with Joint-can and without Joint-can. $M-\theta$ graphs were plotted for both cases and the results of the joint analysis were obtained as the member counters. Decks, piles and Joint-can were modelled simply and the structure-pile-soil interaction effect were considered as an equivalent pile with a length equal to eight times its diameter. The platform was modelled as grouted and has been considered by defining an element of interaction between the pile and leg. The added mass effects (added mass) were considered as masses concentrated at the nodes. The performed analyses include modal, non-linear static and non-linear dynamic analyses.

5.2 Summary of Findings and Conclusion

Based on this study, the effects of joint flexibility on the local and global behaviour of the jacket type offshore platform were investigated. Knowing that tubular connections are flexible and they can dissipate energy when subjected to cyclic forces, one can conclude that disregarding the joint flexibility in the estimation of overall energy dissipation, presents inaccurate results even by considering the Joint-can effect.

Comparing the $M-\theta$ diagrams for three types of joint in x, y and z directions for the two groups of joint (with Joint-can and without Joint-can), it can be concluded that the flexibility of the joints in the group which have Joint-can decreased slightly compared to those without Joint-can.

By running the non-linear static analysis, it was found that the static response of the structure changes with respect to the joints flexibility. These changes increase significantly upon the nonlinear range. In platform SPD7, the deck displacement of the flexible model increases by a maximum of 10% in linear range and up to 40% in non-linear range compared to the rigid model. By comparing the base shear and deck displacement graphs of two platforms can conclude that the platform with rigid joints is considerably stiffer and over-strength and stiffness would be more significant when the inelastic responses are encountered.

Furthermore, ignoring joints flexibility during the design process may result in overestimation of the platform lateral capacity and non-conservative design.

Modal characteristics of the structure with flexible joints have significant differences to those of the structures with rigid joints. The percentage of difference in the vibration period in the first mode for the two platforms is approximately 10%. In addition, significant changes in the form of vibration modes and the effective modal mass were observed.

The structural failure occurs in the connecting area, which can be resolved to some extent in the joints by a Joint-can; the value of failure according to the obtained results has been remarkable in the platform under study.

Based on the dynamic time-history analysis and investigation of the effect of flexibility, it was shown that the base shear values have reduced in flexible joints model by about

30% compared to the rigid joints model, which define that the rigid joints platform is stiffer compared with the flexible joints model. In addition, the comparison of the values of the inter-storey drifts shows that the flexible structure, despite the lower base shear force, experiences a greater lateral displacement and inter-storey drifts compared to the rigid joints model due to the lower stiffness and strength of the jacket structure. However, the displacement values of the flexible structure are at an acceptable level.

5.3 Suggestions for Future Research

According to the analysis conducted on the sea platforms in the present study, the following are recommended for future studies:

a) Evaluation of soil, pile and structure interaction in terms of the flexibility of the joints.
b) Investigating how and when to form the plastic hinges by incremental dynamic analysis in the members and evaluating the results.
c) Investigation on the effect of flexibility for different types of connection.
d) Investigation of the effect of joint flexibility in two jacket platforms of different height.
e) Evaluation of the joint flexibility effect on the pile dimension.
f) Experimental testing of the joints in a sub-frame as a representative of the jacket platform in order to obtain the actual joint response for verification with finite element results.
g) Conducting an analysis based on the Discrete Point method on this platform and verifying the results with finite element models.

REFERENCES

Alanjari, P., Asgarian, B., & Kia, M. (2011). Nonlinear joint flexibility element for the modeling of jacket-type offshore platforms. *Applied Ocean Research*, *33*, 147–157.

API. (1993). *Recommended Practice for Planning, Designing and Constructing Fixed Offshore Platforms—Working Stress Design* (20th ed.). API RP 2A-WSD: American Petroleum Institute.

API. (2000). *Recommended Practice for Planning, Designing and Constructing Fixed Offshore Platforms—Working Stress Design* (21th ed.). API RP 2A-WSD: American Petroleum Institute.

API. (2007). *Recommended practice for planning, designing and constructing fixed offshore platforms–working stress design*. *ERRATA AND SUPPLEMENT 3*. American Petroleum Institute.

Arnold, K. (2007). Volume III: Facilities and construction engineering. In *Petroleum Engineering Handbook* (Vol. III). Richardson, Texas: Society of Petroleum Engineers.

AWS. (1996). Structural welding code/steel. Miami, FL: American Welding Society.

Bijlaard, P. (1955). Stresses from radial loads and external moments in cylindrical pressure vessels. *Welding Journal.(NY)*, 608s–617s.

Billington, C., Lalani, M., & Tebbetl, I. (1982). Background to new formulae for the ultimate limit state of tubular joints. In *Offshore Technology Conference*.

Boland, G. (2013). Oil and Gas Exploration. Retrieved October 1, 2012, from http://oceanexplorer.noaa.gov/explorations/06mexico/background/oil/oil.html

Bouwkamp, J. G., & Hollings, J. P. (1980). Effects of Joint Flexibility on The Response of Offshore Towers. In *12th annual Offshore Technology Conference* (pp. 455–464). Houston, Texas.

Carlyle, R. (2012). Which is the current world record for deepwater drilling, and who holds it? Retrieved November 1, 2012, from http://www.quora.com/Which-is-the-current-world-record-for-deepwater-drilling-and-who-holds-it

Chen, B., Hu, Y., & Tan, M. (1990). Local joint flexibility of tubular joints of offshore structures. *Marine Structures*, 13–19.

Chen, T., Wu, S., & Yang, L. (1990). The Flexibility Behavior of Tubular Joints in Offshore Platforms. In *Ninth International Conference Offshore Mechanic and Arctic Engineering Symposium* (pp. 307–312). Houston: ASME.

Cofer, W. F., & Will, K. M. (1992). A Finite Element technique for ultimate strength analysis of tubular joints. *Engineering Competitions*, *9*, 345–358.

Comartin, C. D., Niewiarowski, R. W., & Rojahn, C. (1996). *ATC-40 Seismic Evaluation and Retrofit of Concrete Buildings Volume 1* (Vol. 1). Redwood City, California: Seismic Safety Commission.

Det Norske Veritas. (1977). *Rules for the design, construction and inspection of fixed offshore structures*. Høvik, Norway.

Dier, A. F. (2005). Tubular Joint Technology for Offshore Structures. *Steel Structure*, *5*(5), 495–502.

E.S.D.E.P. (1994). *The European Steel Design Education Programme*. London, UK.

Efthymiou, M. (1985). *Local rotational stiffness of unstiffened tubular joints*. *Koninklijke Shell Exploratie Produktie Laboratorium Report RKER.85.199.*

Elnashai, A. S., & Gho, w. (1992). Effect of joint Flexibility on Seismic Response Parameters of Steel Jackets. *International Offshore and Polar Engineering Conference*. San Francisco, USA.

Fessler, H., Mockford, P., & Webster, J. (1986a). Parametric Equations for the Flexibility Matrices of Multi-Brace Tubular Joints in Offshore Structures. In *Institute of Civil Engineers*.

Fessler, H., Mockford, P., & Webster, J. (1986b). Parametric Equations for the Flexibility Matrices of Single Brace Tubular Joints in Offshore Structures. In *Institute of Civil Engineers* (Vol. 81, pp. 659–673). Ice Virtual Library.

Fessler, H., & Spooner, H. (1981). Experimental determination of stiffness of tubular joints. In *2nd International Conference on Integrity of Offshore Structures*. University of Glasgow.

Holmås, T., Remseth, S. N., & Hals, T. E. (1985). Approximate Flexibility Modelling of Tubular Joints in Marine Structures. SINTEF Report No.STF71 A85016.

Honarvara, M. R., Bahaaria, M. R., Asgarianb, B., & Alanjarib, P. (2008). Cyclic inelastic behavior and analytical modelling of pile–leg interaction in jacket type offshore platforms. *Applied Ocean Research*, *29*(4), 167–179. doi:10.1016/j.apor.2008.02.001

HSE. (1999). *Dynamic push-over Analysis of jacket Structures*. Great Britain, Health and Safety Executive.

Kawashima, S., & Fujimoto, T. (1984). Vibration analysis of frames with semi-rigid connections. *Computers & Structures, Vol 19*(No.1-2), 85–92.

Kellogg M W. (1956). Design of piping systems. *Journal of the Franklin Institute*. Wiley. doi:10.1016/0016-0032(56)90101-6

Koloušek, V., & McLean, R. (1973). Dynamics in engineering structures. London: Praha-Academia.

Kurobane, Y., Packer, J. A., Wardenier, J., & Yeomans, N. (2004). *Design guide for structural hollow section column connections*. Koln, Germany: TüV-Verlag GmbH.

Lee, J. H., Hino, S., Ohta, T., & Seo, S. T. (2002). Static loading performance of tubular joint in multi-column composite bridge piers. *Memoirs of the Faculty of Engineering, Kyushu University*, *62*(3), 129–137.

Lee, M. M. K., & Llewelyn-Parry, A. (2004). Strength prediction for ring-stiffened DT-joints in offshore jacket structures. *Engineering Structures*, *27*(3), 421–430.

Matsui, C., Morino, S., & Kawano, A. (1984). Lateral-Torsional Buckling of Trusses with Rectangular Tube Sections. In *Proceedings of the Second international Conference* (pp. 199–206). Boston, Massachusetts, USA: Pergamon Press Inc.

Mirtaheri, M., Zakeri, H. A., Alanjary, P., & Assareh, M. A. (2009). Effect of Joint Flexibility on Overall Behavior of Jacket Type Offshore Platforms. *American Journal of Engineering and Applied Sciences*, *2*(1), 25–30.

Recho, N., Ritty, B., & Ott, F. (1990). Numerical Influence of Flexibility on the Fatigue Design of T-Welded Tubular Joints. In *Proceedings of the 9th International Conference Offshore Mechanic and Arctic Engineering Symposium* (pp. 365–371). ASME.

Rodabaugh, E. (1980). Review of data relevant to the design of tubular joints for use in fixed offshore platforms. *Welding Research Council Bulletin No.256, January*.

Sakamoto, S., & Minoshima, N. (1979). Behaviour of T-joint of Octagonal tubes. *Abstract, Annual Meeting ofAIJ*, 1037–1038.

Skallerud, B., & Amdahl, J. (2002). *Nonlinear analysis of offshore structures*. *RESEARCH STUDIES PRESS LTD*. Research Studies Pre; 1st edition (June 15, 2002).

Souissi, R. (1990). Flexibility of tubular joints. *In Tubular Structures-The Third International Symposium Lappeenranta 1989*, (Elsevier Applied Science, London.), 137–146.

SP6-1-300. (2002). SPD7 Wellhead Platform Jacket, Pars Oil and Gas Company, South Pars Gas Field Development, Phase 6, 7 and 8, EPCI Jackets. Iran.

Springfield, J. C. ., & Brunair, R. (1989). End-fixity determination of vibrating structural components. *Computers & Structures*, *33*(2), 453–458. doi:10.1016/0045-7949(89)90017-5

SW ANSYS Academic Teaching. (2011). ANSYS Online Manuals Release 5.5. Retrieved July 1, 2011, from http://mostreal.sk/html/

Tebbett, I. (1982). The reappraisal of steel jacket structures allowing for the composite action of grouted piles. In *14th Annual Offshore Technology Conference, Paper 4194*.

Ueda, Y., & Rashed, S. (1986). Flexibility and yield strength of joints in analysis of tubular offshore structures. In *Proceedings of the Fifth International Symposium on Offshore Mechanics and Arctic Engineering* (Vol. 2, pp. 293–301). Tokyo: ASME.

UEG. (1984). *Node Flexibility and Its Effects on Jacket Structures–A Pilot Study on Two-Dimensional Frames* (UR22 ed.). Underwater Engineering Group.

Van der Vegte, G. J., Koning, C. H. M. de, Puthli, R. S., & Wardenier, J. (1991). The static strength of multiplanar tubular steel X-joints. In *1st International O shore and Polar Engineering Conference* (pp. 42–52).

Vegte, G. Van der. (1995). *The static strength of uniplanar and multiplanar tubular T- and X-joints*. *Civil Engineering*. Delft University of Technology, Delft University Press, Netherlands.

Wang, W., & Chen, Y. (2007). Hysteretic behaviour of tubular joints under cyclic loading. *Journal of Constructional Steel Research*, *63*(10), 1384–1395.

Zayas, V. A., Popov, E. P., & Mahin, S. A. (1980). *Cyclic inelastic behavior of steel offshore structures*. California: University of California, Earthquake Engineering Research Center.